Biodiversity Data Journal 14: e189060
doi: 10.3897/BDJ.14.e189060

Taxonomy & Inventories

Diatoms (Bacillariophyta) of the Salish Sea, Northeast Pacific: annotated checklist and new species reports

Mark Webber[‡,§], Elaine Humphrey[‡,§], Arjan van Asselt[‡], Alice Chang[|], Evan Morien[¶,#], Andrew D. F. Simon[‡,¤]

‡ Institute for Multidisciplinary Ecological Research in the Salish Sea, Galiano Island, Canada
§ Advanced Microscopy Facility, Bob Wright Centre, University of Victoria, Victoria, Canada
| Department of Earth, Ocean and Atmospheric Sciences, University of British Columbia, Vancouver, Canada
¶ Hakai Institute, Heriot Bay, Canada
# Department of Botany and Biodiversity Research Centre, University of British Columbia, Vancouver, Canada
¤ University of Alberta, Edmonton, Canada

Corresponding author: Mark Webber (mwebber@imerss.org), Andrew D. F. Simon (adfsimon@imerss.org)

Academic editor: Anne Thessen

Received: 18 Feb 2026 | Accepted: 08 Apr 2026 | Published: 15 May 2026

Citation: Webber M, Humphrey E, van Asselt A, Chang A, Morien E, Simon ADF (2026) Diatoms (Bacillariophyta) of the Salish Sea, Northeast Pacific: annotated checklist and new species reports. Biodiversity Data Journal 14: e189060. https://doi.org/10.3897/BDJ.14.e189060

Abstract

Background

Diatoms are major primary producers known to respond rapidly to environmental change, making them useful indicators for ecological assessment and monitoring. In the Salish Sea bioregion, diatom records date back to early inventories by Lord (1866) and Bailey and MacKay (1916), followed by scattered surveys throughout the 20th and 21st centuries. Due to this fragmented record, a consolidated regional baseline has been lacking.

New information

We report 924 diatom taxa for the Salish Sea from historical records, voucher specimens and molecular data, forming a curated dataset of 11,469 records. Forty-two species, including six previously unreported genera, are newly recorded for the region, based on combined morphological and molecular evidence. For these taxa, including the recently described *Andrzeja fenestrata*, we provide taxonomic accounts with diagnostic light and electron micrographs. These data establish a baseline record of diatom diversity in the Salish Sea, setting an example for how collaboration amongst community and academic researchers can help establish data foundations for phytoplankton monitoring.

Keywords

biodiversity, eDNA, light microscopy, marine microbiome, metabarcoding, phytoplankton, scanning electron microscopy

Introduction

The Salish Sea is a biodiverse and culturally significant marine ecosystem spanning the coastal waters of south-western British Columbia (BC), Canada, and north-western Washington, USA. Encompassing the Georgia Basin and Puget Sound, this transboundary region forms the traditional territories of Coast Salish peoples, whose stewardship has shaped—and continues to shape—these lands and waters since time immemorial. Today, the Salish Sea, one of six distinct ecoregions within the Cold Temperate Northeast Pacific Province (Spalding et al. 2007), supports nearly nine million people and faces intensifying pressures from urbanisation, industrial activity, and habitat degradation (Sobocinski 2021). Thus, it has been recognized as a globally significant *urban sea*, where dense human populations intersect with highly productive coastal ecosystems (Sobocinski et al. 2022). At this intersection, the region represents an important setting for expanding plankton monitoring networks (United Nations Global Compact 2024), where diatoms—organisms known to respond rapidly to environmental variability (Dixit et al. 1992, Lowery et al. 2020, Sarker et al. 2023, Viljoen et al. 2024)—serve as key biological indicators.

Diatoms (Bacillariophyta) form a dominant lineage of photosynthetic eukaryotes within the Ochrophyta (stramenopiles), a group that ranks amongst the most abundant and species-rich components of aquatic ecosystems. While they are commonly regarded as planktonic primary producers, the majority of their diversity is associated with benthic habitats (Nakov et al. 2018). Currently divided into ten classes (Kociolek et al. 2026), more than 18,000 diatom species have been formally described (Guiry 2024), with total diversity estimated to be much higher — potentially reaching 100,000–200,000 species (Adl et al. 2005, Mann and Vanormelingen 2013, Kociolek and Williams 2015, Mann et al.

2016, Simpson and Eglit 2016, Benoiston et al. 2017, Kociolek et al. 2018, WoRMS Editorial Board 2021).

Diatoms are predominantly unicellular algae, although some taxa form chains of connected cells. Individual cells typically range from 5–200 µm in length, with larger species occasionally reaching 1–2 mm. Diatoms occupy an extensive range of sunlit environments wherever nutrients are available, including marine and freshwater systems and, in some cases, solid substrates, such as soils and even atmospheric particulates. They are amongst the most ecologically successful and productive organisms on Earth, generating much of the organic matter that forms the base of aquatic food webs. Estimated to account for approximately 40% of marine primary production, diatoms contribute about 20% of the global photosynthetic output annually and are responsible for approximately 20–40% of the Planet's oxygen generation (Field et al. 1998, Benoiston et al. 2017, Tréguer et al. 2018). They also play a pivotal role in global biogeochemical cycling — particularly in the cycling of silica, iron and nitrogen — and mediate the transfer of organic carbon and biogenic silica from surface waters to oceanic sediments and other aquatic depositional environments (Nelson et al. 1995, Falkowski et al. 1998, Kooistra et al. 2007, Armbrust 2009, Hoppenrath et al. 2009, Gugi et al. 2015, Medlin 2015, Cermeño 2016).

Fossil evidence and molecular phylogenies indicate that diatoms originated over 200 million years ago (Ma), likely during the early Mesozoic era and became dominant components of marine microalgae communities by the early Cretaceous period (ca. 110–115 Ma) (Vardi et al. 2009, Nakov et al. 2018, Behrenfeld et al. 2021, Pietluch et al. 2024). Yet their deeper evolutionary roots trace back further to the origins of the Ochrophyta, which emerged during the Mesoproterozoic (approximately 1–1.6 billion years ago) in a secondary endosymbiotic event that gave rise to the plastids shared amongst diatoms, brown algae (Phaeophyceae) and other stramenopiles (Armbrust 2009, Medlin 2015, Cermeño 2016, Benoiston et al. 2017, Pietluch et al. 2024).

Diatoms have intricately patterned cell walls (frustules) composed of amorphous silica, embedded proteins (frustulins, pleuralins, silaffins), mono- and polysaccharides (fucose, rhamnose, galactose, mannose, glucuronic acid, xylose) and long-chain polyamines. The external surface is further coated with exopolysaccharides and some genera also incorporate β-chitin in spines and excreted fibres. Each cell has two halves (valves) that fit together like a Petri dish and are connected by girdle bands. Valves contain intricate chambers, struts, tubes and partitions, with numerous pores for gas exchange, nutrient absorption and chemical signalling. These biological processes involve calcium ions, nitric oxide, oxylipins and aldehydes that mediate environmental sensing, defence, population dynamics, sexual reproduction and apoptosis. Frustule shape and patterning are diverse, yet relatively conserved within species, making morphological characters a key basis for taxonomy, typically corroborated by molecular analyses (Kooistra et al. 2007, Vardi 2008, Hoppenrath et al. 2009, Mann and Vanormelingen 2013, Nanjappa et al. 2014, Gugi et al. 2015, Kociolek and Williams 2015, Medlin 2015, Mann et al. 2016, Vasselon et al. 2017, Li et al. 2018).

As major primary producers in marine food webs, diatoms support fisheries that have sustained Coast Salish peoples for millennia (Carlson 2001). Yet, the earliest documented records of diatoms in the Salish Sea date back to the late 19th and early 20th centuries, beginning with the work of Lord (1866) and Bailey and MacKay (1916). Subsequent research along the west coast of North America expanded throughout the 20 th century, with extensive taxonomic and ecological studies by Gran and Angst (1931), Phifer (1932), Cupp (1943), Buchanan (1966), Rao and Lewin (1976), Shim (1976), and Tynni (1986), amongst others. Given the ecological importance of diatoms, integrating these fragmented records into a comprehensive regional baseline is critical amid intensifying pollution and habitat change. To support ongoing research and monitoring, we present an annotated checklist of Salish Sea diatoms, including new records that are verified from morphological and molecular data. This growing dataset, including taxonomic diagnostics, imagery, and references, provides a foundation for the continued study and monitoring of diatom diversity in the Northeast Pacific.

Materials and methods

Study area

The Salish Sea, one of the world's largest and most biologically diverse inland seas, encompasses roughly 7,000 km of coastline, hundreds of islands, and a network of oceanic and estuarine channels ranging from shallow to deep (Sobocinski 2021). Its waters extend from northern Vancouver Island through the southern Gulf Islands in the Strait of Georgia, British Columbia, to the San Juan Islands in Puget Sound, Washington State (Fig. 1). Circulation is driven by Pacific Ocean inflows via the Strait of Juan de Fuca and Johnstone Strait and by freshwater outflows from the Fraser and other rivers, forming a stratified, estuarine system.

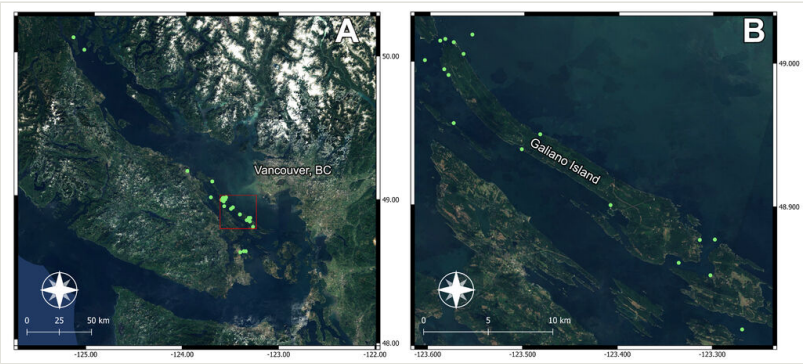

Figure 1.

Map of sampling locations (sampling details in Table 1). **A** Distribution of sampling sites throughout the Salish Sea (green markers). Red frame: area of enlargement around Galiano Island (1B); **B** Sampling sites around Galiano Island (green markers). Imagery: Sentinel-2 cloudless map of the world by EOX IT Services GmbH (Austria; https://s2maps.eu); contains modified Copernicus Sentinel imagery from 2016–2017 (Sentinel Hub 2025).

Sampling was concentrated around Galiano Island (48.9236, -123.4415), within the traditional territories of Hul'qumi'num- and SENĆOŦEN-speaking peoples, with additional sites distributed more broadly across the Salish Sea (Table 1), including Quadra Island, in the territories of the We Wai Kai, Wei Wai Kum, K'ómoks, Klahoose and Xwemalkhwu First Nations. Bounded to the north and south by the major tidal channels Porlier Pass and Active Pass, Galiano Island lies at the interface between waters more directly influenced by Pacific inflow via the Trincomali Channel to the southwest and more stratified, freshwater-influenced waters of the Strait of Georgia to the northeast. Intertidal habitats around the island are dominated by rocky shores formed from sandstones, conglomerates, and shales of the Upper Cretaceous Nanaimo Group (Johnstone et al. 2006). Interspersed shell, sand and mud beaches, together with brackish intertidal zones at the mouths of seasonal and perennial creeks (Simon et al. 2022), provide a diversity of soft-sediment and low-salinity habitats.

Table 1.

Sampling sites, dates and methods. See Fig. 1 for map of site locations.

Site name	Coordinates	Sampling dates	Methods
Active Pass East (APE)	48.8770, -123.2976	05.VIII.2024	20-µm plankton net sample (0–10 m depth)
Active Pass West (APW)	48.8607, -123.3357	05.VIII.2024	20-µm plankton net sample (0–10 m depth)
Chivers Point (CP), Wallace Island, Trincomali Channel	48.9572, -123.5743	25.VI.2022, 27.IX.2025	20-µm plankton net sample (0–4 m depth)
Departure Bay (DB), Nanaimo, public beach	49.2004, -123.9676	06.V.2024	20-µm plankton net sample (0–1 m depth); *Z. marina*; tidal flat sand samples
Dionisio Point (DP), Galiano Island, east lagoon; Hul'qumi'num name: *quelus*'	49.0136, -123.5749	15.VII.2022, 08.V.2025	20-µm plankton net sample (0–1 m depth)
Dionisio Reefs (DR), Porlier Pass	49.0158, -123.5838	08.V.2025	Brushings from unidentified red alga collected at depth by scuba
Gabriola Pass (GP)	49.1291, -123.7030	07.IX.2012	20-µm plankton net sample (0–10 m depth)
Miners Bay Wharf (MBW), Active Pass, Mayne Island	48.8521, -123.3022	20.VII.2022, 31.X.2022	20-µm plankton net sample (0–3 m depth); brushings from the red alga *Scagelia americana*
Montague Harbour Marine Provincial Park (MHMPP), Galiano Island; Hul'qumi'num name: *sumnuw*	48.9007, -123.4079	08.I.2013, VII–VIII.2020, 15.XI.2020, 07.III.2021, 22.VII.2021, 07.XI.2021	Site of multi-year eelgrass (*Z. marina*) microbiota study; morphological investigations combined with molecular sequencing
Navy Channel (NC) (between Mayne Island and Pender Island	48.8144, -123.2685	05.VIII.2024	20-µm plankton net sample (0–10 m depth)

Site name	Coordinates	Sampling dates	Methods
North Saltery Bay (NSB), Beach Access Site 45, Galiano Island	48.9907, -123.5801	24.VII.2024, 11.IX.2025	Sand and mud samples from a tidal flat
Pebble Beach, east side of Galiano Island (PB)	48.9498, -123.4827	25.VI.2020	20-µm plankton net sample (0–2 m depth)
Porlier Pass (PP)	49.0146, -123.5892	25.VI.2022, 18.X.2022, 16.III.2024, 15.IX.2025	20-µm plankton net sample (0–10 m depth)
Quadra Island, Sutil Channel (Q39)	50.0307, -125.0992	09.V.2024	64-µm plankton net sample (unknown depth); macroalgae samples
Quadra Island, beach in front of Hakai Institute labs (Q45)	50.1153, -125.2201	07.V.2024	Water scooped off the beach
Retreat Cove (RC); Hul'qumi'num name: *xetthecum*	48.9393, -123.5021	26.V.2023, 14.VII.2024	Macroalgae samples (*Ceramium pacificum*, *Costaria costata*, *Sarcodiotheca gaudichaudii*, *Ceramothamnion pacificum*,*Polyneura latissima*) collected by scuba during 2023 Galiano Island BioBlitz
Sidney Channel (SC)	48.6439, -123.3439	15.VII.2021	*Z. marina* sample dried on boat deck
Sidney public beach (SPB), Saanich Peninsula	48.6371, -123.4020	12.IX.2025	Brushings from *Z. marina* and from an unidentified filamentous red alga
Sidney Spit (SS), Sidney Island	48.6443, -123.3648	VII.2024	Brushings from *Z. marina*
Spanish Hills Wharf (SHW) (Spanish Hills Public Dock, North Galiano Island Dock), Trincomali Channel	48.9947, -123.5847	14.VII.2005, 21.VII.2006, 15.XII.2009, 26.X.2010, 20.XII.2010, 31.VII.2013, 13.VIII.2013, 20.XI.2019, 07.XII.2029, 30.V.2021, 03.VII.2021, 27.X.2021 (dock samples of *Obelia* sp.), 06.IV.2022, 15.IV.2022, 26.IV.2022, 25.VI.2022, 08.VII.2022, 15.VIII.2022; (almost every month sampling to VII.2025	20-µm plankton net samples (0–6 m depth); *Obelia* sp. (attached to the dock) sample
Strait of Georgia, east Galiano Island, nearshore (SGE-A)	49.0055, -123.5644	05.VII.2022, 26.IX.2022, 16.III.2024	20-µm plankton net sample (0–5 m depth)
Strait of Georgia, east Galiano Island, offshore (SGE-B)	49.0190, -123.5552	15.VII.2022, 26.IX.2022, 18.X.2022	20-µm plankton net sample (0–10 m depth)
Stuart Channel (SC), west of Thetis Island, adjacent to Fraser Point	49.0185, -123.7162	02.VIII.2023	20-µm plankton net sample (0–10 m depth)

Site name	Coordinates	Sampling dates	Methods
Sturdies Bay (SB) ferry dock	48.8767, -123.3135	12.I.2006, 26.V.2023	20-µm plankton net sample taken along the dock walkway (0–3 m depth)
Trincomali Channel (TC)	49.0009, -123.6053	28.VII.2004, 14.VII.2005, 19.VII.2006, 11.VII.2008, 15.XI.2008, 19.VII.2012, 03.VII.2021, 16.III.2024	20-µm plankton net sample (0–10 m depth)

Sample collection and preservation

We collected planktonic, epiphytic, benthic and epipsammic diatoms, sampling the water column with 20-µm and occasionally 60-µm mesh nets and swabbing biofilms from eelgrass (*Zostera marina*) (Jackman et al. 2025), macroalgae, sand and mud. All samples, including host algal substrates, were preserved in formalin (4% final concentration) and stored at 4°C. For microscopy, we brushed eelgrass, macroalgae and other substrates into a small pool of 0.2-µm-filtered marine water using a medium-firm toothbrush. After initial collection, all samples were soaked in deionised and distilled water (dH_2O) to remove salts.

Diatom frustules were typically treated with 10% hydrochloric acid, rinsed with dH_2O and cleaned with 30% hydrogen peroxide to remove organics. When samples contained substantial organic debris, such as fragments of macroalgae or eelgrass, sediment or concentrated mixed phytoplankton, we used a stronger digestion consisting of a 1:1 mixture of concentrated nitric and sulphuric acids and heated in a water bath at 95–100°C for 1.5–5 hours. In some cases, samples were subsequently treated again with 30% hydrogen peroxide, followed by multiple rinses in dH_2O to reach a pH of 6.5–7.

Cleaning times varied with the robustness of the frustules and the amount of organic matter present. Planktonic samples, which typically contained fewer adherent materials, often required noticeably shorter digestion times than macroalgal, benthic or sediment-associated samples. For taxa with lightly silicified frustules, we sometimes digested with only 30% hydrogen peroxide at room temperature for 7–10 days to avoid damaging the frustules (Webber et al. 2011).

For light microscopy (LM), we pipetted samples on to 22 × 22- or 18 × 18-mm glass coverslips and air dried and attached them to glass slides prepared with Naphrax (Brunel Microscopes, UK). We captured LM micrographs using either a Nikon Eclipse TE300 microscope that was equipped with a Tuscen DigiRetna 16-megapixel camera or a Nikon Eclipse E800 microscope that was equipped with bright-field or differential interference contrast (DIC) PlanApo 60× and 100×/1.40 objectives and an NA 1.40 oil condenser, unless otherwise noted and paired with a Zeiss AxioCam MRc5 digital camera (Jackman et al. 2025). For scanning electron microscopy (SEM), we pipetted cleaned samples directly on to 13-mm aluminium SEM stubs or on to 12-mm round glass coverslips that were then mounted on to the 13-mm aluminium stubs.

We isolated living diatoms with an inverted microscope, using drawn sterile Pasteur pipettes or pipettors. We repeatedly rinsed the diatoms in sterile drops of marine water and grew them in f/2 or f/10 media (Algae Research and Supply, Vista, California, USA; Guillard and Ryther (1962)), with the occasional addition of 1–2% antibiotic-antimycotic solution (A5955, Sigma-Aldrich, St. Louis, Missouri, USA) and, infrequently, HESNW growth media (Canadian Center Sfor the Culture of Microorganisms, University of British Columbia, Vancouver, Canada). We grew isolates in styrene well plates, Petri dishes or culture flasks and, depending on the original environment, in temperatures between 11 and 17°C, under 50–80 µmol photons m^{-2} s^{-1} (12:12h light/dark cycle) in an incubator. Successful clones were: 1) imaged live; 2) prepared in 3 × 1.5-ml polytubes for DNA bar coding in 95% ethanol or RNALater® reagent (Thermo Fisher Scientific, USA) and 3) stored in a final concentration of 4% formalin. When time permitted, clones were: 4a) set on to slides with Naphrax and 4b) prepared on SEM stubs.

We cleaned diatom clones that were grown in f/2 or other culture media and had delicate frustules with 30% hydrogen peroxide at room temperature for 5–10 days. We then rinsed the samples to remove salts and either prepared them for LM as described above or filtered them by syringe on to 13-mm-diameter polycarbonate filters (0.8–3-µm pore size), dried them and mounted them on to 13-mm SEM stubs. For both LM and SEM, we occasionally cleaned specimens directly on square or 12-mm round coverslips following Trobajo and Mann (2019). All stubs were sputter-coated with gold and imaged using either a Hitachi S-4800 field-emission SEM or a Hitachi TM4000Plus tabletop SEM at the Advanced Microscope Facility (AMF), University of Victoria (UVic), Victoria, Canada.

For in situ, environmentally prepared samples, we collected 8–10 mm sections of eelgrass leaves or macroalgae, soaked them in dH_2O to remove salts and dehydrated them through an ethanol series (50–100%), followed by three treatments of 100% hexamethyldisilazane (HMDS) (Hazrin-Chong and Manefield 2012, Jackman et al. 2025). Samples were mounted on to conductive carbon stickers (Ted Pella Inc., USA) that were affixed to 13-mm SEM stubs and imaged with the aforementioned SEM models at AMF, UVic. All preserved samples, slides and SEM stubs were deposited in the Webber Lab (IMERSS) collection on Galiano Island, BC or SEM stubs were stored temporarily for use at the AMF, UVic.

For molecular analyses, we concentrated samples by centrifugation into at least three 1.5-ml Eppendorf tubes, two of which were retained at the IMERSS lab as vouchers. We preserved the sub-samples in 95% ethanol (Linke et al. 2010, Lang and Kaczmarska 2011) or 50–60% RNAlater® (Hamilton et al. 2015) and stored them at -18 to -22°C.

Taxonomy and Nomenclature

We followed the valve terminology of Anonymous (1975), Ross et al. (1979), Round et al. (1990) and recent literature where terminology has been revised for specific genera. For *Cocconeis* species, sternum and raphe-sternum valves are abbreviated SV and RSV, respectively, and striae were counted at the valve centre along the apical *hyaline* area and on the opposite margin (Romero 1996).

We verified species and varieties with reference to valid binomials and authorities listed in AlgaeBase (Guiry and Guiry 2025) as the primary reference, adopting the same system of classification used in this resource. Where names could not be resolved through AlgaeBase, we consulted the World Register of Marine Species (WoRMS Editorial Board 2021) and DiatomBase (Kociolek et al. 2018). All taxonomic databases were accessed in 2024 and 2025. For class-level organization, however, taxa were arranged within the three-class diatom framework of Round et al. (1990), with all taxa assigned to Coscinodiscophyceae, Fragilariophyceae, or Bacillariophyceae. This framework was adopted to facilitate a more intuitive morphological navigation of the checklist.

Literature review

We summarised species reported for the Salish Sea from all available references that mentioned diatoms, beginning with Lord (1866). Using online searches, library catalogues and private literature collections of researchers, we included published sources from books, journals, government technical reports, such as Mather et al. (2010) and graduate student theses. All sources that had relevant information are cited in the annotated checklist (Suppl. material 1). We excluded private publications, personal communications and general references.

DNA extraction, PCR and molecular sequencing

We used Illumina metabarcoding and Sanger sequencing to sequence diatom samples from: 1) a published eelgrass epiphyte study (amplicon sequencing, Jackman et al. (2025)) (European Nucleotide Archive accession: PRJEB72893); 2) macroalgal epiphytes collected during the 2023 Galiano Island BioBlitz (amplicon) (ENA accession: PRJEB102646); 3) plankton tows (amplicon) (ENA accession: PRJEB102646) and 4) isolated diatom clones (Sanger sequencing) (ENA accession: ERZ29258993). DNA was extracted using the DNeasy PowerSoil Pro Kit (QIAGEN, Hilden, Germany; catalogue number 47014) following the manufacturer's instructions. Extraction blanks were included to detect potential contamination. DNA from each sample was amplified by PCR, using two primer sets to target general eukaryotes (18S) and diatoms (rbcL), which all contained Illumina adaptors and Golay barcodes, as follows:

- 18S: E572F CYGCGGTAATTCCAGCTC, E1009R and AYGGTATCTRATCRTCTTYG (Caporaso et al. 2012);
- rbcL: Diat_rbcL_708F AGGTGAAGTTAAAGGTTCATACTTDAA, R3 CCTTCTAATTTACCAACAACTG (Vasselon et al. 2017).

Library preparation and sequencing followed the procedures described in Jackman et al. (2025), the only exception being that the PCR chloroplast blocker was not used.

Sequence processing and taxonomic assignment

We processed raw amplicon reads for each amplicon, following the length-variable ITS workflow for DADA2 (v.1.24.0; Callahan et al. (2016)) in R (v.4.2.2; R Core Team (2023)), except where noted. We used Cutadapt (v.4.0; Martin (2011)) to remove primers and DADA2 using default parameters to process reads into amplicon sequence variants (ASV), except for the following modifications: trimRight(5,40), minLen(150,150), (18S V4), trimRight(5,10), minLen(150,150) (rbcL) and setting maxEE to c(4,6) for both datasets. After computing error rates, dereplication and sample inference with default DADA2 settings, we removed samples that had one or fewer identifiable unique sequences from the analysis, merged forward and reverse read pairs, denoised the data by removing ASVs that only appeared in a single sample at less than 0.001 relative abundance and then removed chimeric ASVs using the "removeBimeraDenovo" function with the "pooled" setting from DADA2.

For the 18S data, we performed taxonomic assignment in R using DECIPHER's IDTAXA function (Wright 2019), with PR2 5.0 (Guillou et al. 2013) and SILVA v.138 (Quast et al. 2012) reference databases, using IDTAXA's default threshold for identification (50). For rbcL data, we used BLASTn to query a local copy of the NT database (dated 01-11-2023) from the National Center for Biotechnology Information (NCBI; Bethesda, Maryland, USA), retaining the top 10 hits for each ASV at 96% identity and 50% query coverage. We used Galaxy Tool LCA (Beentjes et al. 2019) to determine a consensus lowest common ancestor (LCA) taxonomy from the BLAST hits for each ASV. We then integrated sequence tables, taxonomy tables and metadata into phyloseq objects (phyloseq v. 1.40.0; McLaren (2020)) and filtered as follows:

- removed off-target ASVs (18S, rbcL: bacteria, macroalgae, vascular plants, *Zostera* spp., unassigned);
- removed samples with < 1,000 reads and ASVs that represented < 0.001% of total reads;
- converted ASV counts ≤ 9 to zero.

Following taxonomic classification, we manually curated the resulting taxon tables by re-evaluating ambiguous or low-confidence assignments using BLAST against the National Center for Biotechnology Information nucleotide database, ensuring consistency with reference taxonomy. Curated taxon tables are provided as supplementary materials (Suppl. materials 3, 4, 5, 6, 7).

Data synthesis

We used R (v.4.5.0; R Core Team (2025)) to process and harmonise diatom occurrence records from: a) the literature review; b) the Global Biodiversity Information Facility (GBIF) and c) the morphological and molecular datasets generated through our sampling. We then filtered records to retain only diatom records that were identified to genus, species or infraspecific level, excluding higher-rank identifications, taxa sampled from freshwater bodies and any questionable reports. As diatom identification often requires detailed

morphological or molecular analysis, we excluded most observations from iNaturalist (iNaturalist 2025) and kept only a subset that we verified directly from our sampling.

We aligned species names with taxonomic standards maintained by AlgaeBase (Guiry and Guiry 2025) and standardised all metadata to Darwin Core (DwC) standards. As the historical record is often insufficiently resolved to determine precisely which infrataxa are encompassed within reported Latin binomials, we retained species-level names alongside infrataxa as warranted. Morphological sources included museum collections, data from past regional monitoring (Del Bel Belluz et al. 2024, Esenkulova and Salinas-Ruiz 2024), as well as vouchers and micrographs that were generated through our sampling. Molecular data included sequences from the European Bioinformatics Institute (EBI; Cambridgeshire, UK) that were aggregated on GBIF (MGnify 2021), along with amplicon and Sanger datasets that were generated through our sampling (Table 2).

Table 2.

Salish Sea diatom records by source: historical literature, molecular data and morphological data. Material that is uniquely contributed through this research is marked 'WL' (Webber Lab) and 'IMERSS', abbreviations corresponding to those used in the annotated checklist (Suppl. material 1). Accession numbers are provided for all molecular data submitted to the European Nucleotide Archive (ENA).

Type	Source	Records	Unique taxa
Literature	Various works cited in annotated checklist	2259	815
Molecular	IMERSS – 2023 Galiano BioBlitz (amplicon) (ENA accession: PRJEB102646)	1365	56
Molecular	Ecological genomics of a seasonally anoxic fjord; Saanich Inlet – data derived from the European Bioinformatics Institute (amplicon) (MGnify 2021)	474	43
Molecular	IMERSS – Plankton samples (amplicon) (ENA accession: PRJEB102646)	432	40
Molecular	*Zostera* epiphyte samples (amplicon) (Jackman et al. 2025) (ENA accession: PRJEB72893)	428	69
Molecular	IMERSS – *Scagelia* epiphyte sample (amplicon) (ENA accession: PRJEB102646)	63	41
Molecular	IMERSS – Diatom clones (Sanger) (ENA accession: ERZ29258993)	6	3
Morphology	Phytoplankton community composition links to environmental drivers across a fjord to shelf gradient on the central coast of British Columbia (Del Bel Belluz et al. 2024)	2354	45
Morphology	Harmful algae in the Strait of Georgia, 2015–2023 (Esenkulova and Salinas-Ruiz 2024)	1338	1
Morphology	WL – Morphological data (LM and SEM micrographs, iNaturalist observations) generated by Webber Lab (iNaturalist 2025)	317	174
Morphology	Continuous plankton recorder survey (CPR Survey) – Marine Biological Association (Lear 2022)	201	20
Morphology	University of British Columbia Herbarium (UBC) – Algae Collection (University of British Columbia Herbarium 2024)	58	5

Type	Source	Records	Unique taxa
Morphology	The Diatom Collection of Franz Josef Weinzierl at the Botanische Staatssammlung München (M) (Staatliche Naturwissenschaftliche Sammlungen Bayerns 2025)	17	16
Morphology	Harmful Algal Event Database (HAEDAT) (Provoost and Enevoldsen 2025)	12	2
Morphology	Brown University Herbarium (BRU) (Brown University Herbarium 2025)	6	4
Morphology	Michigan State University Herbarium (MSC) (Michigan State University Herbarium 2025)	6	5
Morphology	W.S. Turrell Herbarium, Miami University (MU) (W.S. Turrell Herbarium 2025)	6	5
Morphology	The New York Botanical Garden (NY) (Ramirez et al. 2025)	4	3
Morphology	University and Jepson Herbaria, University of California, Berkeley (UC) (Alexander and Gross 2024)	4	1
Morphology	Natural History Museum (London) (NHMUK) (Natural History Museum 2025)	2	2
Morphology	Florida Museum of Natural History (FLAS) (Florida Museum of Natural History 2025)	1	1
Morphology	University of New Hampshire Nature History Collections (NHA) (University of New Hampshire Natural History Collections 2025)	1	1

We concatenated annotations at the species level to build a comprehensive matrix that integrated all source data and identified new records from our sampling, based on historical precedence. Finally, we added fields for synonymy and critical notes, based on our review of the data. The matrix generated from this anlysis was then used to create the annotated checklist available as supplementary materials (Suppl. materials 1, 2). All novel data generated through this study are available as a DwC dataset on the Global Biodiversity Information Facility (Simon et al. 2026); the complete DwC dataset that we used to generate the checklist (synthesising all source data) is also available as supplementary materials (Suppl. materials 8, 9).

In determining new records, we compared the results of our sampling against both the historical record and detections arising from recent molecular surveys. As uncertainties can arise throughout the metabarcoding workflow (Mathieu et al. 2020), we regard detections, based solely on amplicon data, as provisional until they are confirmed morphologically. Thus, we treated as “new” any taxa that were previously unreported in literature or were unrepresented in collection databases, as well as records we verified morphologically that were previously known only from environmental amplicon sequencing. New records are presented as taxon treatments below.

Taxon treatments

Achnanthes groenlandica meridiana Giffen

Nomenclature

Achnanthes groenlandica var. *meridiana* Giffen (1973): 33, figs. 1–4, 619, 620, 621, 625—McIntire and Reimer (1974): pl. II, figs. 3a–c, pl. III; Tynni (1986): 14–15, table 1, pl. 15, fig. 91; Majewska et al. (2017): table 1; Kaleli et al. (2023): 43, pls. 5, 15–16.

Achnanthes groenlandica var. *phinneyi* McIntire and Reimer (1974)—Guiry and Guiry (2025).

Description

In girdle view, valve slightly geniculate, with convex RLV and concave RV. Valves linear-lanceolate with broadly rounded apices, slightly convex in the middle, length 22.9–32 (13.9–46) µm, width 4–5.0 (4–7) µm. RLV: narrow linear sternum, approximately central on valve face. Striae broken into one or two large and transversely elongate areolae. Central areolae occasionally larger than other areolae. Transapical rows of areolae 7–8 (6–8) in 10 µm. RV: moderately broad linear axial sternum. Central area has transverse fascia extending and slightly widening to the margins. Raphe filiform, narrow, broadening moderately near the slightly enlarged, slightly deflected proximal raphe ends. Distal raphe ends curved in the same direction, forming a shallow hook that terminates around the middle of the apices. Striae on both sides of sternum alternate, composed of two large, elliptical, usually transapically elongated areolae: one on valve face, one on mantle. The four or five striae nearest apices are moderately radiate, have smaller areolae and are more
closely spaced than other striae on valve. Transapical rows of areolae 9–10 (8–13) in 10 µm on RV. Puncta on girdle bands next to RV 13–14 (10–12) in 10 µm.

Diagnosis

The lower striae density, more closely spaced areolae near apices, smaller width range, lack of terminal orbiculi and other characteristics of the Galiano Island specimens place them outside of measurements for *Achnanthes pseudogroenlandica* Hendey (Hendey (1964): 177, pl. 28, figs. 9–12; Witkowski et al. (2000): 94, pl. 44, figs. 16–23; Suzuki et al. (2009); Majewska et al. (2017): table 1) and *Achnanthes groenlandica* (Cleve) Grunow, which have a lower striae density range (Witkowski et al. (2000): 89, 90, pl. 44, figs. 1–7). McIntire and Reimer (1974) distinguished *Achnanthes groenlandica* var. *meridiana* (p. 172, pl. 2, figs. 5a and b) from *Achnanthes groenlandica* var. *phinneyi* f. *jadyei*, where the latter has a RLV sternum that is centred within the valve and has more increased striae than the var. *phinneyi*. Our samples contain both forms, however. Since AlgaeBase (Guiry and Guiry 2025)

does not recognise *Achnanthes groenlandica* var. *phinneyi* f. *jadyei*, we have placed both forms within *Achnanthes groenlandica* var. *meridiana*.

Notes

Although this is the first report of an extant *Achnanthes groenlandica* var. *meridiana* within the Salish Sea, Tynni (1986) recorded this taxon as a rare occurrence in the Shine peat deposit (> 5.3 million years old) at a depth of 5.2 m at Squamish Harbor, Washington. The taxon was also identified by McIntire and Reimer (1974) in the Yaquina Estuary, Oregon. iNaturalist ID: 323108312, 323262404 (Fig. 2).

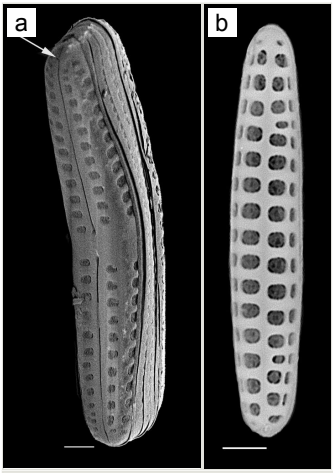

Figure 2.

Achnanthes groenlandica var. *meridiana*:

a: *Achnanthes groenlandica* var. *meridiana*, exterior RV. SEM. Scale bar: 2 µm;
b: *Achnanthes groenlandica* var. *meridiana*, exterior RLV and girdle view. SEM. Scale bar: 2.5 µm.

Actinoptychus adriaticus pumila Grunow

Nomenclature

Actinoptychus adriaticus var. *pumila* Grunow 1883: pl. 121, fig. 3, in Van Heurck (1882)—Lee and Chang (1996).

Description

Valves disc-shaped, diameter 13.5 (13.5–30) µm. Sectors 12, alternately raised and depressed. Externally, valve centre *hyaline* with curved wrinkles forming star-like pattern between sectors. Rimopotulae have medium tube length, are thin and hollow and face away from frustule centre, with slightly bulbous proximal connections to margin on the raised sectors. External rimopotulae located between valve face and

valve mantle is open and round to elliptical in shape. Small *hyaline* area around base of rimopotulae. Hyaline rim on margin of depressed sector. Depressed sectors have a small and faint *hyaline* area in the margin. Areolae in raised sectors 22 (22) in 10 µm, in depressed sectors 14 (14) in 10 µm. Small siliceous nodules scattered on margin surface. Internally, rimopotulae located in the centre of raised sectors.

Notes

iNaturalist ID: 185626241 (Fig. 3).

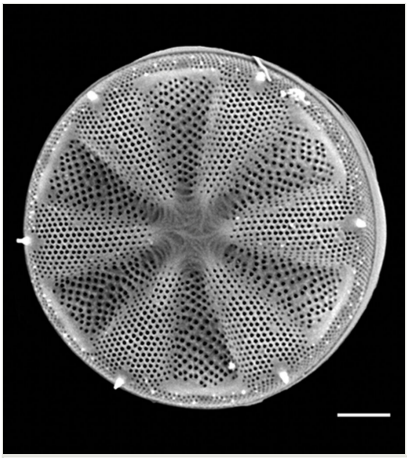

Figure 3.
Actinoptychus adriaticus var. *pumila*, exterior valve view. SEM. Scale bar: 5 µm.

Andrzeja fenestrata Mayama & Kryk

Nomenclature

Andrzeja fenestrata Mayama et al. (2025): 15, 17, table 2, figs. 44–59.

Description

Frustules rectangular, box-like in girdle view. Valve narrowly hemi-lanceolate with acute ends slightly inflated on dorsal side and flat on ventral side, length 8-15.4 (7–16) µm and width 1.5-2.2 (1.3–2.3) µm. Externally, valve face flat, curving roundly into the dorsal mantle. Ridge at juncture between valve face and mantle. External raphe branches short, arcuate and almost fully on the ventral mantle, with a small distal section along the valve face. Raphe proximal ends form drop-shaped holes within slightly curved elevations and distal ends are simple and curved away from marginal ridge. Internally, raphe fissures slightly curved (straight) and located along the face/mantle juncture, proximal ending simple, co-axially symmetrical, with low profile helictoglossa at the distal ends. Areolae elongate, parallel, uniseriate, occluded by

hymens and 14-20 in 10 µm on valve face and dorsal mantle. Striae on ventral mantle, 30-35 (28–30) in 10 µm, are denser than on valve face. Striae elongated below raphe branches, 2-4 and generally 4 (4-5), have oval-shaped areolae between proximal raphe endings, with narrow slits near apices. Epicingulum has 4-5 (4-5) bands, each with a single row of pores.

Notes

In both the Gulf Island specimens of *Andrzeja fenestrata* and in figs. 44-59 in Mayama et al. (2025), the distal raphe often travels a short distance across the ridge on the valve face-mantle juncture into the valve face, ending in a helictoglossa. Specimens of epiphytic and epipsammic *A. fenestrata* from Madagascar and Mozambique, as shown in Mayama et al. (2025), have a distal raphe that often travels a short distance across the ridge on the valve face-mantle juncture into the valve face, ending in a helictoglossa. These morphometric data closely match the epiphytic specimens on the eelgrass *Zostera marina* from the Southern Gulf Islands, BC, Canada. An abundance of *A. fenestrata* colonies were found on the eelgrass *Zostera marina* at Montague Harbour Marine Provincial Park (MHMPP), Galiano Island, BC. Canada, in 2020 to 2022 collections. *Andrzeja fenestrata* has also been observed 30 km from MHMPP on *Z. marina* from Sidney Beach, Sidney, BC. 12 September 2025. iNat: 331457188, 331455851 (Fig. 4).

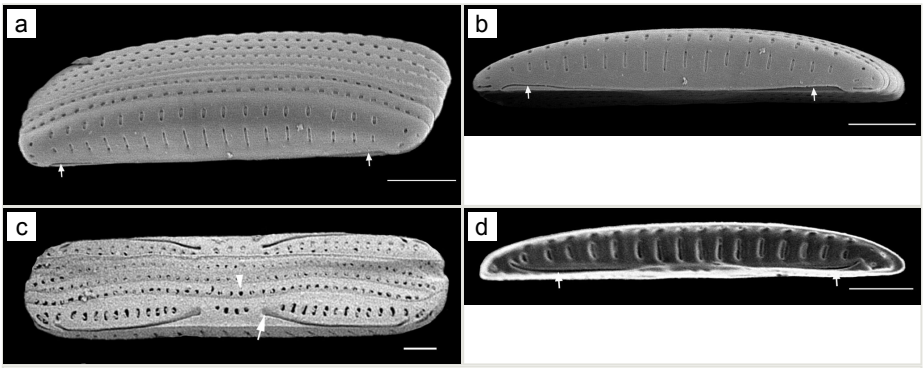

Figure 4.

Andrzeja fenestrata:

a: *Andrzeja fenestrata*, exterior, girdle and valve views. Arrow indicates location of raphe along part of the valve and mantle edge. SEM. Scale bar: 2 µm;

b: *Andrzeja fenestrata*, valve view. Tilted, with a section of ventral valve showing. Arrows indicate location of raphes. SEM. Scale bar: 2 µm;

c: *Andrzeja fenestrata*, ventral valve and girdle views. Short arrow indicates location of four girdle bands with simple singular row of pores. Longer arrow shows raphe on ventral valve side and proximal termination ending in a helictoglossa with a slight rim. SEM. Scale bar: 1 µm;

d: *Andrzeja fenestrata*, interior valve view. Arrows showing distal raphe termination ending in a helictoglossa. Scale bar: 2 µm.

Attheya longicornis R.M.Crawford & C.Gardner

Nomenclature

Chaetoceros septentrionale Østrup (1895): 457, pl. 7, fig. 88.

Attheya septentrionalis Østrup (1895)—Crawford et al. (1994): 41, figs. 42–49.

Attheya longicornis Crawford et al. (1994): 38, figs. 36–41—Hendey (1964); Hasle and Syvertsen (1997): 225; Bérard-Therriault et al. (1999): 38, pl. 22c–h; Orlova et al. (2002); Stonik et al. (2006); Rampen et al. (2009); Sugie and Kuma (2017); Stonik and Efimova (2020).

Description

Solitary marine species, not known to form colonies, except in culture. Valves flat to noticeably concave and lacking spines, spinules and rimoportulae. Length 5.2–6.4 (4–12) µm, 4–7.5 (3–16) µm in the apical axis (wide); pervalvar axis in culture often reported as 2–5 (2–5) times the width. Horns built of many silicious hoops and vary from long, thin, wavy, curly and straight, with horn length averaging 4.3–11 (4–10) times the cell length. Horns initially parallel to pervalvar axis, then may go in different directions. Longitudinal non-spiralling support bands 3 (3–4) in horns. Horns end in spines around an open apical aperture. Plastids per cell 1–2 (1–2). No resting cells or spores have been reported.

Diagnosis

Horns on *A. septentrionalis* are three times the valve length (Crawford et al. 1994; Hasle and Syvertsen 1997; Bérard-Therriault et al. 1999; Orlova et al. 2002; Stonik and Aizdaicher 2016) and are distinctly shorter than our specimens of *A. longicornis*, whose horns are 8–10 times the cell length. *Attheya longicornis* horns are strongly undulate (at least for one valve), as they arise from the valve corners and project parallel to the valvar plane, then often go in different directions. The two species of *Attheya* often differ in the longitudinal support bands in the horns: *A. septentrionalis* has four spiralling bands (Crawford et al. 1994; Stonik et al. 2006). Stonik and Aizdaicher (2016) report that from observations of six species, including *A. longicornis* and *A. septentrionalis*, found in the Sea of Japan, the only reliably different features that are useful for diagnosis between the two species are horn length and the number of longitudinal support rods in the horns. The horns of *A. longicornis* end in spines around an open apical aperture.

Notes

iNaturalist ID: 263094504 (Fig. 5).

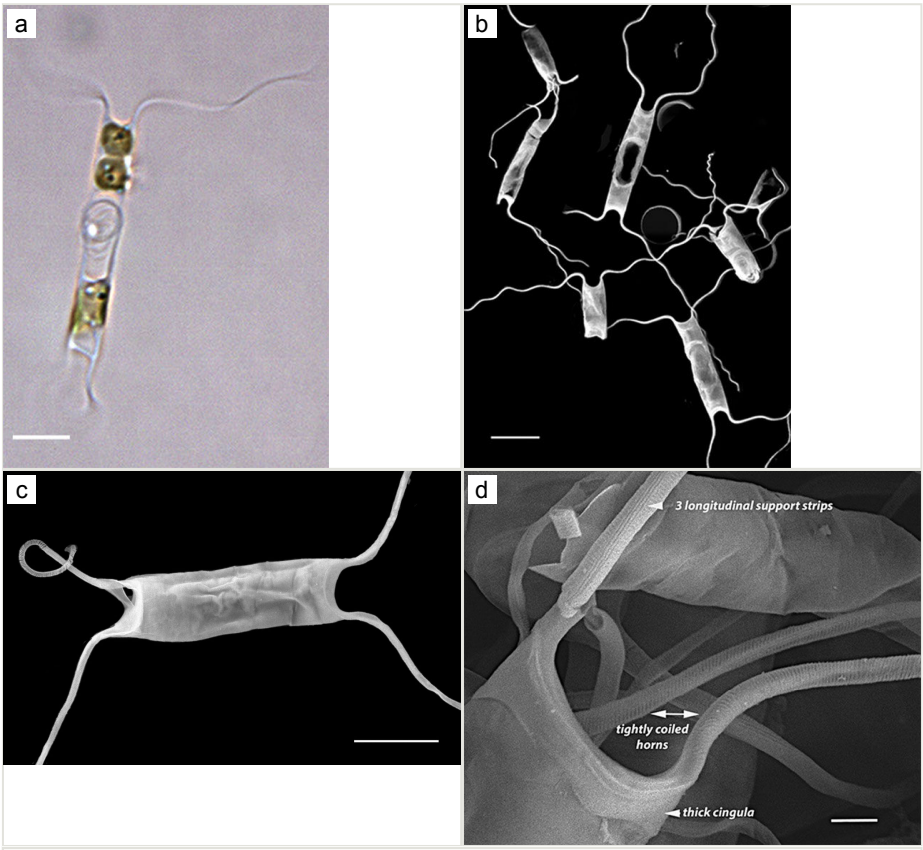

Figure 5.

Attheya longicornis:

a: *Attheya longicornis*, girdle view. LM. Scale bar: 10 µm;
b: *Attheya longicornis*, girdle view. SEM. Scale bar: 10 µm;
c: *Attheya longicornis*, girdle view. SEM. Scale bar: 5 µm;
d: *Attheya longicornis*, girdle view. SEM. Scale bar: 1 µm.

Bacteriastrum hyalinum Lauder

Nomenclature

Bacteriastrum hyalinum Lauder (1864): 8, pl. III, fig. 7—Cupp (1943): 96, figs. 56a–d; Hendey (1964); Hoppenrath et al. (2009): 73; Bosak et al. (2015); Barcode of Life Data System (2024); Guiry and Guiry (2025).

Bacteriastrum varians f. *hyaline* (Lauder) Frenguelli (1928): 543.

Description

Cells cylindrical, diameter 21.4–22 (14–54) µm. Chains are long, straight or slightly curved. Apertures narrow, but distinct. Inner setae 14–22 (12–46) on each valve, with short basal part, orientated almost perpendicular to the chain axis. Hairy appearance due to bifurcations in the pervalvar axis (parallel to chain axis). Forked parts gently curved and usually weakly twisted. Terminal setae not bifurcated and are umbrella-shaped, straight or undulate, stronger than inner setae, 2–3 (2) times longer than valve diameter and with spirally arranged tiny spines. Central process appears as a short, flattened tube on valve exterior and as a simple slit on interior side.

Notes

iNaturalist ID: 315424735 (Fig. 6).

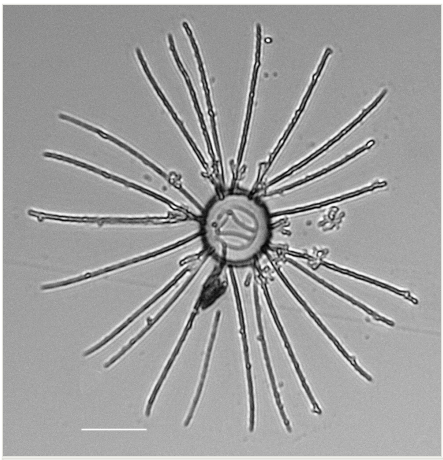

Figure 6.

Bacteriastrum hyalinium, valve view. LM. Scale bar 20 µm.

Bacterosira cf. *constricta* (Gaarder) J.S.Park & J.H.Lee

Nomenclature

Thalassiosira constricta Gaarder (1938): 6, fig. 6; Harris et al. (1995): 125, fig. 15; Hasle and Syvertsen (1997): 69–70; Throndsen et al. (2007): 137.

Bacterosira constricta—Park et al. (2016a).

Description

Frustules rectangular in girdle view, with slightly round valve edge. Cells in chains, often connected by chitin threads extruded from central fultoportulae; rarely solitary. Pervalvar axis length 17.8 (13.5–23.0) µm, sometimes exceeding length of valve

diameter. Cells circular in valve view, diameter 21.9–22.7 (9.8–25.7) µm, with slight depression in centre. Clusters of 2 (0–14) fultoportulae present in valve centrs. Fultoportulae, with raised tubes, located on valve margin, 3–4 (5–7) in 10 µm. Single rimoportulae located mid-way between marginal fultoportulae. Areolar density, 36–44 per 10 µm on valve face, 37–46 per 10 µm on valve margin and 30 (41–51) per 10 µm on valve mantle.

Diagnosis

This specimen from Trincomali Channel has two central, buttressed, strutted processes instead of a cluster of tubes (fultoportulae) in the centre of the valve, which is unusual. Normally, for the two species of this genus, the buttresses are not apparent, though they are mentioned in Harris et al. (1995). All other morphological features of this specimen conform reasonably well with published accounts of *Bacterosira constricta*. This specimen is unlike the only other accepted species, *Bacterosira bathyomphala* (Cleve) Syvertsen & Hasle (Guiry and Guiry 2025). More specimens are required to examine the internal valve and girdle band morphology.

Notes

iNaturalist ID: 259444260. Mol. data: ERS27217975, ERS27218291, ERS27218292, ERS27218293, ERS27218294, ERS27218295, ERS27218296, ERS27218297, ERS27218298 (Fig. 7).

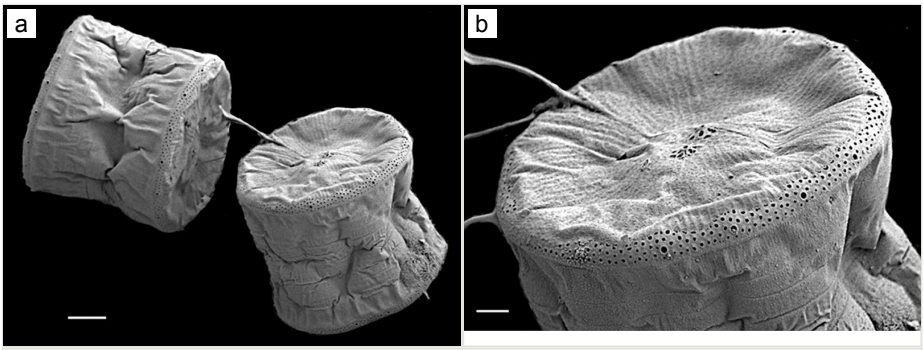

Figure 7.

Bacterosira cf. *constricta*:

a: *Bacterosira* cf. *constricta*, external girdle and valve views. SEM. Scale bar: 5 µm

b: *Bacterosira* cf. *constricta*, external valve and girdle views. SEM. Scale bar: 2 µm.

Campylodiscus bicostatus W.Smith ex Roper

Nomenclature

Campylodiscus bicostatus W.Smith ex Roper (1856): 75, pl. 6, fig. 4 (as '*bi-costatus*') —Sims (1996); Al-Handal et al. (2018): 143, fig. 103; Plinski and Witkowski (2020): 133, fig. 706.

Campylodiscus clypeus var. *bicostata* (W.Smith ex Roper) Hustedt (1930a): 448, fig. 874.

Description

Valve subcircular, convex along apical plane, diameter 57.5 (18–85) µm. Frustule saddle-shaped with round corners. Hyaline band surrounds the oblong central area (depressed elliptical central area). Distinctive radiate heavy costae, 2.5–3 (2.5–3) in 10 µm, do not reach centre of valve. Axial area linear-lanceolate, narrow or slightly expanded. Inner transapical striae 8–9 (9–10) in 10 µm.

Notes

iNaturalist ID: 189680990 (Fig. 8).

Figure 8.
Campylodiscus bicostatus, exterior valve view. LM. Scale bar: 20 µm.

Cocconeis costata hexagona Grunow

Nomenclature

Cocconeis costata var. *hexagona* Grunow 1880: pl. XXX, figs. 15–17, in Van Heurck (1880): pls. I–XXX—Romero and Rivera (1996): 327, figs. 17–34; Riaux-Gobin and Romero (2003): 24, 76, pl. 3; Al-Handal et al. (2022): 420, 425, fig. 50.

Description

Valves hexagonal in outline, with acute to rounded apices, length 14.5–23.1 (9–30) µm, width 8.9–11.9 (5.5–15) µm. SV: sternum relatively broad (narrow), linear, rarely linear-lanceolate. Transapical striae bi- to triseriate (bi- to tetraseriate), parallel, radiate at apices, 6–7 (6–13) in 10 µm. RV: similar to the nominate variety, transapical striae biseriate, parallel in middle becoming radiate towards apices, 18 (6–11) in 10 µm, 40 areolae (30–35) in 10 µm.

Notes

iNaturalist ID: 259362490; 259359045 (Fig. 9).

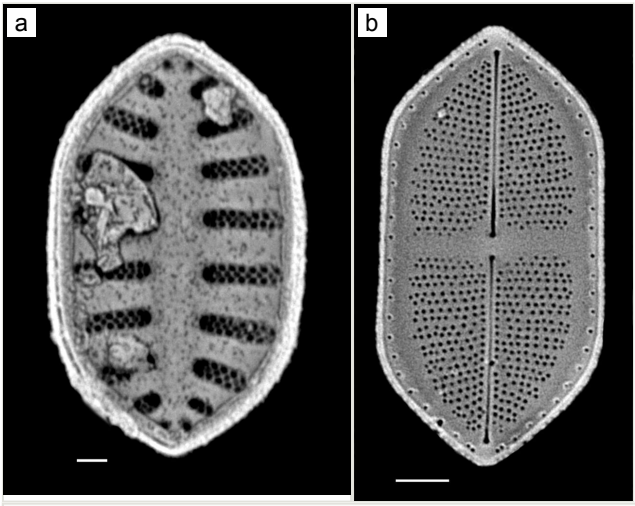

Figure 9.

Cocconeis costata var. *hexagona*:

a: *Cocconeis costata* var. *hexagona*, SV. SEM. Scale bar: 1 µm;
b: *Cocconeis costata* var. *hexagona*, interior SV. SEM. Scale bar: 2 µm.

Cocconeis kerguelensis P.Petit

Nomenclature

Cocconeis kerguelensis Petit (1889): 116, pl. X, fig. 5—Cleve (1895): 182; Bourrelly and Manguin (1950); Desikachary (1988): 7, pl. 506, figs. 1–12.

Description

Valves elliptical, disc-like, length 53.1 (32–55) µm, width 47.9 (38–85) µm. SV: axial area relatively narrow, linear-lanceolate. Striae biseriate, 7 (4–6) in (10) µm, 4 striae at margins, slightly parallel at centre and highly radiate at apices. Areolae 16 (10) in 10 µm. RV (not imaged): raphe ends near margin. Axial area very narrow. Central area has transverse, outwardly narrowed fascia. Striae biseriate, 4 in 10 µm. Areolae 10–12 in 10 µm and crossed near margin by narrow blank band.

Diagnosis

The description above is based on Cleve (1895) and matches well with the images in Desikachary (1988). Only one image of the sternum valve.

Notes

Cocconeis kerguelensis (P.Petit) Cleve 1895 (as *Cocconeis costata* var. *kerguelensis* (P.Petit) Cleve 1895 was reported from the Yaquina Estuary, Oregon, USA by Riznyk (1973: 119, Pl. 5, Figs. 3 and 4). iNaturalist ID: 259379467 (Fig. 10).

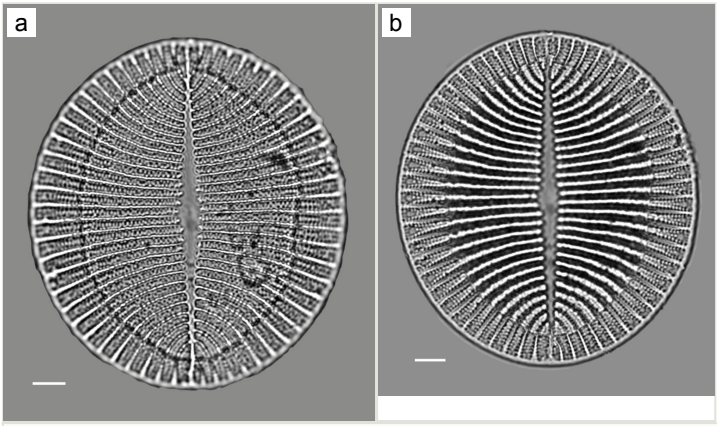

Figure 10.

Cocconeis kerguelensis:

a: *Cocconeis kerguelensis*, SV. LM. Scale bar: 5 µm;
b: *Cocconeis kerguelensis*, SV. LM. Scale bar: 5 µm.

Cocconeis notata P.Petit

Nomenclature

Cocconeis notata Petit (1877): 168, pl. 4, fig. 1—Poulin et al. (1984): 54, figs. 22–25; Siqueiros-Beltrones and Ibarra Obando (1985); De Stefano and Marino (2001): 297, figs. 1–14, 44–46; Sar et al. (2003): 91, fig. 32; Lee et al. (2012): 250, fig. 1.

Description

SV: valves broadly elliptical, length 21.2 (12–29) µm, width 12.9 (6.4–19) µm. Sternum narrow and sigmoid with thin, stauros-like area expanding into a hemispheric *hyaline* area close to valve margin. Striae uniseriate, 10 (9–23) in 10 µm, parallel at the centre and curved to radiate at apices. Areolae round, 10 (10–22) in 10 µm.
RV: valves broadly elliptical, length 23.7–26.9 (12–30) µm, width 15.9–16.2 (5.6–19) µm. A complete fascia reaches valve margin on one side and expands into stirrup-shaped *hyaline* area. Raphe narrow, sigmoid and slightly deflected in opposite directions. Central terminal endings slightly expanded. Transapical striae uniseriate, 16–18 (14–25) in 10 µm, parallel at centre and curved to radiate at apices. Areolae 15–16 (17–24) in 10 µm.

Notes

For the Eastern Pacific, *C. notata* was previously reported by Siqueiros-Beltrones and Ibarra Obando (1985) for the Baja California Peninsula on the Mexican Pacific coast. iNaturalist ID: 259450952 (Fig. 11).

Cocconeis pseudomarginata intermedia Grunow

Nomenclature

Cocconeis pseudomarginata var. *intermedia* Grunow (1867): 13, pl. 1, fig. 6—Joh (2021): 166, figs. 73–76, 88, 89.

Description

Valves elliptical, length 73.2 (26–68) µm, width 60.1 (14–51) µm. SV (note: no SV specimen to date): sternum broadly lanceolate with ends enlarged and pear-shaped, connected to submarginal *hyaline* area, with longitudinal line bisecting striae between sternum and valve margins. Outer surface of sternum longitudinally depressed. Transapical striae radiate towards apices, 25–30 in 10 µm; striae composed of elongated areolae. RV: raphe weakly sigmoid, sternum very narrow with terminal ends expanded and with crescent-shaped *hyaline* area, resulting in raphe distant from apices. Longitudinal depression between raphe and valve margins.

Central area small, rhombic. Transapical striae radiate towards apices, 23 (23–28) in 10 µm in inner parts of valve (Joh 2021).

Diagnosis

This taxon differs from the nominate variety, *Cocconeis pseudomarginata*, in that the raphe is slightly sigmoid and transapical striae of SV are dense (Joh 2021).

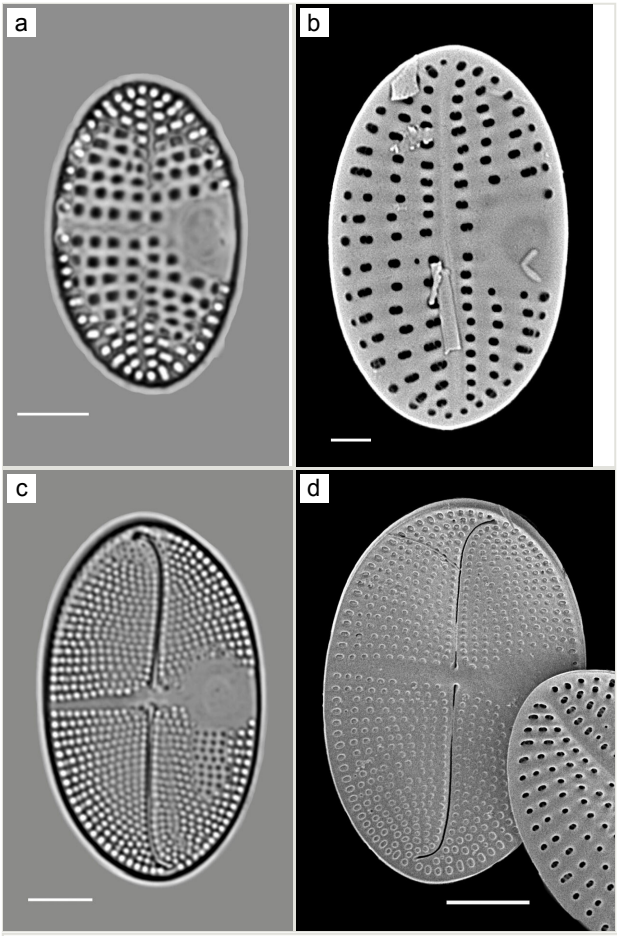

Figure 11.

Cocconeis notata:

a: *Cocconeis notata*, SV. LM. Scale bar: 5 µm;
b: *Cocconeis notata*, SV. SEM. Scale bar: 2 µm;
c: *Cocconeis notata*, RV. LM. Scale bar: 5 µm;
d: *Cocconeis notata*, RV. SEM. Scale bar: 5 µm.

Notes

iNaturalist ID: 259455426 (Fig. 12).

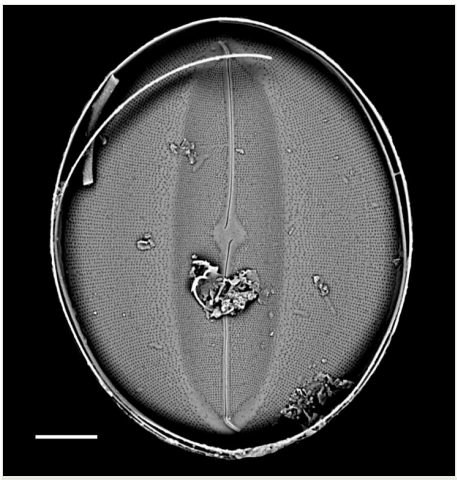

Figure 12.

Cocconeis pseudomarginata var. *intermedia*, RV. SEM. Scale bar: 10 µm.

Cocconeis scutellum posidoniae M.De Stefano, D.Marino & L.Mazzella

Nomenclature

Cocconeis scutellum var. *posidoniae* De Stefano et al. (2000): 235–237, figs. 72–86 —De Stefano et al. (2008); Riaux-Gobin and Witkowski (2017); Riaux-Gobin et al. (2018).

Description

Valves elliptic-oval shaped, length 22.5–48.8 (13–40) µm, width of transapical axis 15.0–34.1 (8–23) µm. SV: Thickly silicified sternum lacks differentiated central area. Striae have radiate arrangement (11–14 in 10 µm), uniseriate in centre of valve to biseriate at margin and triseriate in mantle. Valve-face areolae, 9–13 in 10 µm arranged in apically aligned pattern. RV: Raphe straight and thin with coaxial proximal endings converging in very small central area and distal endings terminating in reduced, submarginal areas. Striae radiate, uniseriate from valve centre to submarginal *hyaline* area, which appears as a thickened rim to internal face of valve. Striae on mantle biseriate. Striae and areolae range from 12–17 (18–23) and from 18–22 in 10 µm, respectively. Papillae with parallel furrows on valvocopula (De Stefano et al. 2000).

Diagnosis

The specimens found on *Z. marina* conform well to the original description (De Stefano et al. 2000; De Stefano et al. 2008), especially the distinctive papillae on the valvocopula.

Notes

iNaturalist ID: 259478500 (Fig. 13).

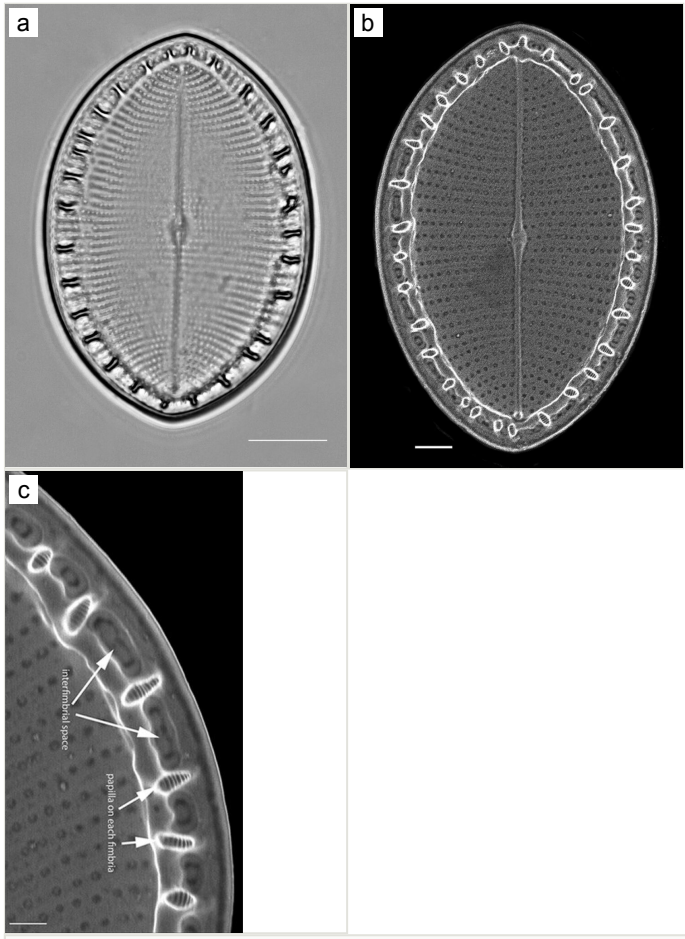

Figure 13.

Cocconeis scutellum var. *posidoniae*:

a: *Cocconeis scutellum* var. *posidoniae*, RV. SEM. Scale bar: 2 µm;
b: *Cocconeis scutellum* var. *posidoniae*, RV. Arrows indicate interfimbial space and papilla on each fimbria. SEM. Scale bar: 1 µm;
c: *Cocconeis scutellum* var. *posidoniae*, RV. SEM. Scale bar:10 µm.

Cyclotella baltica (Grunow) Håkansson

Nomenclature

Cyclotella striata var. *baltica* Grunow 1882: pl. 92, figs. 13–15, in Van Heurck (1882)—Guiry and Guiry (2025).

Cyclotella baltica (Grunow)—Håkansson (2002): 104, 105, figs. 373–380; Hasle and Syvertsen (1997): 33, 34, table 1; Prasad and Nienow (2006); Tanaka (2007): 18, 19, pls. 11–13.

Description

Valve diameter 27.3 (11–67) µm with strong, tangentially undulate central area extending two-thirds (one-half to two-thirds) of the valve diameter. Central area colliculate with 9 (3–11) valve-face fultoportulae arranged in semicircular array on elevated (convex) area. Marginal striae 11–12 (8–16) in 10 µm. Internally, valve-face fultoportulae are surrounded by 3 (2–3) satellite pores. Externally, marginal area striae and interstriae are equal length and continue on to mantle. Mantle fultoportulae 7–8 (8–16) in 10 µm on non-recessed costae. At every second, occasionally third (second to fourth), interstriae are mantle fultoportulae, internally with two satellite pores orientated lengthwise to costae. Costae between mantle fultoportulae often slightly recessed. Internally, rimoportula located on mantle at same level as mantle fultoportulae, with opening running radially in same direction as costa.

Diagnosis

Cyclotella baltica and *C. litoralis* have similar morphologies. The latter species has marginal fultoportulae on recessed costae, often paired with a single costa of separation. In addition, the SHW specimen has a mantle fultoportula (MF) density of 7–8 in 10 µm, which falls within the published data for *C. baltica* and below densities and MF distribution for *C. litoralis* (MF 11–14 in 10 µm) and *C. striata* (MP 8–11 in 10 µm), but recessed on the second to fourth interstria, with absence of valve-face fultoportulae; *C. stylorum* (MF 9–12 in 10 µm, grouped in pairs or triplets); and *C. caspia* (MP 20–28 in 10 µm, every third or fourth interstria, diameter 3.5–22 µm).

Notes

Brackish to marine waters. iNaturalist ID: 265283095 (Fig. 14).

Didymosphenia geminata (Lyngbye) Mart.Schmidt

Nomenclature

Didymosphenia geminata—Schmidt (1899): pl. 214, figs. 7–10; Round et al. (1990): 496, 497; Snoeijs and Balashova (1998): pl. 430; Khan-Bureau et al. (2016): 7, figs. 17–24; Lange-Bertalot et al. (2017): 188, 189, pl. 102, fig. 1.

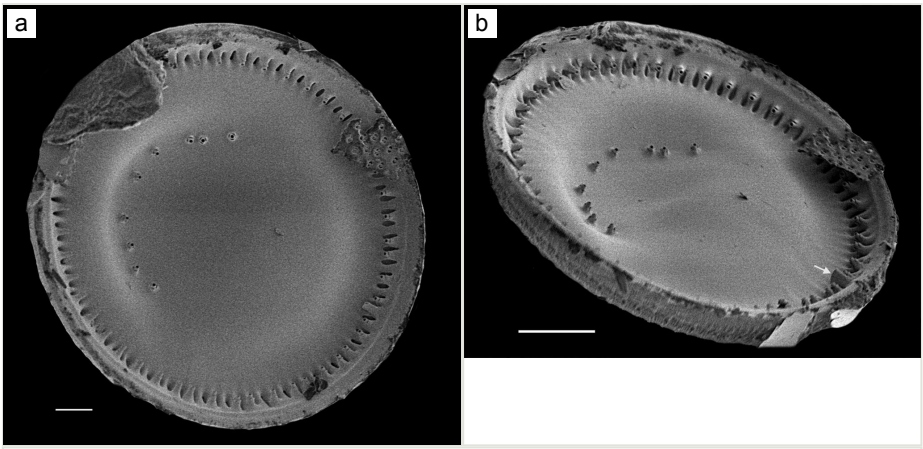

Figure 14.

Cyclotella baltica:

a: *Cyclotella baltica*, interior valve view. SEM. Scale bar: 2.5 µm;
b: *Cyclotella baltica*, interior valve view. Arrow indicates location of the rimoportula. SEM. Scale bar: 5 µm.

Description

Head pole distinct and subcapitate; foot pole rounded to slightly capitate, with distinct constriction of apices and inflated central part. Valve face flat. Length 124.5 (48–161) µm, width 43.6 (25–45) µm, length-to-width ratio 2.9 (1.9–3.9). Stigma number 4–5 (1–7) in a row to one side of central area. Striae uniseriate 10 (7–10) in 10 µm, radiate and becoming parallel to convergent towards poles and of different lengths in middle of valve, circling terminal fissure in head pole. Clear area in foot pole has very small pores where mucilage stalks are secreted. Areolae 12–13 (9–12) in 10 µm. Raphe laterally displaced, mostly straight, with expanded central ends and long, hooked terminal fissures in same direction.

Diagnosis

A distinctive species, especially the row of stigma to one side of the central area and inflation of the valves between the subcapitate poles.

Notes

This is a freshwater epiphytic and epilithic species. Specimens were possibly washed into Galiano Island waters from the Fraser River outflow. iNaturalist ID: 264211715; 318331778 (Fig. 15).

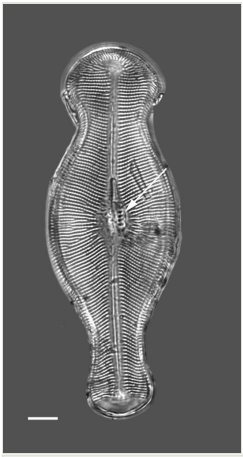

Figure 15.

Didymosphenia geminata, valve view. Arrow indicates a row of five stigma. LM. Scale bar: 10 µm.

Diploneis exemta (A.W.F.Schmidt) Cleve

Nomenclature

Navicula exemta Schmidt (1875): pl. 11, figs. 28, 29.

Diploneis exemta Cleve (1894): 86—Kuntze (1898): 548, 549, 552; Peragallo and Peragallo (1908): 112, pl. 15, figs. 16, 17; López-Fuerte and Siqueiros-Beltrones (2016): 242; Guiry and Guiry (2025).

Schizonema exemtum (A.W.F.Schmidt) Kuntze (1898): 549, 552—Guiry and Guiry (2025).

Description

Valve panduriform with tongue-shaped segments, length 85.0 (60–140) µm, width 21.8 (32–42) µm, 14.1 (16–30) µm at constriction. Central nodule quadrate, moderately large, slightly expanded in apical direction; horns parallel and furrows linear. Striae density 8 (5–6) in 10 µm (8 in 10 µm for *D. exemta* var. *digrediens*), crossed by 1 (1–2) longitudinal lines. Distal to furrow is a line of faint or large puncta, 8 in 10 µm.

Diagnosis

This specimen conforms fairly well to the description in Cleve (1894) and the drawings (figs. 28 and 29) in Schmidt (1875), including shape proportions and is a fairly exact match with the drawing in Peragallo and Peragallo (1908). Exceptions include a slightly higher striae density in Cleve's and Peragallo and Peragallo's descriptions (5–6 in 10 µm) and the row of large puncta that is interrupted in the middle of the valve, distal to the longitudinal furrows as in Peragallo and Peragallo's drawing. Either this specimen is a new variety or it can be placed into the unverified (Guiry and Guiry 2025) variety of *D. exemta* var. *digrediens* Cleve (1894) with a reported striae density of 8 in 10 µm.

Notes

This species is listed as a freshwater species by AlgaeBase (Guiry and Guiry 2025) and has been reported by López-Fuerte and Siqueiros-Beltrones (2016) as epiphytic in the marine waters of Baja California and the Gulf of Mexico.

Diploneis exemta is newly reported for the Pacific coast of North America, with the exception of a fossil report from California. This species is listed by Cleve (1894) from marine waters of the east coast of Madagascar, Tahiti, Kerguelen Island and Campeche Bay in the Gulf of Mexico, with fossils from Oamaru, New Zealand and Santa Monica, California. Cleve reported *Diploneis exemta* cf. *digrediens* from China and a fossil specimen from Hungary. Peragallo and Peragallo (1908) identified *Diploneis exemta* from the English Channel and Banyuls-sur-Mer, Balearic Sea, France. iNaturalist ID: 266785298 (Fig. 16).

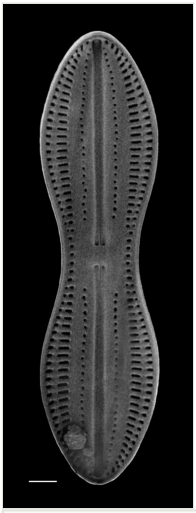

Figure 16.

Diploneis exemta, interior valve view. SEM. Scale bar: 5 µm.

Extubocellulus spinifer (Hargreaves & Guillard) Hasle, Stosch & Syvertsen

Nomenclature

Bellerochea spinifera Hargraves and Guillard (1974): 168, figs. 9–12.

Extubocellulus spinifer—Hasle et al. (1983): 70–73, figs. 362–390, 392; Saunders et al. (2010): 135, 136, fig. 3.14d; Dabek et al. (2019).

Description

Chain-forming. Valves broadly elliptical to circular, length 2.6–2.8 (1.6–3.6) µm, width 2.2–2.3 (1.5–3.0) µm, with shallow mantle. Rectangular in girdle view. Small, raised, short and funnel-like ocelluli located at each apex. Valve face perforated by approximately equidistant larger and unoccluded poroids 50 (50) in 10 µm of diameter 60 (78) nm and smaller and unoccluded poroids 60–70 in 10 µm of diameter 20 nm. Globules or short spines are scattered, or not, on valve face. Occasional tubular processes.

Diagnosis

No vela could be found in any of our specimens (n = 2), which is in accordance with accounts in North American and European literature (Hasle et al. 1983). However, Saunders et al. (2010) reported vela in the poroids (areolae) for their Australian specimens. Tubular processes were not observed in any of those samples.

Notes

iNaturalist ID: 311561542. Mol. data: ERS21395345, ERS27630062 (Fig. 17).

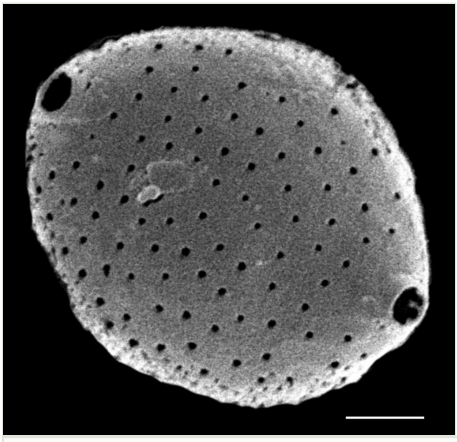

Figure 17.

Extubocellulus spinifer, exterior valve view. SEM. Scale bar 0.5 µm.

Fogedia krammeri Witkowski, Lange-Bertalot, Kociolek & M.Kulikovskiy

Nomenclature

Fogedia krammeri Witkowski et al. (2010): 50, figs. 1, 2—Kim et al. (2022).

Description

Valves moderately variable in outline, from broad-elliptic or broadly elliptic-lanceolate to linear-elliptic, with ends cuneate and terminus shortly protracted and subrostrate. Length 23.5–28.2 (20–30) µm, width 11.7–12.0 (9.5–12.0) µm. Raphe slightly lateral, with two minor undulations at one-quarter distance from central endings and one-quarter distance from terminal endings. External central raphe endings expanded; terminal raphe endings short and slightly bent in same direction. Axial area narrow, linear throughout. Central area forming a shortened, almost rectangular fascia connected to lateral area, with transapical striae interrupted in marginal part on either side. Striae subparallel to slightly radiate proximally to the ends and becoming more strongly radiate distally, where they are very slightly denser at 11–12 (10–12) in 10 µm. Lineolae of the striae comparatively coarse, discernible by LM, 27–30 (26–29) in 10 µm.

Diagnosis

This specimen has similarities to both *Fogedia krammeri* and *F. finmarchica* (Cleve 1895: 28) (Van der Werff and Huls (1975): P.D G XVI. 109; Hendey (1964): 198, pl. 30, fig. 5; Riznyk (1973): 126, pl. 11, fig. 7; Sims (1996): pl. 141, fig. 12; Witkowski et al. (1997)). As noted in Witkowski et al. (2010), *F. finmarchica* has a more lanceolate outline and a higher lineolae density of 35–40 in 10 µm, which is very difficult to resolve by LM. For the MHMPP specimens observed with LM, the valve outline is more broadly elliptic than drawings in the literature for *F. finmarchica*; the lineolae can be resolved and are 27 in 10 µm, matching data for *F. krammeri* and the SEM image from the SHW specimen shows an areolae density of 30 in 10 µm. Additionally, the undulations in the raphe of the SHW specimen (SEM) match the undulations in the images of specimens from San Francisco Bay (Witkowski et al. 2010). Further, the expansion of the raphe endings are more pronounced in *F. krammeri*, matching our specimens. Lastly, most images of *F. finmarchica* show a pronounced lanceolate outline. From these criteria, we place our specimens in *F. krammeri*. This species was previously reported and first described in San Francisco Bay by Witkowski et al. (2010) and was, as far as can be ascertained before this report, the only known locality for *F. krammeri*.

Notes

iNaturalist ID: 312508075, 323689358 (Fig. 18).

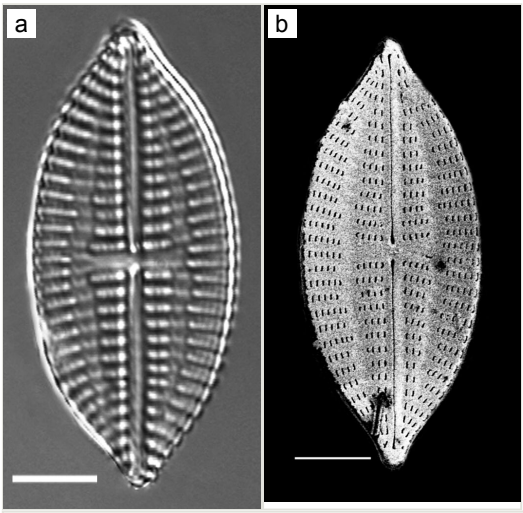

Figure 18.

Fogedia krammeri:

a: *Fogedia krammeri*, exterior valve view. LM. Scale bar: 5 µm;
b: *Fogedia krammeri*, exterior valve view. SEM. Scale bar: 5 µm.

Gomphonemopsis pseudexigua Medlin

Nomenclature

Gomphonemopsis pseudexigua Medlin and Round (1986): 212, figs. 16–18—Krzywda et al. (2019); Witkowski et al. (2000): 222, pl. 61, figs. 17, 18; Pienitz et al. (2003): 58, pl. 17, fig. 21.

Description

Valves linear to narrowly linear lanceolate, length 20.9–26.9 (6–40) µm, width 1.6–1.9 (1.5–5.0) µm. Striae 18–20 (11–22) in 10 µm, elongate to generally round at the poles, slightly parallel to slightly radiate at the apices. Narrow axial area, small rectangular or round central area that reaches the valve margin with a small stria lying in the mantle opposite either side of the central area.

Notes

The specimens from MHMPP fit well with the morphological summary of Krzywda et al. (2019). iNaturalist ID: 189577227. Mol. data: ERS27214058, ERS27214059, ERS27214060, ERS27214061, ERS27214062, ERS27214063, ERS27214064, ERS27214065, ERS27214066, ERS27214067, ERS27214068, ERS27214069, ERS27214070 (Fig. 19).

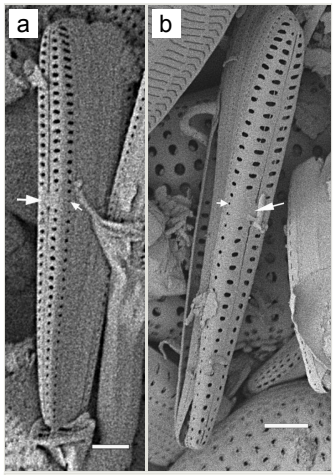

Figure 19.

Gomphonemopsis pseudexigua:

a: *Gomphonemopsis pseudoexigua*, exterior valve view. Large arrow indicates small rectangular central area that reaches the valve margin and small arrow shows the small stria. SEM. Scale bar: 2 µm;

b: *Gomphonemopsis pseudoexigua*, exterior valve view. Large arrow indicates small rectangular central area that reaches the valve margin and small arrow shows the small stria. SEM. Scale bar: 2.5 µm.

Gomphoseptatum aestuarii (Cleve) Medlin

Nomenclature

Gomphomena aestuarii Cleve (1893): 55, pl. 3, fig. 4.

Gomphoseptatum aestuarii—Medlin and Round (1986): 212, figs. 16–18; Witkowski et al. (2000): 222, pl. 61, figs. 17, 18; Pienitz et al. (2003): 58, pl. 17, fig. 21; Li et al. (2020).

Description

Valves linear with obtusely rounded apices, length 10.6–17.7 (9–35) µm, width 2.4–3.5 (2–4.5) µm. Raphe straight, external central endings expanded and relatively distant, axial area narrow. Distal raphe endings bent and slightly recurved in same direction at both apices. Central area transversely expanded into fascia that reaches valve margins. Distinctive pore field in foot pole. Well-developed pseudoseptum at foot pole. Transapical striae 16–20 (16–24) in 10 µm, slightly radiate to parallel at apices and punctate. Striae are crossed by longitudinal rib that runs midway between raphe and valve margin.

Notes

The morphology of *G. aestuarii* found on the red alga *S. americana* at Miners Bay Wharf conforms well to the original description and images in Medlin and Round (1986) for specimens from Oregon, USA and the morphometric data provided by Pienitz et al. (2003) for a specimen from Haida Gwaii, north of the Salish Sea. iNaturalist ID: 258910079 (Fig. 20).

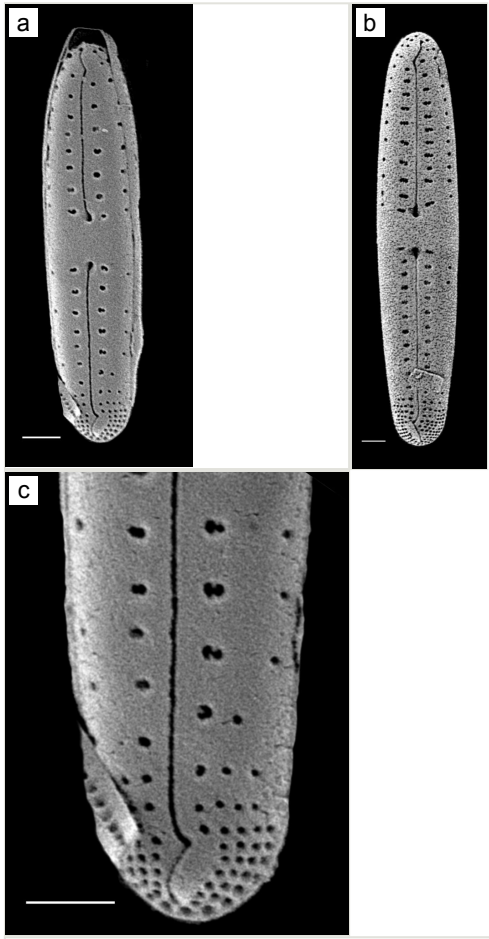

Figure 20.

Gomphoseptatum aestuaril:

a: *Gomphoseptatum aestuaril*, exterior valve view. SEM. Scale bar: 1 µm;
b: *Gomphoseptatum aestuaril*, exterior valve view. SEM. Scale bar: 1 µm;
c: *Gomphoseptatum aestuaril*, exterior valve view, foot pole. SEM. Scale bar: 1 µm.

Gomphoseptatum pseudoseptatum (Giffen) Witkowski, Lange-Bertalot & Metzeltin

Nomenclature

Gomphonema pseudoseptatum Giffen (1970): 13, figs. 29–32—Medlin and Round (1986): 476, 477.

Gomphoseptatum pseudoseptatum—Witkowski et al. (2000): 222, pl. 60, figs. 22–26; Guiry and Guiry (2025).

Description

Frustules in girdle view weakly clavate with distinctive pseudosepta on both apices. Valves linear to linear-lanceolate, gradually tapering from obtusely rounded head pole to slightly produced foot pole. Length 40.7–63.1 (12–33.3) µm, width 4.6–4.9 (2.5–5) µm. Raphe straight, axial area narrow. Central area has moderately wide transverse fascia that extend to margins. Externally, raphe is central, straight and opens slightly laterally. Central raphe endings slightly expanded; pore-like, polar (distal) fissures are bent, hook-like and curved to one side like a question mark, then curve back to centre of pole and are heavily silicified. Transapical striae uniseriate and mostly parallel, 8–9 (10–16) in 10 µm in mid-valve, 12 in 10 µm near poles. Striae crossed by rim of silica that runs around circumference of valve. Half of each stria subdivided into pores with cribra-like complex (30–80 nm pores), round to transapically slightly elongate. Striae towards each apex are reduced to smaller, single, round pores with the same cribra-like feature. Internally, pseudosepta are well-developed and equal-sized. Raphe internal endings straight. Pores closest to central area reduced in size and without marginal pore.

Diagnosis

Morphologically, the illustrations in Giffen (1970), an unpublished image by Giffen (image A1008Sa02: A. Witkowski pers. comm., 07-06-2023) and the description and images of *G. pseudoseptatum* in Witkowski et al. (2000) support placing the two specimens from Galiano Island into *Gomphoseptatum pseudoseptatum*.

Notes

iNaturalist ID: 258910629 (Fig. 21).

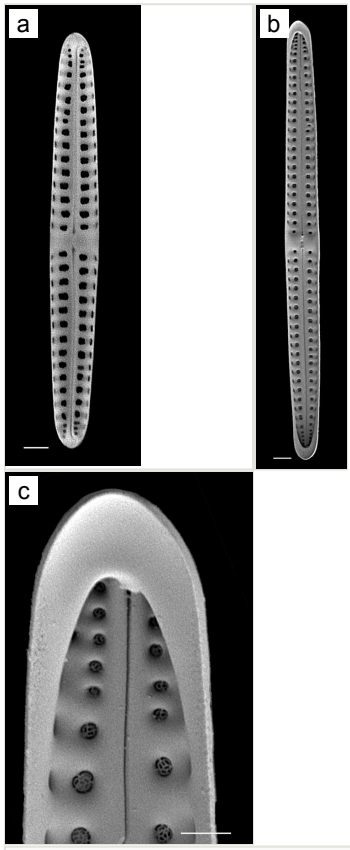

Figure 21.

Gomphoseptatum pseudoseptatum:

a: *Gomphoseptatum pseudoseptatum*, exterior valve view. SEM. Scale bar: 2 µm;
b: *Gomphoseptatum pseudoseptatum*, interior valve view. SEM. Scale bar: 1 µm;
c: *Gomphoseptatum pseudoseptatum*, interior valve view. SEM. Scale bar: 1 µm.

Gyrosigma arcuatum (Donkin) Sterrenburg

Nomenclature

Pleurosigma arcuatum Donkin (1858): 25, pl. 3, fig. 10.

Gyrosigma fasciola var. *arcuatum* (Donkin) Cleve (1894): 116 (as '*arcuata*')—Proshkina-Lavrenko (1950): 249, pl. 82, fig. 7; Jin et al. (1985): 80, pl. 24, fig. 188; Cardinal et al. (1989): 18, fig. 7; Stidolph (1994); Sims (1996): pl. 113, fig. 4; Jahn et al. (2005): 309.

Gyrosigma arcuatum—Jahn et al. (2005): 308.

Description

Distinguished by long, rostrate apices curving in opposite directions and sharply turned out from valve body. Valve distinctly sigmoid, lanceolate to elliptical-lanceolate in central portion, narrowing to long and thin extensions that are bluntly rounded or flattened.
Valve face fairly flat, length 100.9–105.0 (60–150) µm, width 10.6–14.3 (10–24) µm. Axial area and raphe central and sigmoid, appearing slightly eccentric in extensions of some valves. Central area quite small, orbicular or longitudinally elliptical. Central raphe endings slightly deflected to opposite sides. Longitudinal striae, 25–30 (27) in 10 µm and transverse striae, 24–30 in 10 µm, about equal and distinct. Two marginal, thin plastids, almost exactly opposite.

Notes

These three specimens of *Gyrosigma*, with long and narrow apical extensions of the valve and curved in opposite directions, are placed into *Gyrosigma arcuatum* (Donkin) Sterrenburg (Guiry and Guiry 2025), as recommended by Jahn et al. (2005). iNaturalist ID: 254241262, 255788398, 254242421 (Fig. 22).

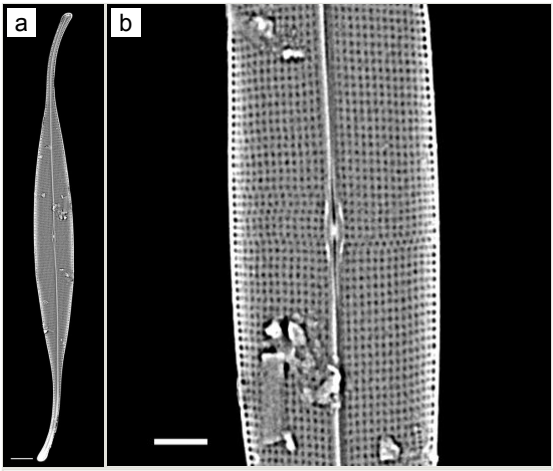

Figure 22.

Gyrosigma arcuatum:

a: *Gyrosigma arcuatum*, exterior valve view. SEM. Scale bar: 5 µm;

b: *Gyrosigma arcuatum*, central area. Exterior valve view. SEM. Scale bar: 2.5 µm.

Homoeocladia spathulatoides (Lobban, Ashworth, Calaor & E.C.Theriot) Lobban & Ashworth

Nomenclature

Nitzschia spathulatoides Lobban et al. (2019): 227, figs. 121–129—Lobban and Ashworth (2022): 5.

Homoeocladia spathulatoides (Lobban, Ashworth, Calaor & E.C.Theriot)—Lobban and Ashworth (2022).

Description

Valves lanceolate, rostrate, length 45.7 (110–125) µm, width ca. 7–8 (ca. 11) µm, generally lying in girdle view. Striae 46–48 (45) in 10 µm, comprising tiny puncta, transapically 68 (66) in 10 µm. Keel straight, central, with distinct spathulate extensions at apices. Fibulae 2–4 in 10 µm. Several rows of pores on the keel apex. Copulae reported with numerous pores arranged in short transapical striae. Plastids apparently two plates against girdle face.

Diagnosis

This specimen is assigned to *Homoeocladia spathulatoides* as it is morphologically distinct from *H. spathulata* (Syn: *N. spathulata*): a) the MHMPP specimen has striae with very small discrete pores vs. the long slits found in *N. spathulata*; b) there are pores over the apex and c) the striae are slightly less dense than *N. spathulata* (Lobban et al. 2019: 226).

Notes

iNaturalist ID: 193640716 (Fig. 23).

Isthmia enervis Ehrenberg

Nomenclature

Isthmia enervis Ehrenberg (1838): 209, pl. 16, fig. 6—Kützing (1844); Smith (1856): pl. 47, fig. F; Van Heurck (1881): XCVI, figs. 1–3; Hendey (1964): 110, 111, pl. XXV, fig. 3, pl. XXV, fig. 2; Round (1984); Round et al. (1990); Sims (1996); Guiry and Guiry (2025).

Description

Cells form branching colonies with large mucilage pads. Cells rhomboid-shaped, heteropolar. Valves elliptical and ovoid, apical axis 70 (48–200) µm, length of whole frustule in girdle view 195–268 (150–300) µm. No transition between valve face and

mantle. Single pseudocellus per cell, with cluster of smaller areolae. Externally, areolae are large, cribrate, suspended by struts, ovoid to quadrate and enclosed by robust silica. In the apical direction, every 2–3 areolae have a pore in the silica mesh framework; in the transapical direction, 1–2 areolae between poroids. Areolae pattern curved, slightly radiate transapically, 2–3 in 10 µm. Areolae size is mostly regular over valve face, becoming smaller at pseudocellus. Girdle bands complete, with smaller areolae than valve and closed by cribra.

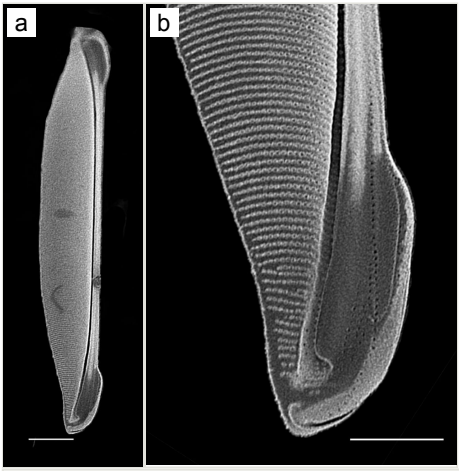

Figure 23.

Homoeocladia spathulatoides:

a: *Homoeocladia spathulatoides*, exterior valve view. SEM. Scale bar: 5 µm;
b: *Homoeocladia spathulatoides*, apex. Exterior valve view. SEM. Scale bar: 2.5 µm.

Notes

iNaturalist ID: 204882487 (Fig. 24).

Licmophora cf. *communis* (Heiberg) Grunow

Nomenclature

Podosphenia communis Heiberg (1863): 76, pl. 6, fig. 23—Guiry and Guiry (2025).

Licmophora communis—Grunow 1881: pl. 48, figs. 8, 9, in Van Heurck (1881); Proshkina-Lavrenko (1950); Van der Werff and Huls (1975): P.A.D. X b. 66; Honeywill (1998): 238, fig. 5a–i; Snoeijs (1993): 65, pl. 51; *Sims (1996)*: 260, pl. 122, figs. 3, 4; Witkowski et al. (2000): 63, pl. 20, fig. 1; Plinski and Witkowski (2020): 57, 246, fig. 221; Romagnoli et al. (2014).

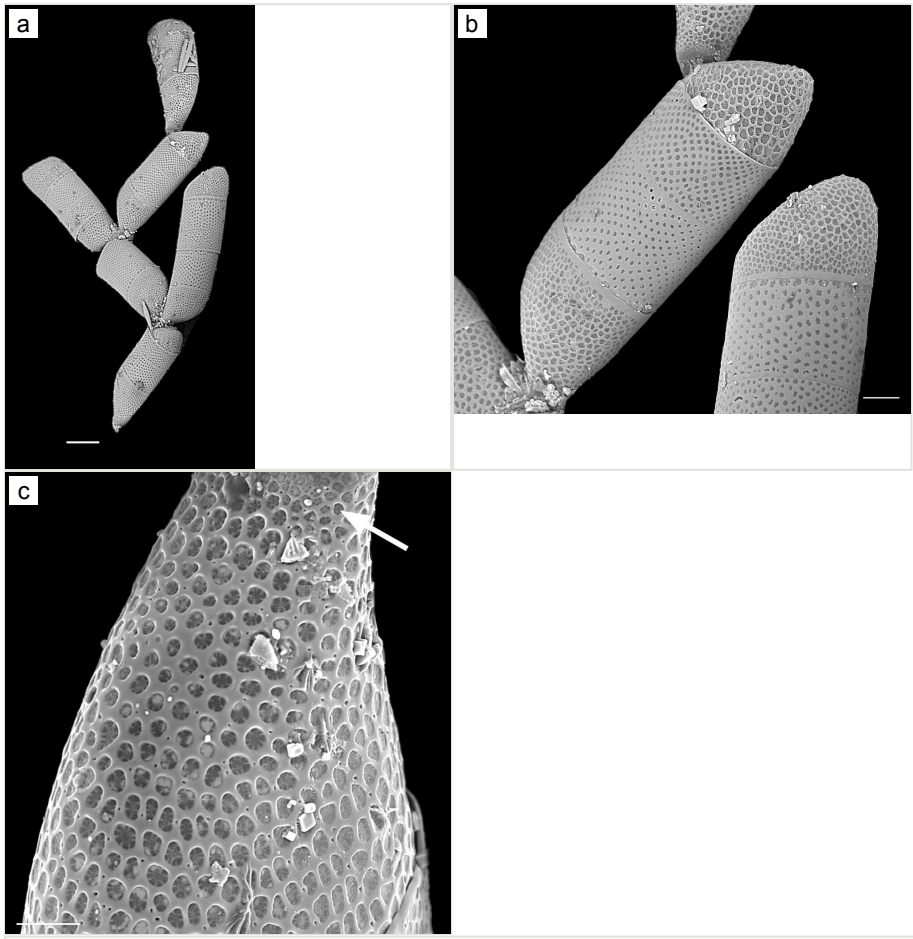

Figure 24.

Isthmia enervis:

a: *Isthmia enervis*, girdle view. SEM. Scale bar: 50 µm;
b: *Isthmia enervis*, girdle and valve views. SEM. Scale bar: 20 µm;
c: *Isthmia enervis*, girdle and valve views. Arrow indicates a gradual reduction in areolae size in the pseudocellus. SEM. Scale bar: 10 µm.

Description

Cells in girdle view wedge-shaped with strongly rounded corners, septa mostly long, rarely fairly short. Valves clavate, head pole broadly rounded, 17.7 (20–60) µm long, 5 (6–15) µm broad. Sternum (very) distinct, transapical striae (robust), 25–30 (11–17) in 10 µm near foot pole to 30–35 (23–30) in 10 µm at head pole. Areolae 50 in 10 µm. Rimoportula at head pole with short stalk.

Diagnosis

For now, this single valve from Galiano Island will be assigned to *Licmophora* cf. *communis* until more specimens are imaged, even though this specimen fits well with the published data.

Notes

iNaturalist ID: 263351671 (Fig. 25).

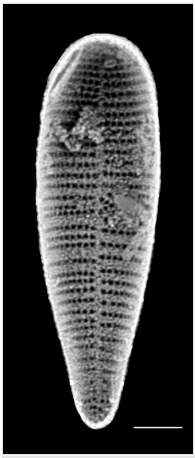

Figure 25.

Licmophora cf. *communis*, interior valve view. SEM. Scale bar: 2 µm.

Licmophora tincta (C.Agardh) Grunow

Nomenclature

Licmophora tincta Agardh (1828): 32 (no measurements given)—Grunow (1868): 35; Proshkina-Lavrenko (1950): 20, pl. 6, fig. 11a, b; Hendey (1964): 168; *Sims (1996)*: pl. 123, fig. 3; Honeywill (1998): 239.

Licmophora paradoxa var. *tincta* (Agardh) Hustedt (1931): 77, fig. 607—Guiry and Guiry (2025).

Description

Wedge-shaped cells in girdle view with wide round head pole. Valves clavate with broadly rounded poles; valve margin slightly concave near foot pole. Septa distinctly deep. Length 66.0–90.2 (30–140) µm, width 8.5–12.5 (7–18) µm, sternum distinct. Transapical striae fine, 29–34 (27–30) in 10 µm at head pole, 26–30 (23–32) in 10 µm at foot pole, 26–29 striae in 10 µm in mid-valve. Transapical areolae 50 in 10 µm, elongate near sternum (elongate to round). Two rimoportulae per cell (Honeywill

1998). Basal rimoportula has very short stalk and wide internal lips. Multiscissura has 14–15 (10) slits.

Diagnosis

Due to the high striae count at both poles, we assigned this specimen to *Licmophora tincta* (C.Agardh) Grunow, syn. *Licmophora paradoxa* var. *tincta* (Agardh) Hustedt. *Licmophora tincta* is very similar to *L. paradoxa*; however, this specimen has more striae at 33 in 10 µm (Proshkina-Lavrenko (1950): 20, pl. 6, fig. 11a, b).

Notes

Licmorphora paradoxa (Lyngbye) C. Agardh was previously reported by Shim (1976) in the Strait of Georgia, Salish Sea. iNaturalist ID: 195808793 (Fig. 26).

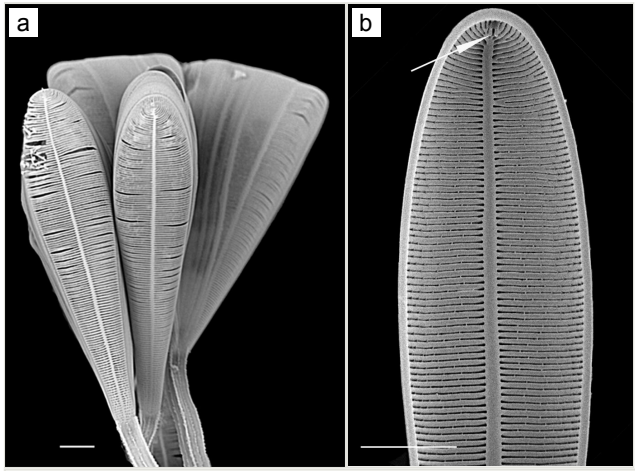

Figure 26.

Licmophora tincta:

a: *Licmophora tincta*, exterior valve view. SEM. Scale bar: 5 µm;
b: *Licmophora tincta*, interior valve view. Arrow indicates rimoportula. SEM. Scale bar: 5 µm.

Minidiscus proschkinae (Makarova) J.S.Park & J.H.Lee

Nomenclature

Thalassiosira proschkinae Makarova et al. (1979): 922, pl. 1, figs. 1–7—Snoeijs (1993): 113, pl. 99; Hasle and Syvertsen (1997): 84, table 14, pl. 13; Hoppenrath et al. (2007): 59, fig. 24e.

Minidiscus proschkinae—Park et al. (2017); Li et al. (2020); Guiry and Guiry (2025).

Description

Forms chains of 2–3 cells, linked by mucilage thread extruded from central fultoportula. Cells circular with flattened valve face or slightly convex, with sharp-angled mantle. Diameter 11.7 (3–11.5) µm. Single rimoportula located on valve surface adjacent to central fultoportula, both without external tubes and with a single areola in between. Areolae in tangential rows, 30–35 (25–30) in 10 µm, at valve centre. Marginal fultoportula processes (MFPs), without external tubes, 6 (6–8) closely spaced, 5 (1.24–1.91 µm) separation, processes 2.75 in 10 µm.

Diagnosis

The external rimoportula and central fultoportula, both without external tubes and close together, the MFPs without external tubes and the unique ornamentation of the valve surface place this specimen in *Minidiscus proschkinae*. Our molecular data from Trincomali Channel and plankton from Miners Bay Wharf, Mayne Island, support the presence of *Minidiscus proschkinae*.

Notes

Previously identified in Haida Gwaii, BC, by Pienitz et al. (2003). iNaturalist ID: 260112129 (Fig. 27).

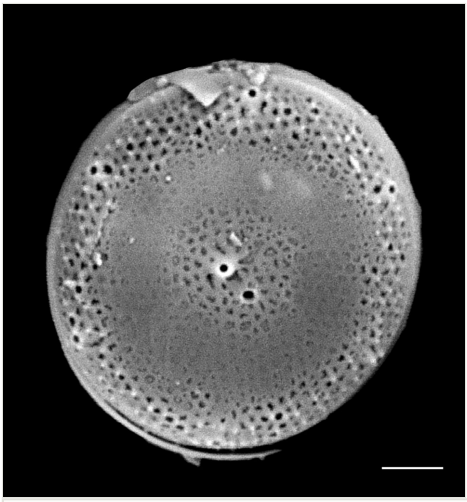

Figure 27.

Minidiscus proschkinae, exterior valve view. SEM. Scale bar: 2 µm.

Neocalyptrella robusta (G.Norman ex Ralfs) Hernández-Becerril & Meave

Nomenclature

Rhizosolenia robusta Ralfs 1861: 866, pl. VIII, fig. 42, in Pritchard (1861)—Cupp (1943).

Neocalyptrella robusta—Hernández-Becerril and Meave del Castillo (1996); Hernández-Becerril and Maeve del Castillo (1997): 329; Hasle and Syvertsen (1997); Sunesen and Sar (2007); Hoppenrath et al. (2009); Yun and Lee (2011); Boonprakob et al. (2021); Guiry and Guiry (2025).

Description

Cells in valvar cross section elliptical; cells in girdle view sigmoid, curved and crescent-shaped. Length 227–240 (in culture) to 477 (500–1000) µm, diameter 59 (109, in culture) (40–400) µm. Valves noticeably conical, with longitudinal undulations converging near truncated apex. Valve apex has calyptra, which bears a needle-like external tube or process that is a complex rimportula. Valve areolae 13–20 in 10 µm arranged in regular, straight striations and with secondary quincunx pattern of 22–25 in 10 µm.

Notes

The morphology of these LM images agrees with literature, especially the images and description in Sunesen and Sar (2007). Only observed in December. Rare in Galiano Island waters. iNaturalist ID: 48460936 (Fig. 28).

Parlibellus delognei ellipticus (Lobban) E.J.Cox

Nomenclature

Parlibellus delognei f. *ellipticus* (Lobban)—Cox (1988): 21.

Description

Parlibellus delognei f. *ellipticus* (Lobban) E.J.Cox is more elliptical-rhomboid-shaped and lacks occasional puncta (carinoportula) in central area compared to the typical form. Length 45.4–62.8 (42–50) µm, width 12.7–19.4 (13–17) µm, striae 20–23 (19–20) in 10 µm, areolae 24 in 10 µm.

Notes

Naturalist ID: 256411671. Mol. data: ERS27214058, ERS27214059, ERS27214060, ERS27214061, ERS27214062, ERS27214063, ERS27214064, ERS27214065, ERS27214066, ERS27214067, ERS27214068, ERS27214069, ERS27214070,

ERS21395346, ERS21395352, ERS21395359, ERS21395365, ERS21395369, ERS27630064, ERS21395356, ERS27217975, ERS27218291, ERS27218292, ERS27218293, ERS27218294, ERS27218295, ERS27218296, ERS27218297, ERS27218298 (Fig. 29).

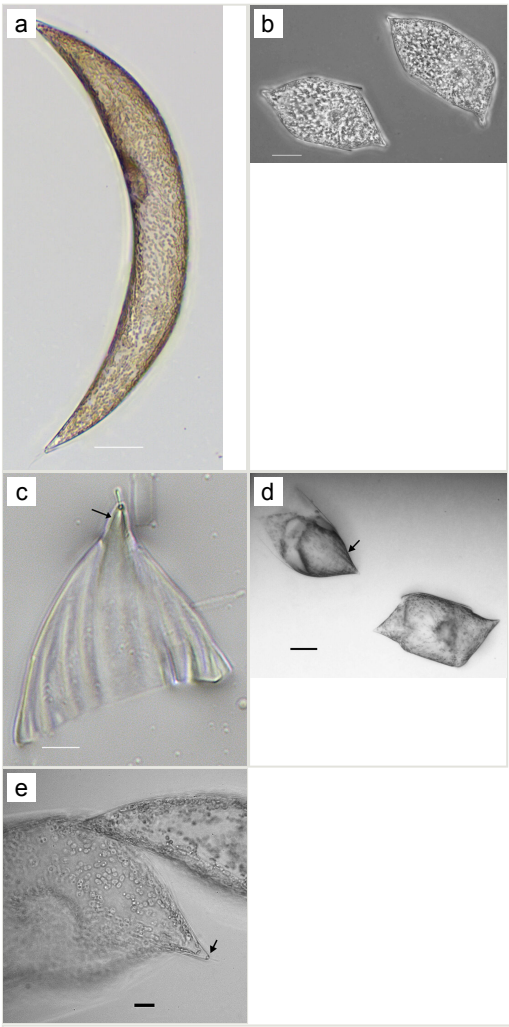

Figure 28.

Neocalyptrella robusta:

a: *Neocalyptrella robusta*, live, girdle view. LM. Scale bar: 50 µm;
b: *Neocalyptrella robusta*, live, in culture. LM. Girdle view. Scale bar: 50 µm;
c: *Neocalyptrella robusta*, LM, girdle view. Arrow indicates calyptra. LM. Scale bar: 20 µm;

d: *Neocalyptrella robusta*, clones. Girdle view. Large arrow indicates longitudinal undulations converging on apex. LM. Scale bar: 50 µm;
e: *Neocalyptrella robusta*, clones. Girdle view. Arrow indicates calyptra. LM. Scale bar: 10 µm.

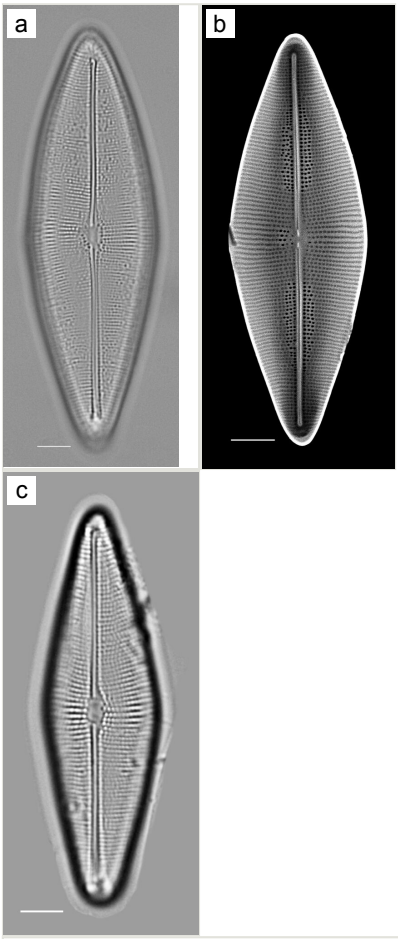

Figure 29.

Parlibellus delognei f. *ellipticus*:

a: *Parlibellus delognei* f. *ellipticus*, LM exterior valve view. LM. Scale bar: 5 µm;
b: *Parlibellus delognei* f. *ellipticus*, interior valve view. SEM. Scale bar: 5 µm;
c: *Parlibellus delognei* f. *ellipticus*, LM, exterior valve view. LM. Scale bar: 5 µm.

Proschkinia complanatula (Hustedt ex Simonsen) D.G.Mann

Nomenclature

Amphora complanata Grunow 1867: 25—Van der Werff and Huls (1975): P.D G XVI. 109; Guiry and Guiry (2025).

Navicula complanatula Hustedt ex Simonsen (1987): 479, pl. 735, figs. 1–10.

Proschkinia complanatula—Mann 1990: 675, in Round et al. (1990): 596, 597; Majewska et al. (2019); Kim et al. (2020): 10–12, fig. 4; Plinski and Witkowski (2020): 115, 324, fig. 576.

Description

Cells solitary, usually positioned in girdle view, rectangular with rounded corners and with numerous, moderately broad bands, 9 (7–8) in 10 µm. Valves lanceolate, slightly arched, with acutely rounded apices, length 64.7 (30–58) µm, width 7.4 (5.5–8.0) µm. Raphe straight and linear with proximal ends close and distal ends strongly hooked. Transapical uniseriate striae parallel at centre, 18 (12–17) in 10 µm, becoming slightly convergent and denser near apices, 22 (17–20) in 10 µm. Central area asymmetric with striae more distant than towards the apices, producing a stauros-like structure. Fistula located in central area on primary side of valve.

Notes

iNaturalist ID: 188679253 (Fig. 30).

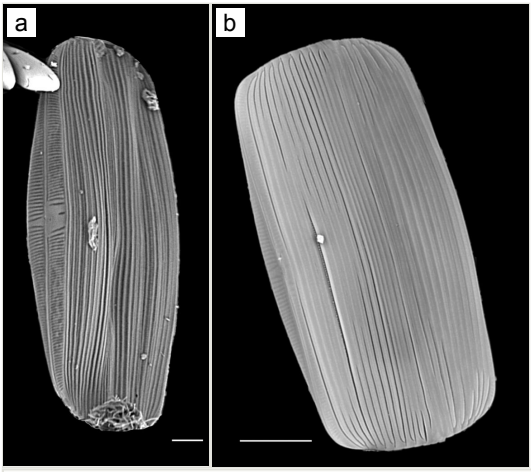

Figure 30.

Proschkinia complanatula:

a: *Proschkinia complanatula*, girdle and valve views. SEM. Scale bar: 5 µm;
b: *Proschkinia complanatula*, girdle view. SEM. Scale bar: 10 µm.

Seminavis robusta D.B.Danielidis & D.G.Mann

Nomenclature

Seminavis robusta Danielidis and Mann (2002): 440, figs. 39–53—Wachnicka and Gaiser (2007); Kaleli et al. (2023).

Description

Valves strongly dorsiventral, frustules semi-lanceolate to rhombic-lanceolate, ends more or less obtusely rounded. Length 61.5 (34–104) µm, width 11.5 (6.5–13.5) µm. Margins convex dorsal with straight to slightly convex ventral margins. On dorsal side, axial area more expanded and rounded than on ventral side. Longitudinal raphe straight and displaced to ventral side. Externally, central raphe branches are slightly deflected ventrally and proximal raphe ends are deflected ventrally at apices. Dorsal striae slightly radiate in middle, 14 (12–20.7) in 10 µm and slightly denser 18 (15–18) in 10 µm at apices. Ventral striae at centre 14 (11–15) in 10 µm and at ends 17 (12–18). Middle striae are shorter than the others. Solitary cells.

Notes

This specimen from Retreat Cove conforms well with descriptions and data in literature. However, this specimen differs slightly from the description of Danielidis and Mann (2002) by having slightly radiate striae at the apices. iNaturalist ID: 263684273. Mol. data: ERS27214058, ERS27214059, ERS27214060, ERS27214061, ERS27214062, ERS27214063, ERS27214064, ERS27214065, ERS27214066, ERS27214067, ERS27214068, ERS27214069, ERS27214070, ERS21395352, ERS21395356, ERS21395359, ERS21395369, ERS21395365 (Fig. 31).

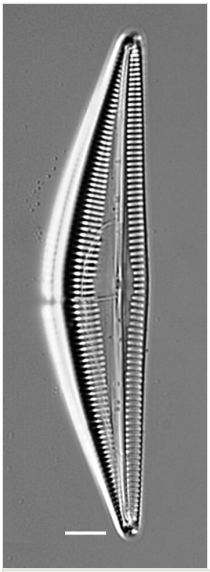

Figure 31.

Seminavis robusta, LM, valve view. LM. Scale bar: 5 µm.

Shionodiscus endoseriatus (Hasle & Fryxell) Alverson, Kang & Theriot

Nomenclature

Thalassiosira endoseriata Fryxell and Hasle (1977): 78, pl. 8, figs. 45–49—Fryxell and Hasle (1980); Rivera Ramírez (1981): 68, figs. 145–157; Mahood et al. (1986): 146, fig. 91; Hasle and Syvertsen (1997): 81, 82, pl. 13; Guiry and Guiry (2025).

Shionodiscus endoseriatus—Alverson et al. (2006); Wilks and Armand (2017).

Description

Diameter 30.0–54.1 (20–60) µm. Valve face flat or slightly convex. Irregular ring of 8–10 (4–14) central fultoportulae. Rimoportula is 7 (6) areolae from the margin towards centre of valve. Areolae usually fasciculate, 8–12 (11–18) in 10 µm at valve centre. MFP 6–8 (5–6) in 10 µm and extending into interior of frustule.

Notes

Specimens from the Strait of Georgia conform well with the published data. iNaturalist ID: 259613928 (Fig. 32).

Shionodiscus frenguelliopsis (Fryxell & Johansen) Alverson, Kang & Theriot

Nomenclature

Thalassiosira frenguelliopsis Johansen and Fryxell (1985): 168, figs. 6, 67, 68, 71, 81—Sar et al. (2002): 378, 379, figs. 2–6, table 3; Guiry and Guiry (2025).

Shionodiscus frenguelliopsis—Alverson et al. (2006): 259; Wilks and Armand (2017): tables 2, 11.

Description

Valves circular and flat, diameter 18.2 (12–34) µm, no external projections of processes. Areolae pattern on valve face irregularly eccentric to irregularly linear. Striae 28–30 (24–30) in 10 µm, areolae 20–22 (12–26) in 10 µm from centre towards mantle and 24 (18–20) near mantle. One (1) sub-central fultoportula off-centre and operculate. Rimoportula is between margin and centre, transverse (radial), 6–7 (5.8–8) areolae from the sub-central process. Ten MFPs are long and extend out internally, 3 in 10 µm, 10–11 areolae between MFPs, 4.1–5.5 (5–10) µm apart.

Notes

The morphometric data of this specimen are sufficient to place it as *S. frenguelliopsis*. iNaturalist ID: 301822368 (Fig. 33).

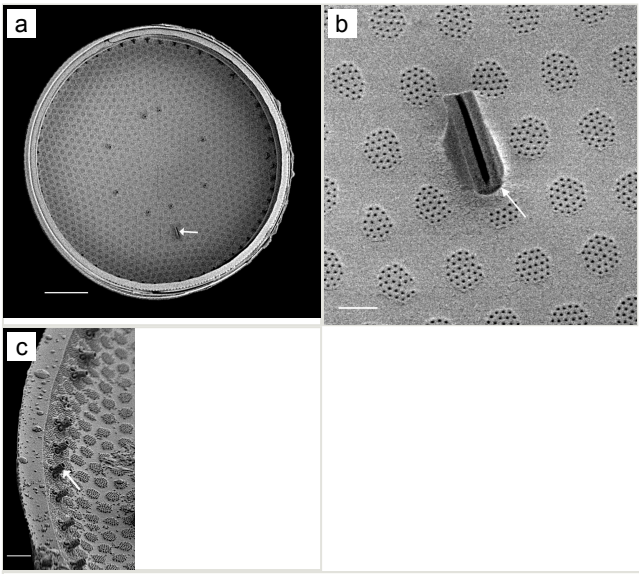

Figure 32.

Shionodiscus endoseriatus:

a: *Shionodiscus endoseriatus*, interior valve view. Arrow indicates rimoportula. SEM. Scale bar: 5 µm;

b: *Shionodiscus endoseriatus*, interior valve view. Arrow indicates rimoportula orientated radially, taking the place of an areola arranged in a radial row. SEM. Scale bar: 0.5 µm;

c: *Shionodiscus endoseriatus*, interior valve view. Arrow shows the marginal strutted processes extending into the interior. SEM. Scale bar: 1 µm.

Shionodiscus karianus Georgiev & Gololobova

Nomenclature

Shionodiscus karianus *Georgiev and Gololobova (2022)*.

Description

Valves circular and heavily silicified, diameter 30.8 (26–54) µm, no external projections of processes. Areolae pattern on valve face curved in tangential rows or in sectors of radial or sub-radial rows. Striae 10 in 10 µm, areolae 7 (7–11) in 10 µm from centre towards mantle and 8 (8–13) near mantle zone. Areolae loculate with internal domed cribra, slightly elevated relative to surrounding *hyaline* area, 6–7 (10–16) cribrum pores in 1 µm. One (1) central fultoportula process (CFP), operculate with

4 (4) satellite struts, 4 (4) pores with cowlings. Rimoportula radially orientated and located 1 (0–2) areolae, 1.2 µm (1.3–3.4) µm distance, from CFP. Four (4) marginal fultoportula processes (MFP), strutted, have 4 satellite pores, 15 (13–35) per valve. MFP internally long, more or less evenly placed around valve margin, 1.6 (1.5–2.4) in 10 µm, 4–6 (2–7) areolae between processes and 1.7–2.8 (2.7–6.5) µm apart.

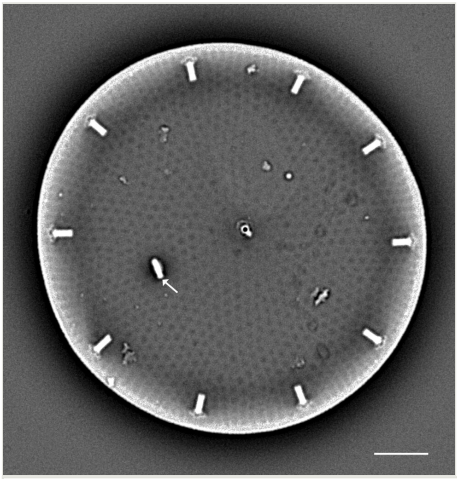

Figure 33.

Shionodiscus frenguelliopsis, interior valve view. Arrow indicates location of the rimoportula. SEM. Scale Bar: 2.5 µm.

Diagnosis

External valves, girdle band images and external valve ultrastructural details are lacking at this time. The *Shionodiscus* species closest to this specimen are *S. bioculatus*, *S. bioculatus* var. *exiguus*, *S. biporus*, *S. centrus*, *S. gaarderae* and *S. variantius*. All have an operculate CFP with a rimoportula that is located nearby or midway between the valve margin and CFP. All of the above species have areolae densities that are over double that of the SHW specimen. Only *S. bioculatus* and *S. gaarderae* have a rimoportula that is immediately adjacent to a central areola; however, the separation is more than 1 areolae distant, valve areolae density is too high, at 16–23 in 10 µm and MFP are 5–7 µm apart (Hasle and Syvertsen (1997): table 14, Ferrario et al. (2018): table 1, Georgiev and Gololobova (2022): table 2). Although *S. bioculatus* has been previously reported in the Salish Sea, the morphometric data of this SHW specimen are more than adequate to place it as *Shionodiscus karianus*.

Notes

iNaturalist ID: 322791476 (Fig. 34).

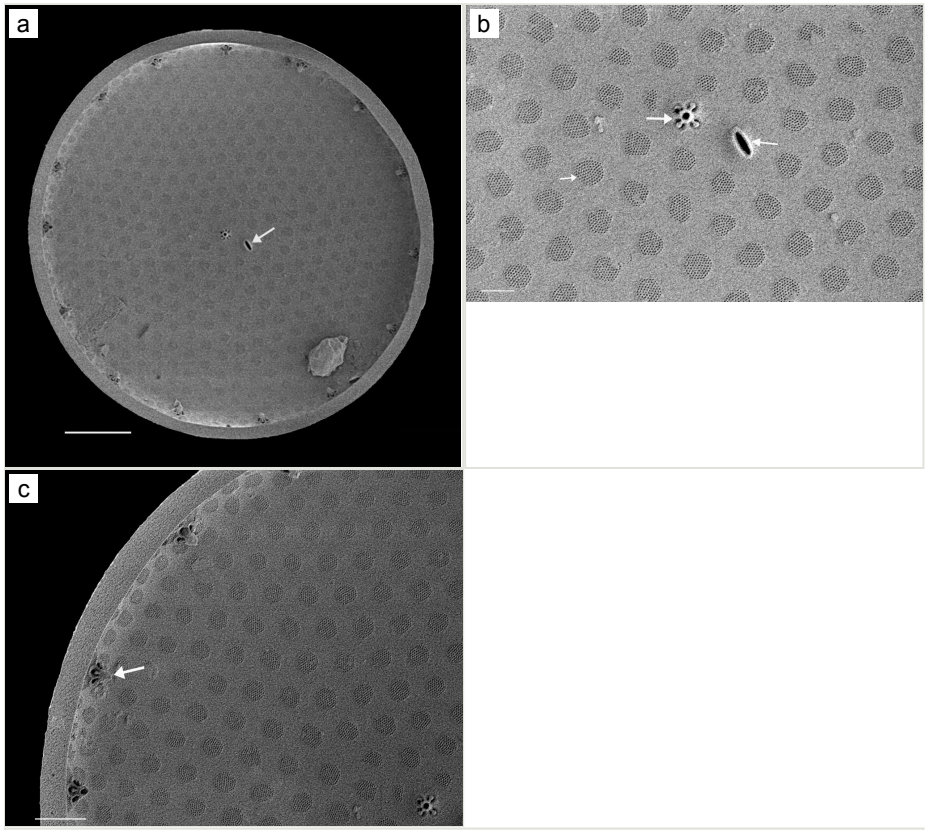

Figure 34.

Shionodiscus karianus:

a: *Shionodiscus karianus*, interior valve view. Arrow indicates location of the rimoportula. SEM. Scale Bar: 5 µm;

b: *Shionodiscus karianus*, central interior valve view. Arrows indicate, in decreasing size, the location of: the operculate central fultoportula (CFP), rimoportula and cribrate areolae. SEM. Scale Bar: 1 µm;

c: *Shionodiscus karianus*, interior valve view. Arrow indicates a marginal process that extends internally. SEM. Scale Bar: 2 µm.

Shionodiscus oestrupii (Ostenfeld) A.J.Alverson, S.-H.Kang & E.C.Theriot

Nomenclature

Coscinosira oestrupii Ostenfeld (1900): 52—Fryxell and Hasle (1980); Hasle and Syvertsen (1997): 81, 82, pl. 13.

Shionodiscus oestrupii—Alverson et al. (2006): 258; Wilks and Armand (2017); Guiry and Guiry (2025).

Description

Diameter 21.7–23.9 (7–60) µm, pervalvar axis half to twice the diameter. Valve face flat or slightly convex. Mantle low and rounded. Areolae usually larger in central part of valve than closer to the margin, sometimes in sublinear array. One nearly central strutted fultoportula. Rimoportulae is 3–4 areolae from central process. Areolae 9 (6–12) in 10 µm at valve centre. MFPs 3–4 in 10 µm, 0.96–1.1 (0.8–1.9) µm between MFPs.

Notes

iNaturalist ID:142951511, 142950297 (Fig. 35).

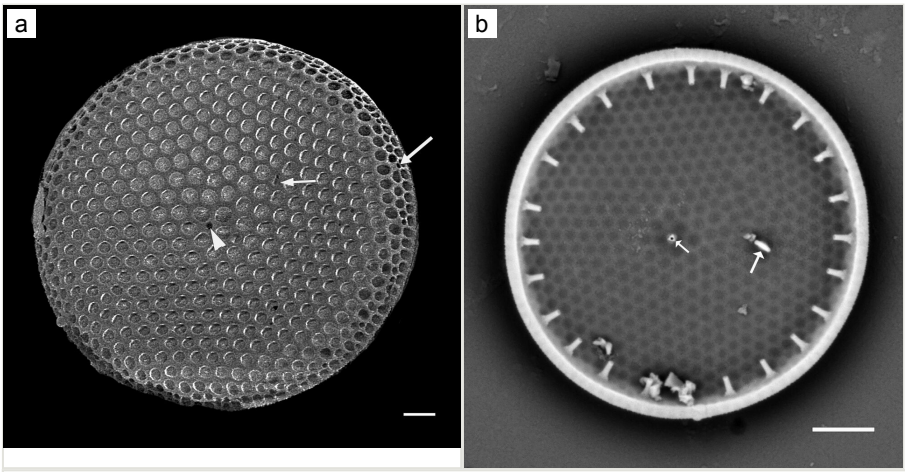

Figure 35.

Shionodiscus oestrupii:

a: *Shionodiscus oestrupii*, exterior valve view. Shortest arrow is location of the central process; medium arrow is the location of the exit hole of labiate process; longest arrow is exit hole of a marginal process. SEM. Scale Bar: 2.0 µm;
b: *Shionodiscus oestrupii*. internal valve view. Small arrow shows the central fultoportula and larger arrow is the rimoportula. Note: MFPs extend internally and not externally. SEM. Scale bar: 2 µm.

Sundstroemia pungens (A.Cleve) Medlin, Lundholm, Boonprakob & Moestrup

Nomenclature

Rhizosolenia pungens *Cleve-Euler (1937)*: 43, fig. 10—Hasle and Syvertsen (1997): 157; Bérard-Therriault et al. (1987); Bérard-Therriault et al. (1999): 37, pl. 21g, m; Hoppenrath et al. (2009): 63, fig. 27a–c; Yun and Lee (2011): 142–145: fig. 1A–F.

Sundstroemia pungens—Medlin et al. (2021): 242; Boonprakob et al. (2021): 162–164, figs. 106–118; Guiry and Guiry (2025).

Description

Cells solitary and narrow, diameter 16.0 (4–20) µm, length up to 213.2 (150–589) µm without processes, process length (85–276) µm. Valves conical. External processes long, almost straight and needle-like. Basal part of process narrow, abruptly swollen for about half its length, narrow again and gently tapering towards tip. Otarium absent. Girdle composed of segments in two dorsiventral columns. Numerous chloroplasts.

Diagnosis

Very similar in morphology to *Sundstroemia setigera*. However, the narrow basal section, then a swollen zone of the process in *S. pungens* (seen in LM and SEM), differentiates it from *S. setigera*, which has a long and continuously shaped narrow process.

Notes

Sundstroemia pungens is found in the plankton throughout most of the year, but more frequently observed in the Trincomali Channel and Porlier Pass in September and October. A small bloom of *S. setigera* occurred at SHW on 21 July 2025. iNaturalist ID: 259931970, 315872333. Mol. data: SRS969492, SRS966492 (Fig. 36).

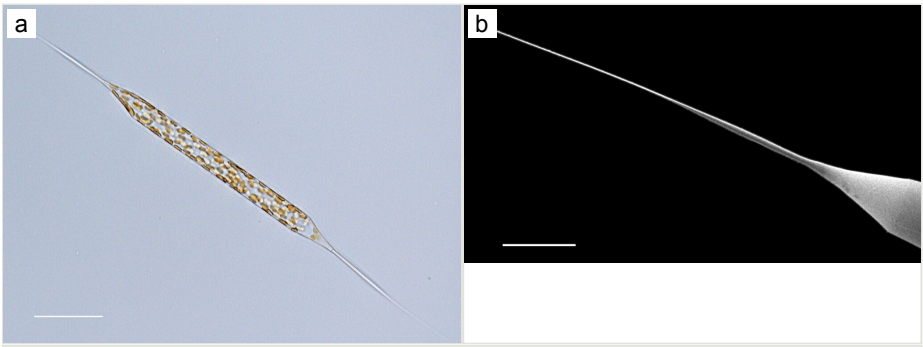

Figure 36.

Sundstroemia pungens:

a: *Sundstroemia pungens*, live cell, girdle view. LM. Scale bar: 50 µm;
b: *Sundstroemia pungens*, valve and a distinctive process abruptly swollen for about half its length. SEM. Scale bar: 20 µm.

Tabellaria cf. *quadriseptata* B.M.Knudson

Nomenclature

Tabellaria quadriseptata Knudson (1952): 436, figs. I–N—Patrick and Reimer (1966): 105, pl. 1, fig. 3; Flower and Battarbee (1985); Sims (1996): pl. 284, figs. 6, 7; Plinski and Witkowski (2020): 56, fig. 212.

Description

Colonies of zigzag filaments, linked together at corners by mucilage pads. Valve median and apical inflations approximately same width. Apical inflations not distinctly capitate as in *Tabellaria fenestrata*. Axial area narrow. Valves linear with parallel margins between inflated area and poles. Length 70.7 (23–130) µm, width 5.7 (6–9) µm. Septa straight and few, usually four. Single rimoportula located adjacent to axial area at edge of central inflation, at base of valve shaft or periphery of median inflation. Striae density 14 (13–20) in 10 µm. Marginal spines short, length up to 1 µm, with equal distribution.

Diagnosis

The morphometric data of the MBW specimen fit the descriptions in literature for *T. quadriseptata*: approximately the same width for median and apical inflations (5.7 and 4.7 µm, respectively), parallel margins, location of the rimoportula and the presence of relatively equally spaced spines along the margins. However, currently there are no images of the septa, so the specimen is assigned *T.* cf. *quadriseptata*.

Notes

iNaturalist ID: 259219380 (Fig. 37).

Thalassiosira allenii H.Takano

Nomenclature

Thalassiosira allenii Takano (1965): 4, pl. 1: figs. 9–11, pl. 2: fig. 1—Hasle (1978a); Hasle and Syvertsen (1997): 51, table 7, pl. 4; Jameson and Hallegraeff (2010): 57, fig. 2.18B, C; Li et al. (2013): 85, 86, figs. 2–5; Hernández-Becerril et al. (2015); Park et al. (2016); Efimova et al. (2023).

Description

Valve diameter 17.2 (5–20) µm. Areolae on valve face 22–24 (18–28) in 10 µm in fasciculate pattern, with smaller areolae 30–40 in 10 µm on narrow valve mantle. Central, non-prominent, central process (fultoportula) located next to one, two or three larger areolae. Valve may be covered by minute granules (not observed). Marginal

processes long and coarse, 6 (5–9) in 10 µm. External rimoportula, single and prominent, takes place of and is occasionally very slightly inside of the ring of marginal strutted process. Mantle narrow, oblique and angled, 5 (2–3) areolae wide.

Diagnosis

Thalassiosira allenii differs from *T. nordenskioeldii* in that the former has a lower mantle in girdle view, a higher areolae density on the valve face and mantle, marginal processes that are closer together and have no collars, processes that are stouter and mantle areolae that are smaller than those in *T. nordenskioeldii*.

Notes

iNaturalist ID: 259835781 (Fig. 38).

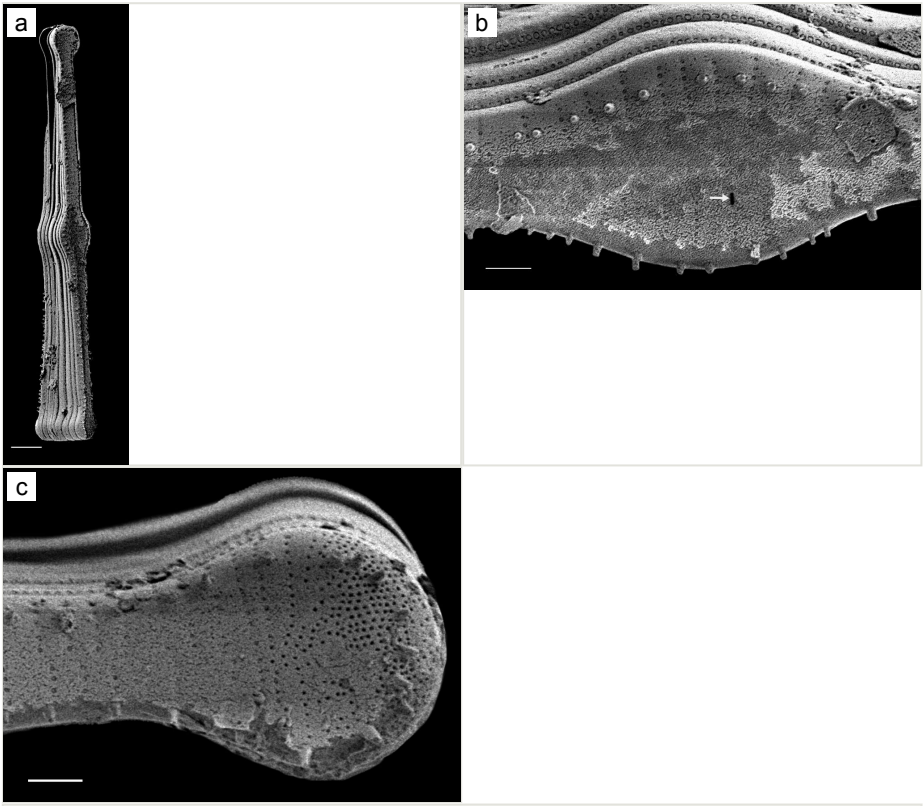

Figure 37.

Tabellaria cf. *quadriseptata*:

a: *Tabellaria* cf. *quadriseptata*, external girdle and valve views. SEM. Scale bar: 5 µm;
b: *Tabellaria* cf. *quadriseptata*, external valve view. Inflated central area, arrow shows external opening of the rimoportula. SEM. Scale bar: 1 µm;
c: *Tabellaria* cf. *quadriseptata*, valve view, external apical pore field. SEM. Scale bar: 1 µm.

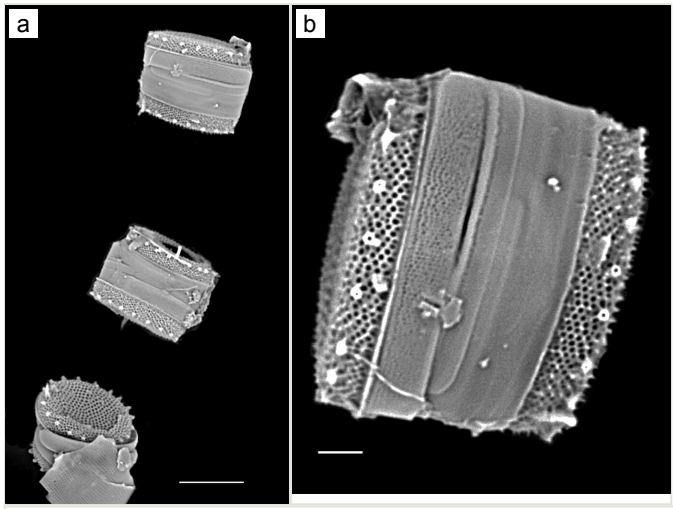

Figure 38.

Thalassiosira allenii:

a: *Thalassiosira allenii*, girdle and valve views. SEM. Scale bar: 10 µm;
b: *Thalassiosira allenii*, girdle view. SEM. Scale bar: 2 µm.

Thalassiosira curviseriata Takano

Nomenclature

Thalassiosira curviseriata Takano (1983): 32—Hallegraeff (1984); Hasle and Syvertsen (1997); Hoppenrath et al. (2007); Li et al. (2014); Park et al. (2016).

Description

Cells discoid, diameter 13.1 (5–14) µm. Valve face flat with central concavity. Areolae in radial rows, siliceous granules all over valve surface, occasional silicious spinules on surface. One sub-central strutted process. Central process adjacent to a more or less off-centred annulus. One marginal ring of five conspicuous winged strutted processes, two wings per process opposed into two or three branches. Marginal processes 2–3 (2–3) in 10 µm, 5.1–5.9 µm apart.

Notes

This specimen conforms with morphometric data from Hallegraeff (1984), Hasle and Syvertsen (1997), Hoppenrath et al. (2007), Li et al. (2014) and Park et al. (2016). Mol. Data: ENA:ERS27630061. iNaturalist ID: 142613095 (Fig. 39).

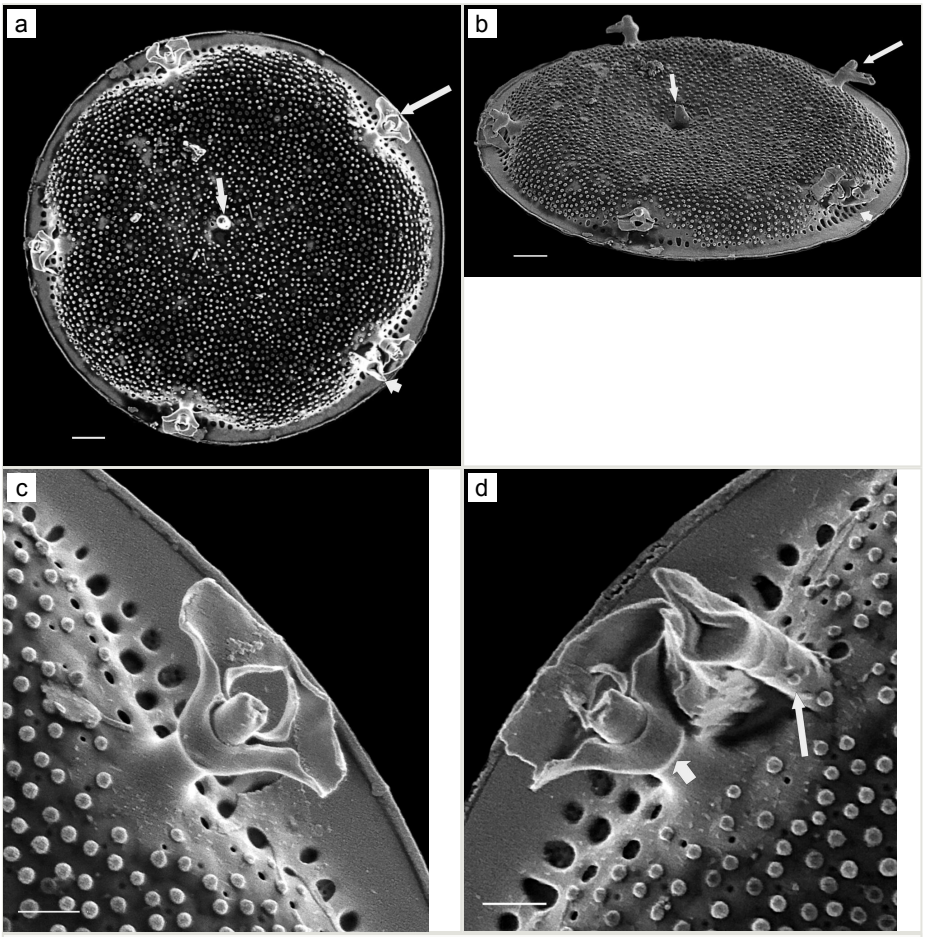

Figure 39.

Thalassiosira curviseriata:

a: *Thalassiosira curviseriata*, external valve view. Smallest arrow indicates the external rimoportula, mid-size arrow shows the central process and the largest arrow indicates a winged marginal process (MSP). SEM. Scale bar: 1 µm;

b: *Thalassiosira curviseriata*, external valve view of the distinctive winged MSP. SEM. Scale bar: 400 nm;

c: *Thalassiosira curviseriata*, external valve view, image of a winged MSP next to the external rimoportula, oblique angle. SEM. Scale bar: 1 µm;

d: *Thalassiosira curviseriata*, external valve view, image of central process (1), annulus (2) and (3) long spinules. SEM. Scale bar: 400 nm.

Thalassiosira minima Gaarder

Nomenclature

Thalassiosira minima Gaarder (1951): 31, fig. 18—Hasle (1980): 167, figs. 1–17; Rivera Ramírez (1981): 90–94, pl. 36–38; figs. 226–245; Harris et al. (1995): 119, table 1, fig. 14; Hasle and Syvertsen (1997): 65, table 9; Bérard-Therriault et al. (1999): 25, 26, pl. 11g–f; Li et al. (2014): 388, figs. 50–54.

Description

Valve diameter 9.9 (5–15) µm. Valve face flat and slightly depressed in the centre; mantle low and bevelled. Two central processes. Areolae arranged in radial or fasciculate rows and decrease slightly in size (increase in density) from 28 (22–40) in 10 µm near centre to 32 (30–50) in 10 µm towards valve margin. Normally two (2) fultoportulae, seldom one or three, present near valve centre and always surrounded by several larger areolae. MFPs, 4 (4–5) in 10 µm, each bearing external tube and keeping one areola inside from a small siliceous granule. One marginal rimoportula, with long external tube, included in MFPs.

Notes

iNaturalist ID: 259931970 (Fig. 40).

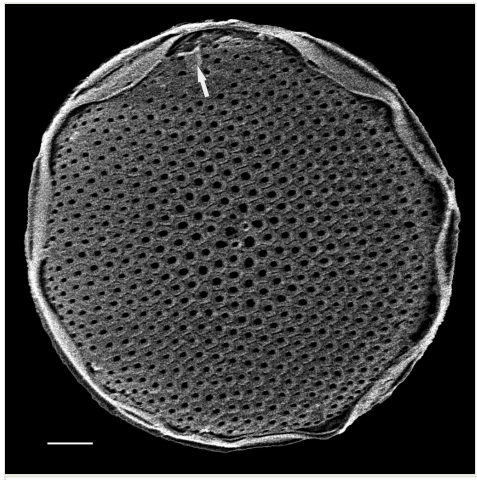

Figure 40.

Thalassiosira minima, external valve view. Arrow indicates location of the rimoportulae. SEM. Scale bar: 1 µm.

Thalassiosira oceanica Hasle

Nomenclature

Thalassiosira oceanica Hasle (1983): 220, table 1, figs. 1–18—Harris et al. (1995): 121, figs. 8, 26; Hasle and Syvertsen (1997): 56, 57, table 7; Bérard-Therriault et al. (1999): 26, pl. 11d; Hoppenrath et al. (2007): 59, fig. 24a; Li et al. (2014): 390, fig. 62.

Description

Cells rectangular in girdle view, pervalvar axis slightly shorter than cell diameter 6.8–7.3 (3.0–12.0) µm. Valve has fine ornamentation of silicious radial ribs and poroidal areolation, 50–60 (40–60) areolae in 10 µm. Valve has undulating marginal ridge. One central strutted process, located slightly sub-central. Single marginal ring of 4–6 (3–8) relatively widely spaced strutted processes in 10 µm without external tubes, 2 µm apart. One labiate process close to one marginal strutted process. Valve rim has ribs.

Notes

The morphometric data of this specimen fit the description in literature and is supported by molecular data. iNaturalist ID: 259589003. Mol. data: SRS968559, SRS964086, SRS966570, SRS1690317, SRS966764, SRS969492, SRS968562, SRS966566, SRS968542, SRS966614, SRS967659, SRS968132, SRS964211, SRS966901 (Fig. 41).

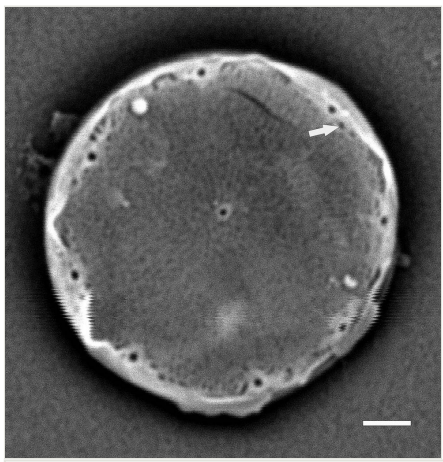

Figure 41.

Thalassiosira oceanica, external valve view. Arrow shows location of rimoportula adjacent to an external marginal process. SEM. Scale bar: 1 µm.

Thalassiosira cf. *visurgis* Hustedt

Nomenclature

Thalassiosira visurgis Hustedt (1957): 207, pl. 1: figs 1-4—Simonsen (1987): 439, pl. 657, figs. 1–9; Hasle (1978b): 263, 264, figs. 1–4; Mahood et al. (1986): 138, figs. 56–61, 95, 96; Aké-Castillo et al. (1999): 497, figs. 45, 46; Li et al. (2013): 104, 105, figs. 126–128.

Description

Valve face flat, concave or convex; diameter 14.0 (12.5–18.0) µm. Areolae arranged in linear or eccentric lines, 10 (12–15) in 10 µm on valve face, 28–32 (17–20) in 10 µm on mantle. One fultoportula present in centre close to large areola. Valve margin characterised by ring of disorganised fultoportulae, 4–5 (4–10) in 10 µm and distinctly short and dentate external tubes. Two rimoportulae with external tubes having variable length and smooth openings, separated 120°–180° apart, located on opposite sides and slightly inside ring of marginal fultoportulae, with each rimoportula taking the place of a fultoportula. Valve mantle ornamented with ribbed rim. Fine silicious granules on valve extend to margin.

Diagnosis

Some variability in morphological characters exists within specimens identified as *T. visurgis* in literature. The number and position of MFSs in the Galiano Island specimen are similar to those described by Hasle (1978b) and Li et al. (2013), but dissimilar to those observed in Mahood et al. (1986). The MHMPP specimen has both a pronounced ribbed margin and two slightly larger external tubes (indicated by arrows in Fig. 42) that are presumably rimoportulae with smooth openings, as they are in the correct position, but that are shorter than described in literature, with the exception of fig. 3a in Hasle (1978b). The major difference between the MHMPP specimen and literature describing *T. visurgis* is the organisation of the marginal processes. If we compare *T. visurgis*, as described in Hasle (1978b), Mahood et al. (1986) and Li et al. (2013), with *T. elsayedii* (Fryxell 1975), the latter species has the following characteristics: 1) areolae appear smaller, but are similar in density, at 9–11 in 10 µm; 2) external processes have spines; 3) the number of striations (ribbed margin) are more numerous and 4) Fryxell (1975) makes no mention of granulation on the valve surface, nor do granules appear in her images. Thus, *T. elsayedii* is similar to *T. visurgis* in having two labiate processes on opposite sides of the valve, but is dissimilar in four other characteristics. The MHMPP specimen is unlikely to be *T. baltica*, which has 2–9 central strutted processes. However, the marginal process patterning in *T. baltica* is clearly in two rows, which is somewhat similar to the MHMPP specimen. Until we study more material, we will consider the MHMPP specimen to be *T.* cf. *visurgis*, as it fits most closely with descriptions in literature.

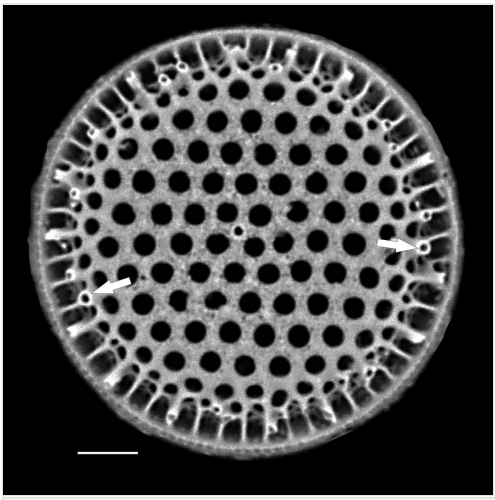

Figure 42.

Thalassiosira cf. *visurgis*, external valve view, arrows indicate the locations of the two rimoportula. SEM. Scale bar: 2 µm.

Notes

iNaturalist ID: 260003450 (Fig. 42).

Trigonium quinquelobatum (Greville) A.Mann

Nomenclature

Triceratium quinquelobatum Greville (1866): 83, pl. IX, fig. 21—Tempère and Peragallo (1908): pl. 104, fig. 2; Mann (1925): 171; Hustedt (1930b): 820, fig. 482.

Trigonium quinquelobatum—Mann (1925): 171.

Trigonium arcticum var. *quinquelobatum* (Greville) Desikachary and Ranjitha (1986): 7, pl. 68, fig. 4; Guiry and Guiry (2025).

Description

Valve pentagonal in outline and thickly silicified. Length between adjacent and slightly non-equidistant corners 96.7–118.6 (61) µm. Convex sides. Areolae coarsely polygonal, many hexagonal, arranged in radiating and decussating rows, 2–6 (2–6) in 10 µm in mid-valve and finer approaching corners. Areolae 4–6 in 10 µm approaching pseudocelli immediately transition to tri- to bi-lobed pores 12–13 in 10 µm, then 16–19 in 10 µm into the slightly elevated pseudocelli. Some lines of areolae discontinuous from margin. Areolae flattened and occluded by a silica layer (vela), usually 2.3–5 µm wide, with distinct papilla in middle of many areola (only observed

with LM) and ring of 5–13 (average 9) small, round pores formed by attachment spokes (rotae). Central sub-circular areola surrounded by rosette of 7–9 slightly smaller areolae, often elliptically-elongated. Externally, exit holes of rimoportulae round and inconspicuous, with 12–17 small protuberances scattered in centre of valve face. Internally, rimoportulae equally small and stalkless with tiny slits, occasionally with multiple openings. Unraised pores scattered across external and internal surfaces, round to oval, connected to loculate chambers. Narrow septum of valve wall occurs at each corner. Mantle deep, steep and vertical. Girdle deep with closed bands containing transverse rows of seven areolae in 10 µm. Silica nodules and short spines occur along edge of valvocopula.

Diagnosis

The genera *Trigonium* and *Triceratium* are in desperate need of revision. AlgaeBase (Guiry and Guiry 2025) lists occurrences of *Trigonium quinquelobatum* from the Philippines (Mann 1925), Colombia (Lozano-Duque et al. 2010) and Korea (Lee et al. 1995). The original description is a fossil from a deposit in Spain (Greville (1866): 83, pl. IX: fig. 21) that conforms well with our pentagonal specimens found in Porlier Pass. AlgaeBase notes a report from Cuba (Foged (1984); no mention of *T. quinquelobatum*, yet a different genus, *Triceratium pentacrinus*, is illustrated in pl. 23, figs. 3, 4). The genus *Trigonium* is readily separated from *Triceratium*, as the former has pseudocelli and the latter has true ocelli that have a distinctive silica ring around the pore field (Ashworth et al. 2013). *Triceratium formosum* Brightwell (Brightwell (1856): 274, pl. 17, fig. 8) is not a *Triceratium*, since it lacks true ocelli and is quadrangular in outline. *Triceratium formosum* f. *quinquelobata* (Hustedt (1930b): 819, 820, fig. 482), as Hustedt notes, is likely synonymous with the above-described *T. quinquelobatum* (Greville 1866). Unlike in the triangular- and quadrangular-shaped *Trigonium arcticum* and var. *quadratum* found in Salish Sea waters, *T. quinquelobatum* has a distinctive papilla (seen with LM), possibly due to the size and shape of the foramina in the centre of most areolae, a characteristic noted by Mann (1925), who designated the pentagonal form as a separate species. Additionally, *T. quinquelobatum* has a central areola surrounded by 7–9 slightly smaller areolae, giving the appearance of a spiral rosette. No silica granules were observed around the areolae, as is commonly found on *Trigonium arcticum* and var. *quadratum*.

Notes

Trigonium quinquelobatum is rare in Salish Sea waters, so far found only once on a leafy red alga at depth in Porlier Pass, near Dionisio Point, Galiano Island. iNaturalist ID: 259931970, 300280287 (Fig. 43 and Fig. 44).

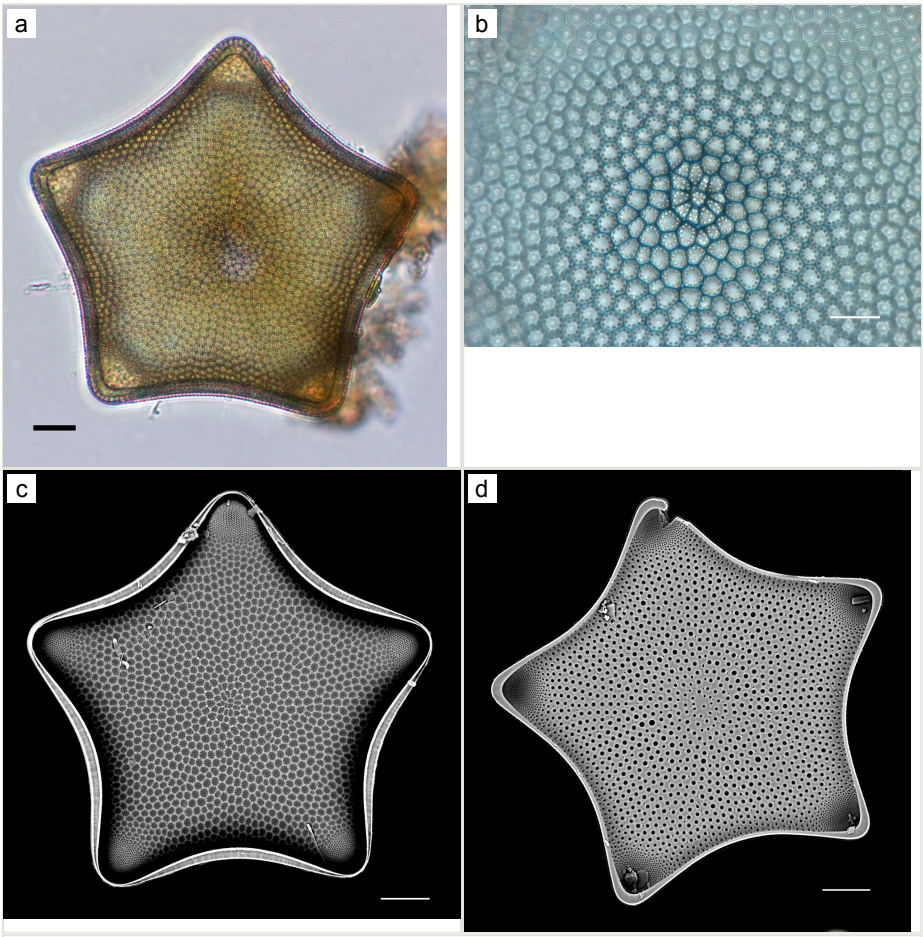

Figure 43.

Trigonium quinquelobatum:

a: *Trigonium quinquelobatum*, live cell, valve view. LM. Scale bar: 20 µm;
b: *Trigonium quinquelobatum*, external valve, cleaned cell, with distinctive central areolae rosette. Stack of five images in polarised light. LM. Scale bar: 10 µm;
c: *Trigonium quinquelobatum*, external valve view. SEM. Scale bar: 20 µm;
d: *Trigonium quinquelobatum*, internal valve view. SEM. Scale bar: 10 µm.

Analysis

Through systematic review of literature and synthesis of existing data, including morphological and molecular data from our sampling, we report 924 diatom species/ infrataxa for the Salish Sea. These reports represent three classes, 13 subclasses, 40 orders, 80 families and 207 genera, which together reflect a broad range of morphological diversity (Fig. 45). Of these records, 42 constitute novel reports of taxa that were previously unreported for the region (Table 3). In total, we synthesised 11,469

records, of which 9,049 were resolved to genus, species or infrataxon (Suppl. material 8), in alignment with the names reported in the annotated checklist (Suppl. material 1).

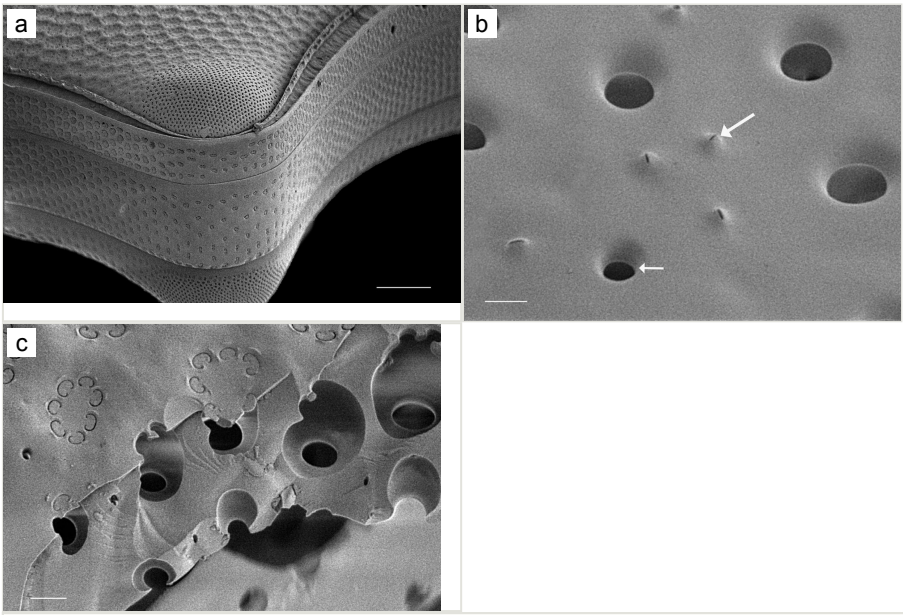

Figure 44.

Trigonium quinquelobatum:

a: *Trigonium quinquelobatum*, external valve and girdle views. Large pseudocellus and girdle bands of an intact cell, partial cleaning. SEM. Scale bar: 15 µm;
b: *Trigonium quinquelobatum*, internal valve, small arrow indicates the central areolae, larger arrow shows one of the stalkless rimoportulae. SEM. Scale bar: 1 µm;
c: *Trigonium quinquelobatum*, cross-section of the valve showing the cribra and loculate chambers of a semi-cleaned frustule. SEM. Scale bar: 1 µm.

Discussion

This work establishes a baseline record of diatom diversity reported for the Salish Sea. Drawing on historical records dating from the 1860s to present, together with existing collections and our recent taxonomic and molecular analysis of plankton, eelgrass, macroalgae, benthic and epipsammic samples, we have added 42 species (including six new genera) to the regional record, bringing the total to 924 taxa. Supporting this work are 31 amplicon sequence libraries now publicly accessible via the European Nucleotide Archive (ENA accession: PRJEB102646) and a small set of Sanger sequence data (ENA accession: ERZ29258993). Together, these resources form the foundation for an ongoing effort involving both community and academic research scientists to document and validate the regional diatom diversity.

Table 3.

New reports for the Salish Sea (2011–2026). Locations: Chivers Point (CP), Wallace Island; Departure Bay (DB), Nanaimo; Dionisio Reefs (DR), Porlier Pass; Strait of Georgia, east Galiano Island, offshore (SGE-B); Dionisio Point (DP), Galiano Island (Hulq'umi'num: *quelus*); Lochside Waterfront Park (LWP), Sidney, Vancouver Island; Miners Bay Wharf (MBW), Mayne Island; Montague Harbour Marine Provincial Park (MHMPP), Galiano Island (Hulq'umi'num: *sumnuw*); North Saltery Bay (NSB), Galiano Island; Porlier Pass (PP); Quadra Island, beach in front of Hakai Institute labs (Q45); Retreat Cove (RC), Galiano Island (Hulq'umi'num: *xetthecum*; Sidney Channel (SC); Spanish Hills Wharf (SHW); Trincomali Channel (TC); Sturdies Bay (SB), Galiano Island. Vouchers at Webber Lab (WL) are identified as light microscope (LM) slides and scanning electron microscope (SEM) stubs.

Taxon	**Location**	**Voucher**
Achnanthes groenlandica var. *meridiana* Giffen	DR, MHMPP	WL-SEM-108; WL-SEM-109; WL-SEM-110
Actinoptychus adriaticus var. *pumila* Grunow	CP	WL-SEM-90
Andrzeja fenestrata Mayama & Kryk	LWPMHMPP	WL-SEM-3-1; WL-SEM-60-3
Attheya longicornis R.M.Crawford & C.Gardner	SHW	WL-SEM-113
Bacteriastrum hyalinum Lauder	PP	WL-LM-51
Bacterosira cf. *constricta* (Gaarder) J.S.Park & J.H.Lee	SHW	WL-SEM-9
Campylodiscus bicostatus W.Smith ex Roper	MHMPP	WL-LM-42
Cocconeis costata var. *hexagona* Grunow	Q45, SB	WL-LM-24; WL-SEM-75
Cocconeis kerguelensis P.Petit	SHW	WL-LM-26
Cocconeis notata P.Petit	SHW	WL-LM-20
Cocconeis pseudomarginata var. *intermedia* Grunow	RC	WL-SEM-77
Cocconeis scutellum var. *posidoniae* M.De Stefano, D.Marino & L.Mazzella	MHMPP	WL-LM-37
Cyclotella baltica (Grunow) Håkansson	SHW	WL-SEM-91
Didymosphenia geminata (Lyngbye) Mart.Schmidt	PP	WL-LM-46
Diploneis exemta (A.W.F.Schmidt) Cleve	SHW	WL-SEM-92
Extubocellulus spinifer (Hargreaves & Guillard) Hasle, Stosch & Syvertsen	NSB	WL-SEM-93
Fogedia krammeri Witkowski, Lange-Bertalot, Kociolek & M.Kulikovskiy	MHMPP, SHW	WL-LM-43; WL-SEM-94
Gomphonemopsis pseudexigua Medlin	SHW	WL-SEM-118
Gomphoseptatum aestuarii (Cleve) Medlin	MBW	WL-SEM-103
Gomphoseptatum pseudoseptatum (Giffen) Witkowski, Lange-Bertalot & Metzeltin	MHMPP	WL-SEM-107
Gyrosigma arcuatum (Donkin) Sterrenburg	MHMPP, RC, SB	WL-SEM-3; WL-SEM-37; WL-SEM-116
Homoeocladia spathulatoides (Lobban, Ashworth, Calaor & E.C.Theriot) Lobban & Ashworth	MHMPP	WL-SEM-66

Taxon	Location	Voucher
Isthmia enervis Ehrenberg	SC	WL-SEM-6
Licmophora cf. *communis* (Heiberg) Grunow	RC	WL-SEM-96
Licmophora tincta (C.Agardh) Grunow	SHW	WL-SEM-89
Minidiscus proschkinae (Makarova) J.S.Park & J.H.Lee	CP	WL-SEM-97
Neocalyptrella robusta (G.Norman ex Ralfs) Hernández-Becerril & Meave	SHW	WL-LM-50; WL-SEM-66-7
Parlibellus delognei f. *ellipticus* (Lobban) E.J.Cox	MHMPP, RC	WL-LM-29; WL-SEM-16
Proschkinia complanatula (Hustedt ex Simonsen) D.G.Mann	MHMPP	WL-SEM-105
Seminavis robusta D.B.Danielidis & D.G.Mann	RC	WL-LM-44
Shionodiscus endoseriatus Hasle & Fryxell) Alverson, Kang et Theriot	SGE-B	WL-SEM-72
Shionodiscus frenguelliopsis (Fryxell & Johansen) Alverson, Kang & Theriot	DB	WL-SEM-106
Shionodiscus karianus Georgiev & Gololobova	SHW	WL-SEM-111
Shionodiscus oestrupii (Ostenfeld) A.J.Alverson, S.-H.Kang & E.C.Theriot	RC, SGE-B	WL-SEM-18; WL-SEM-71
Sundstroemia pungens (A.Cleve) Medlin, Lundholm, Boonprakob & Moestrup	PP	WL-LM-45
Tabellaria quadriseptata B.M.Knudson	MBW	WL-SEM-74
Thalassiosira allenii H.Takano	MHMPP, PP	WL-SEM-63
Thalassiosira curviseriata Takano	MHMPP	WL-SEM-44
Thalassiosira minima Gaarder	MHMPP, NSB	WL-SEM-99; WL-SEM-100
Thalassiosira oceanica Hasle	PP	WL-SEM-65
Thalassiosira cf. *visurgis* Hustedt	MHMPP	WL-SEM-99
Trigonium quinquelobatum (Greville) A.Mann	DR	WL-LM-47; WL-SEM-102

This comprehensive baseline creates new opportunities for future work in the Salish Sea, such as investigations of regional and global diatom biogeography (e.g. Mazur-Marzec et al. 2024, Williams 2025), assessments of human-mediated dispersal events (Villac et al. 2017), broader ecological studies including the marine microbiome (e.g. Mazur-Marzec et al. 2024, Jackman et al. 2025) and long-term monitoring of environmental change (e.g. Bopp et al. 2005, Edwards et al. 2022). These potential applications underline the value of a well-resolved regional inventory for addressing persistent shortfalls in biodiversity knowledge (Hortal et al. 2015).

Notable reports include taxa previously unreported for the Pacific coast of North America (e.g. *Trigonium quinquelobatum*) and those previously known only from warmer waters, such as *Cocconeis kerguelensis* (Indian Ocean), *Isthmia enervis* and *Neocalyptrella robusta* (California). As we resolve a clearer picture of the regional diversity, taxonomic gaps are also becoming apparent: *Trigonium*, *Triceratium*, *Hyalodiscus*, small-celled araphids and the substantial undescribed diversity within *Cocconeis*, all emerge as clear

priorities for future taxonomic work. Ecological patterns have also emerged: for example, *Tabularia*, a species-poor, yet abundant genus, stands out as a dominant component of epiphytic assemblages on eelgrass and macroalgae (Jackman et al. 2025). In contrast, genera such as *Auliscus*, *Biddulphia* and *Mastogloia*, are species-poor and rare in the Salish Sea despite being more diverse and widespread elsewhere, raising questions about the factors limiting their regional occurrence.

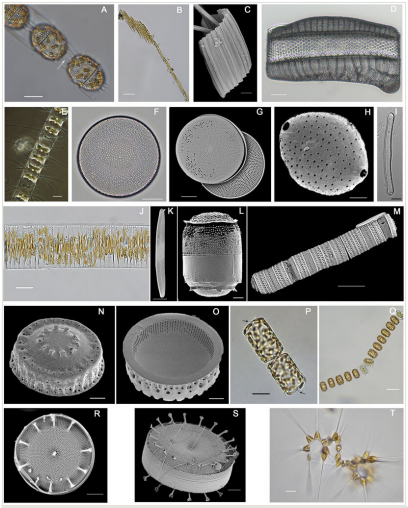

Figure 45.

Examples of diatoms (by subclass) found within the Salish Sea. **A** Archaegladiopsophycidae: *Stephanopyxis niponnica*. Girdle view. Arrow shows a continuous process between cells. LM. iNat: 45809431; **B** Bacillariophycidae: *Bacillaria paxillifera*. Live. Girdle view. LM. iNat: 192871056; **C** *Bacillaria paxillifera*. Girdle view and partial valve view. SEM. iNat: 192871056; **D** Biddulphiophycidae: *Isthmia nervosa*. Girdle and valve views. LM. iNat: 194751473, 5197632; **E** Chaetocerotophycidae: *Chaetoceros didymus*. Live. Girdle view. LM. iNat. 4849241; **F** Coscinodiscophycidae: *Coscinodiscus radiatus*. Exterior valve view. LM, cleaned. iNat: 40703800; **G** *Coscinodiscus radiatus*. Exterior and interior valve views. SEM. iNat: 40702227; **H** Cymatosirophycidae: *Extubocellulus spinifer*. Exterior valve view. SEM. iNat: 311561542; **I** Eunotiophycidae: *Eunotia formica*. Valve view. LM, cleaned. iNat: 316197977; **J** Fragilariophycidae: *Fragilaria striatula*. Exterior girdle view. LM. iNat: 243251313; **K** *Fragilaria striatula*. Exterior valve view, single frustule, tilted. Arrow indicates the exit hole of the single rimoportula. SEM. iNat: 243251313; **L** Melosirophycidae: *Melosira nummuloides*. Girdle view. SEM. iNat: 205351626; **M** Paraliophycidae: *Paralia* cf. *sulcata*. Girdle view. SEM. iNat: 4873115, 189407891; **N** *Paralia sulcata*. Exterior valve view. iNat: 189407891; **O** *Paralia sulcata*. SEM. Interior valve view. iNat: 189407891; **P** Rhizosoleniophycidae: *Dactyliosolen fragilissimus*. Girdle view. Arrows indicate the location of the external process on each valve. LM. iNat: 50047033; **Q** Thalassiosirophycidae: *Thalassiosira nordenskioeldii*. Chain of cells. Girdle view. LM. iNat: 111064233; **R** *Thalassiosira nordenskioeldii*. Valve view. SEM. iNat: 143410067; **S** *Thalassiosira nordenskioeldii*. Girdle and valve views. SEM. iNat: 201221176; **T** Urneidophycidae: *Asterionellopsis glacialis*. Live. Girdle and valve views. LM. iNat: 111057760, 98753620. Scale bars: D = 50 µm; Q = 40 µm; B, J, T = 25 µm; A, E–G, I, M, P = 20 µm; C, K = 10 µm; R, S = 5 µm; L, N, O = 2 µm; H = 0.5 µm.

While our work showcases the contributions that community science can make to phycology (Bahls 2015), we acknowledge the many challenges that impede reliable diatom identification — challenges that have historically hindered professional and amateur diatomist alike. Looking back, we acknowledge the consequences of the Linnaean shortfall for the reliability of the historical record: as taxonomic knowledge has expanded over the last century, species concepts and diagnostic criteria have changed substantially, as well as the tools we use to study diatoms. Historical identifications should thus be interpreted with the appropriate discretion. Looking forward, we also recognise the implications of the Darwinian shortfall: given the inherent limitations of short-read metabarcoding and the incomplete availability of reference sequences, molecular identifications likewise warrant cautious interpretation.

Addressing these challenges today requires an integrated approach that combines molecular, morphological and culture-based techniques. Our results highlight the value of microscopy and cloning as complementary to environmental DNA, especially while marine diatom reference sequences remain under-represented in molecular databases (Hamsher et al. 2013, Chen et al. 2024, Mazur-Marzec et al. 2024, Jackman et al. 2025). Light microscopy remains essential for clarifying certain diagnostic features (e.g. partecta in *Mastogloia*), while SEM is indispensable for resolving ultrastructural traits, including areolae architecture and small rimoportulae that cannot be seen under LM (Li et al. 2018). Culture isolation and cloning yield the most reliable validation by enabling LM, SEM and molecular analyses to be performed on near-axenic and axenic material (Rad-Menéndez et al. 2015, Witkowski et al. 2016; Mönnich et al. 2020). However, establishing and maintaining cultures remains a major bottleneck; the work is time-consuming, technically demanding and constrained by limited personnel and resources. Access to authoritative diatom monographs, reference books and historical literature — much of it unavailable in digital form — has also proven crucial for accurate diatom identification.

As we sample a broader range of habitats, our integrative morphological and molecular approach continues to yield new records of small, taxonomically problematic and cryptic taxa, including the recently described *Andrzeja fenestrata*, as well as *Extubocellulus* sp., *Gedaniella* sp., *Opephora*-like and other small-celled raphids and araphids (Vaulot et al. 2008, Li et al. 2018, Pérez-Burillo et al. 2022, Jackman et al. 2025, Mayama et al. 2025). These findings demonstrate that community science can fill major data gaps through the generation of high-resolution datasets (Theobald et al. 2015, Chandler et al. 2017, Peter et al. 2021), highlighting its potential to play a more central role in the global research community (Simon et al. 2022). Although community science contributions to biodiversity monitoring have been valued at roughly US$2.5 billion annually (Theobald et al. 2015, Chandler et al. 2017), substantial geographic and taxonomic gaps remain and much of the data never reaches the peer-reviewed literature (Theobald et al. 2015, Chandler et al. 2017). Our study demonstrates how sustained collaboration between community scientists and research institutes can bridge these gaps by partnering community expertise and observation with access to microscopy and molecular technologies (Bahls 2015). Based on these early results, we anticipate that this approach will continue to

reveal overlooked diversity while strengthening the baseline record for phytoplankton monitoring in the Salish Sea.

Acknowledgements

We honour all Indigenous peoples who hold rights and responsibilities in the Salish Sea as the stewards of this rich biocultural region since time immemorial. Our many thanks go to the late Andrzej Witkowski of the University of Szczecin, Poland; Oscar Romero of the University of Bremen, Germany; Matt Ashworth of the University of Texas, USA; and Maria Gololobova and Anton Georgiev of the M.V. Lomonosov Moscow State University for their collaboration and assistance. We acknowledge Melanie Quenneville and Ron Read for helping with SEM imaging at the University of Victoria's Advanced Microscopy Facility; Emily Adamczyk, Andrea Jackman, Laura Parfrey and Siobhan Schenk (UBC Parfrey Lab) for providing valuable input and support with molecular sequencing; Kevin Fraser, Dan White and Ian Young for sampling trips on their boats; and Dave "Zeus" Cochrane, Jamie van Dam, Emily Greenan, Rafael Hoekstra, Laurel Jacobson, David Leehr, Henry Mcgee and Tieg Mowbray for their assistance with collecting samples and lab work. Thanks to Hitachi High-Technologies Canada Inc. for the loan of the tabletop TM4000Plus SEM to Elaine Humphrey. Lastly, we acknowledge Danja Currie-Olsen, Heather Earle, Kelly Fretwell, Tyrel Froese, Colleen Kellogg, Matt Lemay, Zach Monteith, Amelia Nimmon, Angeleen Olson and Carolyn Prentice from the Hakai Institute for supporting field and lab work during the 2023 Galiano BioBlitz. Finally, we thank our reviewers for their helpful suggestions, which greatly improved the quality of this work.

Author contributions

MW, AvA and AS sourced, entered, organised and curated data from the historical literature. MW, AvA, EH and AS collected samples and prepared and made slides and SEM stubs. MW, AvA and EH took LM and SEM images and processed/adjusted images for publication. MW and AvA collected samples for molecular analysis. EM and AS processed molecular samples and analysed molecular data. MW identified diatoms, including new reports and evaluated historical records. AS coded algorithms for aggregating and integrating species occurrence data into the annotated checklist; MW, AS and EM analysed and conducted quality control of the data. MW, AC, AS, AvA, EM and EH wrote and edited the paper.

References

- Adl S, Simpson AB, Farmer M, Andersen R, Anderson R, Barta J, Bowser S, Brugerolle G, Fensome R, Fredericq S, James T, Karpov S, Kugrens P, Krug J, Lane C, Lewis L, Lodge D, Lynn D, Mann D, McCourt R, Mendoza L, Moestrup Ø, Mozeley-Standridge S, Nerad T, Shearer C, Spiegel F, Taylor FJRM (2005) The new higher level classification of

eukaryotes and taxonomy of protists. Journal of Eukaryotic Microbiology 52 (5): 399-451. https://doi.org/10.1111/j.1550-7408.2005.00053.x

- Agardh CA (1828) Icones algarum europaeorum. Représentation d'algues européenes suive de celle des espèces exotiques les plus remarquables récemment découvertes. Fascicle 1. Leopold Voss, Leipzig, Germany.
- Aké-Castillo JA, Hernández-Becerril DU, Meave del Castillo ME (1999) Species of the genus *Thalassiosira* (Bacillariophyceae) from the Gulf of Tehuantepec, Mexico. Botanica Marina 42 (6): 487-503. https://doi.org/10.1515/BOT.1999.056
- Alexander J, Gross J (2024) The University and Jepson herbaria -- algae. Occurrence dataset. Version 1.12. Berkeley Natural History Museums, Berkeley, California, USA. URL: https://doi.org/10.15468/2axacp
- Al-Handal AY, Thomas EW, Pennesi C (2018) Marine benthic diatoms in the newly discovered coral reefs, off Basra coast, Southern Iraq. Phytotaxa 372 (2): 111-152. https://doi.org/10.11646/phytotaxa.372.2.1
- Al-Handal AY, Torstensson A, Wulff A (2022) Revisiting Potter Cove, King George Island, Antarctica, 12 years later: new observations of marine benthic diatoms. Botanica Marina 65 (2): 81-103. https://doi.org/10.1515/bot-2021-0066
- Alverson AJ, Kang SH, Theriot EC (2006) Cell wall morphology and systematic importance of *Thalassiosira ritscheri*, with a description of *Shionodiscus* gen. nov. Diatom Research 21 (2): 215-262. https://doi.org/10.1080/0269249X.2006.9705667
- Anonymous (1975) Proposals for a standardization of diatom terminology and diagnoses. Nova Hedwigia, Beihefte 53: 323-354.
- Armbrust EV (2009) The life of diatoms in the world's oceans. Nature 459: 185-192. https://doi.org/10.1038/nature08057
- Ashworth MP, Nakov T, Theriot EC (2013) Revisiting Ross and Sims (1971); toward a molecular phylogeny of the Biddulphiaceae and Eupodiscaceae (Bacillariophyceae). Journal of Phycology 49 (6): 1207-1222. https://doi.org/10.1111/jpy.12131
- Bahls LL (2015) The role of amateurs in modern diatom research. Diatom Research 30 (2): 209-210. https://doi.org/10.1080/0269249X.2014.988293
- Bailey LW, MacKay AH (1916) Diatoms from the eastern coast of Vancouver Island. Transactions of the Royal Society of Canada, series 3, 9 (4): 141-174.
- Barcode of Life Data System (2024) BOLD Systems. Version 5. BOLD Systems. URL: https://boldsystems.org
- Beentjes KK, Speksnijder AGCL, Schilthuizen M, Hoogeveen M, Pastoor R, van der Hoorn BB (2019) Increased performance of DNA metabarcoding of macroinvertebrates by taxonomic sorting. PLOS One 14 (12): e0226527. https://doi.org/10.1371/journal.pone.0226527
- Behrenfeld MJ, Halsey KH, Boss E, Karp-Boss L, Milligan AJ, Peers G (2021) Thoughts on the evolution and ecological niche of diatoms. Ecological Monographs 91 (3): e01457. https://doi.org/10.1002/ecm.1457
- Benoiston AS, Ibarbalz FM, Bittner L, Guidi L, Jahn O, Dutkiewicz S, Bowler C (2017) The evolution of diatoms and their biogeochemical functions. Philosophical Transactions of the Royal Society B 372: 20160397. https://doi.org/10.1098/rstb.2016.0397
- Bérard-Therriault L, Cardinal A, Poulin M (1987) Les diatomées (Bacillariophyceae) benthiques de substrats durs des eaux marines et saumâtres du Québec. 8. Centrales. Le Naturaliste Canadien 114: 81-103.

- Bérard-Therriault L, Poulin M, Bossé L (1999) Guide d'identification du phytoplancton marin de l'estuaire et du Golfe du Saint-Laurent incluant également certains protozoaires. Publication spéciale canadienne des sciences halieutiques et aquatiques 128. National Research Council Canada, Ottawa, Canada, 387 pp.
- Boonprakob A, Lundholm N, Medlin LK, Moestrup Ø (2021) The morphology and phylogeny of the diatom genera *Rhizosolenia*, *Proboscia*, *Pseudosolenia* and *Neocalyptrella* from the Gulf of Thailand and the Andaman Sea. Diatom Research 36 (3): 143-184. https://doi.org/10.1080/0269249X.2021.1957719
- Bopp L, Aumont O, Cadule P, Alvain S, Gehlen M (2005) Response of diatoms distribution to global warming and potential implications: a global model study. Geophysical Research Letters 32 (19): L19606. https://doi.org/10.1029/2005GL023653
- Bosak S, Supraha L, Nanjappa D, Kooistra WHCF, Sarno D (2015) Morphology and phylogeny of four species from the genus *Bacteriastrum* (Bacillariophyta). Phycologia 54 (2): 130-148. https://doi.org/10.2216/14-62
- Bourrelly P, Manguin E (1950) Contribution à l'étude de la flore algale d'eau douce de Madagascar: Le Lac de Tsimbazaza. Mémoires de l'Institut scientifique de Madagascar B2: 161-191.
- Brightwell T (1856) Further observations on the genus *Triceratium*, with descriptions and figures of new species. Quarterly Journal of Microscopical Science 4: 272-276.
- Brown University Herbarium (2025) Brown University - algae. Occurrence dataset. Brown University, Providence, Rhode Island, USA. URL: https://doi.org/10.15468/kpsj8r
- Buchanan RJ (1966) A study of the species composition and ecology of the protoplankton of a British Columbia inlet. PhD thesis. University of British Columbia, Vancouver, Canada, 301 pp. https://doi.org/10.14288/1.0104566
- Callahan BJ, McMurdie PJ, Rosen MJ, Han AW, Johnson AJA, Holmes SP (2016) DADA2: High-resolution sample inference from Illumina amplicon data. Nature Methods 13 (7): 581-583. https://doi.org/10.1038/nmeth.3869
- Caporaso JG, Lauber CL, Walters WA, Berg-Lyons D, Huntley J, Fierer N, Owens SM, Betley J, Fraser L, Bauer M, Gormley N, Gilbert JA, Smith G, Knight R (2012) Ultra-high-throughput microbial community analysis on the Illumina HiSeq and MiSeq platforms. The ISME Journal 6 (8): 1621-1624. https://doi.org/10.1038/ismej.2012.8
- Cardinal A, Poulin M, Bérard-Therriault L (1989) New criteria for species characterization in the genera *Donkinia*, *Gyrosigma* and *Pleurosigma* (Naviculaceae, Bacillariophyceae). Phycologia 28 (1): 15-27. https://doi.org/10.2216/i0031-8884-28-1-15.1
- Carlson KT (Ed.) (2001) A Stó:lō-Coast Salish historical atlas. Douglas & McIntyre Ltd. in association with University of Washington Press and Stó:lō Heritage Trust, Vancouver, Canada; Seattle, USA; Chilliwack, Canada, 208 pp.
- Cermeño P (2016) The geological story of marine diatoms and the last generation of fossil fuels. Perspectives in Phycology 3 (2): 53-60. https://doi.org/10.1127/pip/2016/0050
- Chandler M, See L, Copas K, Bonde AZ, López BC, Danielsen F, Legind JK, Masinde S, Miller-Rushing A, Newman G, Rosemartin A, Turak E (2017) Contribution of citizen science towards international biodiversity monitoring. Biological Conservation 213 (part B): 280-294. https://doi.org/10.1016/j.biocon.2016.09.004
- Chen X, Wei Q, Niu Y, Jiang X (2024) Complementary roles of eDNA metabarcoding and microscopy in plankton monitoring across seven habitats. Journal of Plankton Research 46 (6): 555-566. https://doi.org/10.1093/plankt/fbae052

- Cleve-Euler A (1937) Undersökningar över Öresund: Sundets plankton. 1. Sammansättning och fördelning. Lunds Universitets Arsskrift 33 (9): 1-51.
- Cleve PT (1893) Sur quelques espèces nouvelles ou peu connues (Suite). Le Diatomiste 2 (15): 55-58.
- Cleve PT (1894) Synopsis of the naviculoid diatoms. Part I. Kongliga Svenska Vetenskaps Akademiens Handlingar, series 4, 26 (2): 1-194.
- Cleve PT (1895) Synopsis of the naviculoid diatoms. Part II. Kongliga Svenska Vetenskaps Akademiens Handlingar 27 (3): 1-219.
- Cox EJ (1988) Taxonomic studies on the diatom genus *Navicula* V. The establishment of *Parlibellus* gen. nov. for some members of Navicula sect. Microstigmaticae. Diatom Research 3 (1): 9-38. https://doi.org/10.1080/0269249X.1988.9705014
- Crawford RM, Gardner C, Medlin LK (1994) The genus *Attheya*. I. A description of four taxa and the transfer of *Gonioceros septentrionalis* and *G. armatus*. Diatom Research 9 (1): 27-51. https://doi.org/10.1080/0269249X.1994.9705286
- Cupp EE (1943) Marine plankton diatoms of the west coast of North America. Bulletin of the Scripps Institute of Oceanography 5 (1): 1-238.
- Dabek P, Ashworth MP, Górecka E, Krzywda M, Bornman TG, Sato S, Witkowski A (2019) Toward a multigene phylogeny of the Cymatosiraceae (Bacillariophyta, Mediophyceae) II: morphological and molecular insights into the taxonomy of the forgotten species *Campylosira africana* and of *Extubocellulus*, with a description of two new taxa. Journal of Phycology 55 (2): 425-441. https://doi.org/10.1111/jpy.12831
- Danielidis DB, Mann DG (2002) The systematics of *Seminavis* (Bacillariophyta): the lost identities of *Amphora angusta*, *A. ventricose* and *A. macilenta*. European Journal of Phycology 37 (3): 429-448. https://doi.org/10.1017/S0967026202003724
- Del Bel Belluz J, Jackson JM, Kellogg CTE, Peña MA, Giesbrecht IJW, Hobson LA (2024) Phytoplankton community composition links to environmental drivers across a fjord to shelf gradient on the central coast of British Columbia. Frontiers in Marine Science 11: 1458677. https://doi.org/10.3389/fmars.2024.1458677
- Desikachary TV, Ranjitha DKA (1986) Marine fossil diatoms from India and Indian Ocean region. In: Desikachary TV (Ed.) Atlas of diatoms. Fascicle 1. Madras Science Foundation, Madras, India, 8 pp.
- Desikachary TV (1988) Marine diatoms of the Indian Ocean region. In: Desikachary TV (Ed.) Atlas of diatoms. Fascicle 5. Madras Science Foundation, Madras, India, 13 pp.
- De Stefano M, Marino D, Mazzella L (2000) Marine taxa of *Cocconeis* on leaves of *Posidonia oceanica*, including a new species and two new varieties. European Journal of Phycology 35 (3): 225-242. https://doi.org/10.1080/09670260010001735831
- De Stefano M, Marino D (2001) Comparison of *Cocconeis pseudonotata* sp. nov. with two closely related species, *C. notata* and *C. diruptoides*, from *Posidonia oceanica* leaves. European Journal of Phycology 36 (4): 295-306. https://doi.org/10.1080/09670260110001735458
- De Stefano M, Romero OE, Totti C (2008) A comparative study of *Cocconeis scutellum* Ehrenberg and its varieties (Bacillariophyta). Botanica Marina 51 (6): 506-536. https://doi.org/10.1515/BOT.2008.058
- Dixit SS, Smol JP, Kingston JC, Charles DF (1992) Diatoms: powerful indicators of environmental change. Environmental Science & Technology 26 (1): 22-33. https://doi.org/10.1021/es00025a002

- Donkin AS (1858) On the marine Diatomaceae of Northumberland with a description of eighteen new species. Transactions of the Microscopical Society of London, series 2, 6: 12-34.
- Edwards M, Beaugrand G, Kléparski L, Hélaouët P, Reid PC (2022) Climate variability and multi-decadal diatom abundance in the northeast Atlantic. Communications Earth & Environment 3: 162. https://doi.org/10.1038/s43247-022-00492-9
- Efimova KV, Shulgina MA, Shevchenko OG (2023) Intraspecific heterogeneity, multiple allelism and morphological divergence between morphotypes of *Thalassiosira allenii* (Bacillariophyta) from the Sea of Japan. Phycologia 62 (4): 352-365. https://doi.org/10.1080/00318884.2023.2231783
- Ehrenberg CG (1838) Die Infusionsthierchen als vollkommene Organismen. Ein Blick in das tiefere organische Leben der Natur. Verlag von Leopold Voss, Leipzig, Germany, 548 pp.
- Esenkulova S, Salinas-Ruiz P (2024) Harmful algae in the Strait of Georgia, 2015–2023. Sampling event dataset. Version 1.9. Pacific Salmon Foundation. https://doi.org/10.48689/736c4721-db8e-4116-a5f8-d9084126b135
- Falkowski PG, Barber RT, Smetacek V (1998) Biogeochemical controls and feedbacks on ocean primary production. Science 281 (5374): 200-206. https://doi.org/10.1126/science.281.5374.200
- Ferrario ME, Almandoz GO, Cefarelli AO, Beszteri B, Akselman R, Fabro E, Cembella A (2018) *Shionodiscus gaarderae* sp. nov. (Thalassiosirales, Thalassiosiraceae), a bloom-producing diatom from the southwestern Atlantic Ocean, and emendation of Shionodiscus bioculatus var. bioculatus. Diatom Research 33 (1): 25-37. https://doi.org/10.1080/0269249X.2017.1423112
- Field CB, Behrenfeld MJ, Randerson JT, Falkowski P (1998) Primary production of the biosphere: integrating terrestrial and oceanic components. Science 281 (5374): 237-240. https://doi.org/10.1126/science.281.5374.237
- Florida Museum of Natural History (2025) University of Florida Herbarium - macroalgae. Occurrence dataset. Florida Museum of Natural History, Gainesville, Florida, USA. URL: https://doi.org/10.15468/q69whp
- Flower RJ, Battarbee RW (1985) The morphology and biostratigraphy of *Tabellaria quadriseptata* (Bacillariophyceae) in acid waters and lake sediments in Galloway, southwest Scotland. British Phycological Journal 20 (1): 69-79. https://doi.org/10.1080/00071618500650081
- Foged N (1984) Freshwater and littoral diatoms from Cuba. Bibliotheca Diatomologica 5. J. Cramer, Vaduz, Liechtenstein, 243 pp.
- Frenguelli J (1928) Diatomeas del Océano Atlántico frente a Mar del Plata (República Argentina). Anales del Museo Nacional de Historia Natural 34: 497-572.
- Fryxell GA (1975) Three new species of *Thalassiosira*, with observations on the occluded process, a newly observed structure of diatom valves. Beihefte Nova Hedwigia 53: 57-82.
- Fryxell GA, Hasle GR (1977) The genus *Thalassiosira*: species with a modified ring of central strutted processes. In: Simonsen R (Ed.) Proceedings from the fourth symposium on recent and fossil marine diatoms, Oslo, August 30–September 3, 1976. Beihefte zur Nova Hedwigia 54. J. Cramer, Vaduz, Liechtenstein, 414 pp.
- Fryxell GA, Hasle GR (1980) The marine diatom *Thalassiosira oestrupii*: structure, taxonomy and distribution. American Journal of Botany 67 (5): 804-814. https://doi.org/10.1002/j.1537-2197.1980.tb07709.x

- Gaarder KR (1938) Phytoplankton studies from the Tromsø District 1930-31. Tromsø Museums Arshefter, Naturhistorisk Avd 55 (1): 1-159.
- Gaarder KR (1951) Bacillariophyceae from the “Michael Sars” North Atlantic deep-sea expedition 1910. Report on the scientific results of the “Michael Sars” North Atlantic deep-sea expedition 1910 2 (2): 1-36.
- Georgiev AA, Gololobova MA (2022) *Shionodiscus karianus* sp. nov. (Thalassiosirales, Thalassiosiraceae), a new planktonic diatom from the Kara Sea and notes on some morphological characters of *Shionodiscus* taxa. Diatom Research 37 (3): 273-292. https://doi.org/10.1080/0269249X.2022.2122576
- Giffen MH (1970) New and interesting marine and littoral diatoms from Sea Point, near Cape Town, South Africa. Botanica Marina 13 (2): 81-87. https://doi.org/10.1515/botm.1970.13.2.81
- Giffen MH (1973) Diatoms of the marine littoral of Steenberg's Cove in St. Helena Bay, Cape Province, South Africa. Botanica Marina 16 (1): 32-48. https://doi.org/10.1515/botm.1973.16.1.32
- Gran HH, Angst EC (1931) Plankton diatoms of Puget Sound. Publications–Puget Sound Biological Station 7: 417-514.
- Greville RK (1866) Descriptions of new and rare diatoms. Series XX. Transactions of the Microscopical Society, New Series 14 (1): 77-86. https://doi.org/10.1111/j.1365-2818.1866.tb05074.x
- Grunow A (1867) Diatomeen auf Sargassum von Honduras, gesammelt von Linding. Hedwigia 6 (1-3).
- Grunow A (1868) Algae. In: Fenzl E, et al. (Ed.) Reise der österreichischen Fregatte Novara um die Erde in den Jahren 1857, 1858, 1859 unter den Befehlen des Commodore B. von Wüllerstorf-Urbair. Botanischer Theil. Erster Band. Sporenpflanzen. Aus der Kaiserlich Königlichen Hof- und Staatsdruckeri in Commission bei Karl Gerold's Sohn, Vienna, Austria, 104 pp.
- Gugi B, Costaouee TL, Lerouge P, Helbert W, Bardor M (2015) Diatom-specific oligosaccharide and polysaccharide structures help to unravel biosynthetic capabilities in diatoms. Marine Drugs 13 (9): 5993-6018. https://doi.org/10.3390/md13095993
- Guillard RRL, Ryther JH (1962) Studies of marine planktonic diatoms: I. *Cyclotella nana* Hustedt and *Detonula confervacea* (Cleve) Gran. Canadian Journal of Microbiology 8 (2): 229-239. https://doi.org/10.1139/m62-029
- Guillou L, Bachar D, Audic S, Bass D, Berney C, Bittner L, Boutte C, Burgard G, de Vargas C, Decelle J, del Campo J, Dolan JR, Dunthorn M, Edvadsen B, Holzmann M, Kooistra WHCF, Lara E, Le Bescot N, Logares R, Mahé F, Massana R, Montresor M, Morard R, Not F, Pawlowski J, Probert I, Sauvadet A-, Siano R, Stoeck T, Vaulot D, Zimmerman P, Christen R (2013) The protist ribosomal reference database (PR2): a catalog of unicellular eukaryote Small Sub-Unit rRNA sequences with curated taxonomy. Nucleic Acids Research 41 (D1): D597-D604. https://doi.org/10.1093/nar/gks1160
- Guiry MD (2024) How many species of algae are there? A reprise. Four kingdoms, 14 phyla, 63 classes and still growing. Journal of Phycology 60 (2): 214-228. https://doi.org/10.1111/jpy.13431
- Guiry MD, Guiry GM (2025) AlgalBase. https://www.algaebase.org. Accessed on: 2025-10-20.
- Håkansson H (2002) A compilation and evaluation of species in the general *Stephanodiscus*, *Cyclostephanos* and *Cyclotella* with a new genus in the family

Stephanodiscaceae. Diatom Research 17 (1): 1-139. https://doi.org/10.1080/0269249X.2002.9705534

- Hallegraeff GM (1984) Species of the diatom genus *Thalassiosira* in Australian waters. Botanica Marina 27: 495-514. https://doi.org/10.1515/botm.1984.27.11.495
- Hamilton PB, Lefebvre KE, Bull RD (2015) Single cell PCR amplification of diatoms using fresh and preserved samples. Frontiers in Microbiology 6: 1084. https://doi.org/10.3389/fmicb.2015.01084
- Hamsher SE, LeGresley MM, Martin JL, Saunders GW (2013) A comparison of morphological and molecular-based surveys to estimate the species richness of *Chaetoceros* and *Thalassiosira* (Bacillariophyta) in the Bay of Fundy. PLOS One 8 (10): e73521. https://doi.org/10.1371/journal.pone.0073521
- Hargraves PE, Guillard RR (1974) Structural and physiological observations on some small marine diatoms. Phycologia 13 (2): 163-172. https://doi.org/10.2216/i0031-8884-13-2-163.1
- Harris ASD, Medlin LK, Lewis J, Jones KJ (1995) *Thalassiosira* species (Bacillariophyceae) from a Scottish sea-loch. European Journal of Phycology 30 (2): 117-131. https://doi.org/10.1080/09670269500650881
- Hasle GR (1978a) Some *Thalassiosira* species with one central process (Bacillariophyceae). Norwegian Journal of Botany 25: 77-110.
- Hasle GR (1978b) Some freshwater and brackish water species of the diatom genus *Thalassiosira* Cleve. Phycologia 17 (3): 263-292. https://doi.org/10.2216/i0031-8884-17-3-263.1
- Hasle GR (1980) Examination of *Thalassiosira* type material: *T. minima* and *T. delicatula* (Bacillariophyceae). Norwegian Journal of Botany 27: 167-173.
- Hasle GR (1983) The marine, planktonic diatoms *Thalassiosira oceanica* sp. nov. and *T. partheneia*. Journal of Phycology 19 (2): 220-229. https://doi.org/10.1111/j.0022-3646.1983.00220.x
- Hasle GR, von Stosch HA, Syvertsen EE (1983) Cymatosiraceae, a new diatom family. Bacillaria 6: 9-156.
- Hasle GR, Syvertsen EE (1997) Marine diatoms. In: Thomas CR (Ed.) Identifying marine phytoplankton. Academic Press, San Diego, USA, 874 pp. https://doi.org/10.17031/1629
- Hazrin-Chong NH, Manefield M (2012) An alternative SEM drying method using hexamethyldisilazane (HMDS) for microbial cell attachment studies on sub-bituminous coal. Journal of Microbiological Methods 90 (2): 96-99. https://doi.org/10.1016/j.mimet.2012.04.014
- Heiberg PA (1863) Conspectus criticus diatomacearum danicarum. Kritisk oversigt over de danske Diatomeer. Wilhelm Priors Forlag, Copenhagen, Denmark, 135 pp. https://doi.org/10.5962/bhl.title.68738
- Hendey NI (1964) An introductory account of the smaller algae of British coastal waters. Part V: Bacillariophyceae (Diatoms). Ministry of Agriculture, Fisheries and Food, Fishery Investigations, series 4. Her Majesty's Stationery Office, London, UK, 317 pp.
- Hernández-Becerril DU, Meave del Castillo ME (1996) The marine planktonic diatom *Rhizosolenia robusta* (Bacillariophyta): morphological studies support its transfer to a new genus, *Calyptrella* gen. nov. Phycologia 35 (3): 198-203. https://doi.org/10.2216/i0031-8884-35-3-198.1

- Hernández-Becerril DU, Maeve del Castillo ME (1997) *Neocalyptrella*, gen. nov., a new name to replace *Calyptrella* Hernández-Becerril et Maeve. Phycologia 36 (4): 329. https://doi.org/10.2216/i0031-8884-36-4-329.1
- Hernández-Becerril DU, Salazar-Paredes J, Barón-Campis SA (2015) Morphology and morphological changes of the marine planktonic diatom *Thalassiosira allenii* Takano (Bacillariophyta) during culture. In: Witkowski J, Williams D, Kociolek JP (Eds) Diatoms and the counting relevance of morphology to studies on taxonomy, systematics and biogeography. Nova Hedwigia, Beiheft 144. J. Cramer, Stuttgart, Germany, 228 pp.
- Honeywill C (1998) A study of British *Licmophora* species and a discussion of its morphological features. Diatom Research 13 (2): 221-271. https://doi.org/10.1080/0269249X.1998.9705450
- Hoppenrath M, Beszteri B, Drebes G, Halliger H, Van Beusekom JEE, Janisch S, Wiltshire KH (2007) *Thalassiosira* species (Bacillariophyceae, Thalassiosirales) in the North Sea at Helgoland (German Bight) and Sylt (North Frisian Wadden Sea)—a first approach to assessing diversity. European Journal of Phycology 42 (3): 271-288. https://doi.org/10.1080/09670260701352288
- Hoppenrath M, Elbrachter M, Drebes G (2009) Marine phytoplankton. Selected microphytoplankton species from the North Sea around Helgoland and Sylt. Schweizerbart Science Publishers, Stuttgart, Germany, 264 pp.
- Hortal J, De Bello F, Diniz-Filho JAF, Lewinsohn TM, Lobo JM, Ladle RJ (2015) Seven shortfalls that beset large-scale knowledge of biodiversity. Annual Review of Ecology, Evolution, and Systematics 46: 523-549. https://doi.org/10.1146/annurev-ecolsys-112414-054400
- Hustedt F (1930a) Bacillariophyta (Diatomeae) Zweite Auflage. In: Pascher A (Ed.) Die Süsswasser-Flora Mitteleuropas. Heft 10. Verlag von Gustav Fischer, Jena, Germany, 466 pp.
- Hustedt F (1930b) Die Kieselalgen Deutschlands, Österreichs und der Schweiz unter Berücksichtigung der übrigen Länder Europas sowie der angrenzenden Meeresgebiete VII (1). In: Anonymous (Ed.) Rabenhorst's Kryptogamen Flora Deutschland, Österreich und der Schweiz. Akademische Verlagsgesellschaft m.b.h., Leipzig, Germany, 920 pp.
- Hustedt F (1931) Die Kieselalgen Deutschlands, Österreichs und der Schweiz unter Berücksichtigung der übrigen Länder Europas sowie der angrenzenden Meeresgebiete VII (2). In: Anonymous (Ed.) Rabenhorst's Kryptogamen Flora von Deutschland, Österreich und der Schweiz. Akademische Verlagsgesellschaft m.b.h., Leipzig, Germany, 176 pp.
- Hustedt F (1957) Die Diatomeenflora des Flußsystems der Weser im Gebiet der Hansestadt Bremen. Denkschrift über den heutigen ökologischen Zustand der Wasserstraßen im bremischen Staatsgebiet auf Grund der Kieselalgen-Flora mit Beziehung auf die Abwasserverhältnisse. Abhandlungen der Naturwissenschaftlichen Verein zu Bremen 34 (3): 181-440.
- iNaturalist (2025) iNaturalist research-grade observations. Occurrence dataset. iNaturalist.org. URL: https://doi.org/10.15468/ab3s5x
- Jackman AS, Schenk S, Adamczyk EM, Herrin MJ, van Asselt A, Humphrey E, Witkowski A, Morien E, Webber M, Parfrey LW (2025) Integrating DNA sequencing and morphological identification enhances understanding of epiphytic diatom diversity and ecology. Botany 103: 1-14. https://doi.org/10.1139/cjb-2024-0100

- Jahn R, Sterrenburg FA, Kusber WH (2005) Typification and taxonomy of *Gyrosigma fasciolata* (Ehrenberg) J.W. Griffith et Henfrey. Diatom Research 20 (2): 305-311. https://doi.org/10.1080/0269249X.2005.9705639
- Jameson I, Hallegraeff GM (2010) Planktonic diatoms. In: Hallegraeff GM, Bolch CJ, Hill DR, Jameson I, LeRoi JM, McMinn A, Murray S, de Salas MF, Saunders K (Eds) Algae of Australia. Phytoplankton of temperate coastal waters. Australian Biological Resources Study/CSIRO Publishing, Canberra, Australia, 432 pp.
- Jin D, Cheng Z, Lin J, Liu S (1985) The marine benthic diatoms of China, volume 1. China Ocean Press, Beijing, People's Republic of China; Springer Verlag, Berlin–New York, 313 pp.
- Johansen JR, Fryxell GA (1985) The genus *Thalassiosira* (Bacillariophyceae): studies on species occurring south of the Antarctic Convergence Zone. Phycologia 24 (2): 155-179. https://doi.org/10.2216/i0031-8884-24-2-155.1
- Joh G (2021) Distribution of the genus *Cocconeis* (Bacillariophyceae) along the Seogwipo coast of Jeju Island, South Korea. Phytotaxa 528 (3): 149-179. https://doi.org/10.11646/phytotaxa.528.3.1
- Johnstone PD, Mustard PS, MacEachern JA (2006) The basal unconformity of the Nanaimo Group, southwestern British Columbia: a Late Cretaceous storm-swept rocky shoreline. Canadian Journal of Earth Sciences 43 (8): 1165-1181. https://doi.org/10.1139/e06-046
- Kaleli A, Krzywda M, Car A, Zglobicka I, Kurzydlowski K, Plocinski T (2023) Diatoms associated with loggerhead sea turtles (*Caretta caretta* Linnaeus, 1758) carapace from the Mediterranean Sea coast of Turkey. Diatom Monographs 20. Koeltz Botanical Books, Oberreifenberg, Germany, 201 pp.
- Khan-Bureau DA, Morales EA, Ector L, Beauchene MS, Lewis LA (2016) Characterization of a new species in the genus *Didymosphenia* and of *Cymbella janischii* (Bacillariophyta) from Connecticut, USA. European Journal of Phycology 51 (2): 203-216. https://doi.org/10.1080/09670262.2015.1126361
- Kim H, Khim JS, Witkowski A, Park J (2022) A new species of *Fogedia* (Bacillariophyceae) from tidal flats of Northeast Asia. Phytotaxa 554 (1): 77-84. https://doi.org/10.11646/PHYTOTAXA.554.1.6
- Kim SY, Witkowski A, Park JG, Gastineau R, Ashworth MP, Kim BS, Mann DG, Li C, Igersheim A, Plocinski T, Yoo YD, Chung SO, Theriot EC (2020) The taxonomy and diversity of *Proschkinia* (Bacillariophyta), a common but enigmatic genus from marine coasts. Journal of Phycology 56 (4): 953-978. https://doi.org/10.1111/jpy.12998
- Knudson BM (1952) The diatom genus *Tabellaria*. Annals of Botany, New Series 16: 421-440. https://doi.org/10.1093/oxfordjournals.aob.a083325
- Kociolek J, Ashworth MP, Alverson A (2026) A phylogenetic classification of diatoms (Bacillariophyta). Journal of Phycology 62 (1): 44-67. https://doi.org/10.1111/jpy.70125
- Kociolek JP, Williams DM (2015) How to define a diatom genus? Notes on the creation and recognition of taxa, and a call for revisionary studies of diatoms. Acta Botanica Croatia 74: 195-210. https://doi.org/10.1515/botcro-2015-0018
- Kociolek JP, Balasubramanian K, Blanco S, Coste M, Ector L, Liu Y, Kulikovskiy M, Lundholm N, Ludwig T, Potapova M, Rimet F, Sabbe K, Sala S, Sar E, Taylor J, Van de Vijver B, Wetzel CE, Williams DM, Witkowski A, Witkowski J (2018) DiatomBase. https://www.diatombase.org. Accessed on: 2025-10-25.

- Kooistra WH, Gersonde R, Medlin K, Mann D (2007) The origin and evolution of the diatoms: their adaptation to a planktonic existence. In: Falkowski PG, Knoll AH (Eds) Evolution of primary producers in the sea. Academic Press, San Diego, USA, 456 pp. https://doi.org/10.1016/B978-012370518-1/50012-6
- Krzywda M, Gastineau R, Bąk M, Dąbek P, Górecka E, Chengxu Z, Lange-Bertalot H, Li CL, Witkowski A (2019) Morphology and molecular phylogeny of *Gomphonemopsis sieminskae* sp. nov. isolated from brackish waters of the East China Sea coast. Plant and Fungal Systematics 64 (1): 17-24. https://doi.org/10.2478/pfs-2019-0003
- Kuntze O (1898) Revisio generum plantarum. Vol. 3. Arthur Felix, Leipzig, Germany, 576 pp.
- Kützing FT (1844) Die Kieselschaligen Bacillarien oder Diatomeen. W. Köhne, Nordhausen, Germany, 152 pp. https://doi.org/10.5962/bhl.title.64360
- Lange-Bertalot H, Hofmann G, Werum M, Cantonati M (2017) Freshwater benthic diatoms of Central Europe: over 800 common species used in ecological assessment. English edition with updated taxonomy and added species. Koeltz Botanical Books, Oberreifenberg, Germany, 942 pp.
- Lang I, Kaczmarska I (2011) A protocol for a single-cell PCR of diatoms from fixed samples: method validation using *Ditylum brightwellii* (T. West) Grunow. Diatom Research 26 (1): 43-49. https://doi.org/10.1080/0269249X.2011.573703
- Lauder HS (1864) On new diatoms. Transactions of the Microscopical Society of London, New Series 12: 3-6.
- Lear D (2022) Continuous plankton recorder survey (CPR survey). Sampling event dataset. Version 1.3. The Marine Biological Association of the UK, Devon, UK. URL: https://doi.org/10.17031/1629
- Lee JH, Chang M (1996) Morphological variations of the marine diatom genus *Actinoptychus* in the coastal waters of Korea. Algae, the Korean Journal of Phycology 11 (4): 365-374.
- Lee JH, Lee SD, Park JS (2012) New record of diatom species in Korean coastal waters. Korean Journal of Environmental Biology 30 (3): 245-271.
- Lee K, Choi JK, Lee JH (1995) Taxonomic studies on diatoms in Korea. II. Check-list. Algae, the Korean Journal of Phycology 10 (supplement): 13-89.
- Li CL, Witkowski A, Ashworth MP, Dabek P, Sato S, Zglobicka I, Witak M, Khim JS, Kwon CJ (2018) The morphology and molecular phylogenetics of some marine diatom taxa within the Fragilariaceae, including twenty undescribed species and their relationship to *Nanofrustulum*, *Opephora* and *Pseudostaurosira*. Phytotaxa 355 (1): 1-104. https://doi.org/10.11646/phytotaxa.355.1.1
- Linke B, Schröder K, Arter J, Gasperazzo T, Woehlecke H, Ehwald R (2010) Extraction of nucleic acids from yeast cells and plant tissues using ethanol as medium for sample preservation and cell disruption. Biotechniques 49 (3): 655-657. https://doi.org/10.2144/000113476
- Li Y, Zhao Q, Lü S (2013) The genus *Thalassiosira* off the Guangdong coast, South China Sea. Botanica Marina 56 (1): 83-110. https://doi.org/10.1515/bot-2011-0045
- Li Y, Zhao QL, Lü SH (2014) Taxonomy and species diversity of the diatom genus *Thalassiosira* (Bacillariophyceae) in Zhejiang coastal waters, the East China Sea. Nova Hedwigia 99 (3-4): 373-402. https://doi.org/10.1127/0029-5035/2014/0170

- Li Y, Guo XH, Lundholm N (2020) Molecular phylogeny and taxonomy of the genus *Minidiscus* (Bacillariophyceae), with description of *Mediolabrus* gen. nov. Journal of Phycology 56 (6): 1443-1456. https://doi.org/10.1111/jpy.13038
- Lobban CS, Ashworth MP, Calaor JJM, Theriot EC (2019) Extreme diversity in fine-grained morphology reveals fourteen new species of conopeate *Nitzschia* (Bacillariophyta: Bacillariales). Phytotaxa 401 (4): 199-238. https://doi.org/10.11646/PHYTOTAXA.401.4.1
- Lobban CS, Ashworth MP (2022) *Homoeocladia* C.Agardh reinstated for bilaterally symmetrical conopeate *Nitzschia* species (Bacillariaceae, Bacillariophyta). Notulae Algarum 267: 1-9. URL: https://www.notulaealgarum.com
- López-Fuerte FO, Siqueiros-Beltrones DA (2016) A checklist of marine benthic diatoms (Bacillariophyta) from Mexico. Phytotaxa 283 (3): 201-258. https://doi.org/10.11646/phytotaxa.283.3.1
- Lord JK (1866) The naturalist in Vancouver Island and British Columbia. In two volumes. Vol. II. Richard Bentley, London, England, 375 pp. https://doi.org/10.5962/bhl.title.48504
- Lowery CM, Bown PR, Fraass AJ, Hull PM (2020) Ecological response of plankton to environmental change: thresholds for extinction. Annual Review of Earth and Planetary Sciences 48: 403-429. https://doi.org/10.1146/annurev-earth-081619-052818
- Lozano-Duque Y, Vidal LA, Navas SG (2010) Check-list of diatoms (Bacillariophyta) reported from the Colombian Caribbean Sea. Boletín de Investigaciones Marinas y Costeras 39 (1): 83-116. https://doi.org/10.25268/bimc.invemar.2010.39.1.144
- Mahood AD, Fryxell GA, Mcmillan M (1986) The diatom genus *Thalassiosira*: species from the San Francisco Bay system. Proceedings of the California Academy of Sciences 44 (8): 127-156.
- Majewska R, De Stefano M, Ector L, Balaños F, Frankovich TA, Sullivan MJ, Ashworth MP, Vijver B (2017) Two new epizoic *Achnanthes* species (Bacillariophyta) living on marine turtles from Costa Rica. Botanica Marina 60 (3): 303-318. https://doi.org/10.1515/bot-2016-0114
- Majewska R, Bosak A, Frankovich TA, Ashworth MP, Sullivan MJ, Robinson NJ, lazo-Wasem EA, Pinou T, Nel R, Manning S, Van de Vijver B (2019) Six new epibiotic *Proschkinia* (Bacillariophyta) species and new insights into the genus phylogeny. European Journal of Phycology 54 (4): 609-631. https://doi.org/10.1080/09670262.2019.1628307
- Makarova IV, Genkal SI, Kuzmin GV (1979) Species of the genus *Thalassiosira* Cl. (Bacillariophyta), found in continental water bodies of the USSR. Botanicheskii Zhurnal 64 (7): 921-927.
- Mann A (1925) Marine diatoms of the Philippine Islands. Bulletin of the United States National Museum 100 (6, part 1): 1-182.
- Mann DG, Vanormelingen P (2013) An inordinate fondness? The number, distributions, and origins of diatom species. Journal of Eukaryotic Microbiology 60 (4): 414-420. https://doi.org/10.1111/jeu.12047
- Mann DG, Crawford RM, Round FE (2016) Bacillariophyta. In: Archibald JM, Simpson AG, Slamovits CH (Eds) Handbook of the protists. Springer Cham, Cham, Switzerland, 1,657 pp. https://doi.org/10.1007/978-3-319-28149-0
- Martin M (2011) Cutadapt removes adapter sequences from high-throughput sequencing reads. EMBnet.journal 17 (1): 10-12. https://doi.org/10.14806/ej.17.1.200

- Mather L, MacIntosh K, Kaczmarska I, Klein G, Martin JL (2010) A checklist of diatom species reported (and presumed native) from Canadian coastal waters. Canadian Technical Report of Fisheries and Aquatic Sciences 2881. Fisheries and Oceans Canada, St. Andrews, Canada, 84 pp. URL: https://publications.gc.ca/site/eng/9.568417/publication.html
- Mathieu C, Hermans SM, Lear G, Buckley TR, Lee KC, Buckley HL (2020) A systematic review of sources of variability and uncertainty in eDNA data for environmental monitoring. Frontiers in Ecology and Evolution 8: 135. https://doi.org/10.3389/fevo.2020.00135
- Mayama S, Witkowski A, Kryk A, Ribeiro L, Rybak M (2025) Novel marine diatom genera with raphe on the valve mantle: *Periraphis* gen. nov. and *Andrzeja* gen. nov. (Bacillariophyceae). Nova Hedwigia 120 (1-4): 7-27. https://doi.org/10.1127/nova_hedwigia/2025/1100
- Mazur-Marzec H, Andersson AF, Błaszczyk A, Dąbek P, Górecka E, Jankowska K, Jurczak-Kurek A, Kaczorowska AK, Kaczorowski T, Karlson B, Kataržytė M, Kobos J, Kotlarska E, Krawczyk B, Łuczkiewicz A, Piwosz K, Rybak B, Rychert K, Sjöqvist C, Surosz W, Szymczycha B, Toruńska-Sitarz A, Węgrzyn G, Witkowski A, Węgrzyn A (2024) Biodiversity of microorganisms in the Baltic Sea: the power of novel methods in the identification of marine microbes. FEMS Microbiology Reviews 48 (5): fuae024. https://doi.org/10.1093/femsre/fuae024
- McIntire CD, Reimer CW (1974) Some marine and brackish-water *Achnanthes* from Yaquina estuary, Oregon (U.S.A.). Botanica Marina 17 (3): 164-175. https://doi.org/10.1515/botm.1974.17.3.164
- McLaren MR (2020) Silva SSU taxonomic training data formatted for DADA2. Silva version 138. Zenodo. URL: https://zenodo.org/records/3731176
- Medlin LK, Round FE (1986) Taxonomic studies of marine gomphonemoid diatoms. Diatom Research 1 (2): 205-225. https://doi.org/10.1080/0269249X.1986.9704970
- Medlin LK (2015) Evolution of the diatoms: major steps in their evolution and a review of the supporting molecular and morphological evidence. Phycologia 55 (1): 79-103. https://doi.org/10.2216/15-105.1
- Medlin LK, Boonprakob A, Lundholm N, Moestrup Ø (2021) On the morphology and phylogeny of the diatom species *Rhizosolenia setigera*: comparison of the type material to modern cultured strains, and a taxonomic revision. Nova Hedwigia, Beiheft 151: 223-247. https://doi.org/10.1127/nova-suppl/2021/223
- MGnify (2021) Ecological genomics of a seasonally anoxic fjord; Saanich Inlet. Sampling event dataset. European Molecular Biology Laboratory, European Bioinformatics Institute (EMBL-EBI), Cambridgeshire, UK. URL: https://doi.org/10.15468/yw9wpv
- Michigan State University Herbarium (2025) Michigan State University algae. Occurrence dataset. Michigan State University, East Lansing, Michigan, USA. URL: https://doi.org/10.15468/dey5s9
- Mönnich J, Tebben J, Bergemann J, Case R, Wohlrab S, Harder T (2020) Niche-based assembly of bacterial consortia on the diatom *Thalassiosira rotula* is stable and reproducible. The ISME Journal 14 (6): 1614-1628. https://doi.org/10.1038/s41396-020-0631-5
- Nakov T, Beaulieu JM, Alverson AJ (2018) Accelerated diversification is related to life history and locomotion in a hyperdiverse lineage of microbial eukaryotes (diatoms, Bacillariophyta). New Phytologist 219 (1): 462-473. https://doi.org/10.1111/nph.15137

- Nanjappa D, D'Ippolito G, Gallo C, Zingone A, Angelo F (2014) Oxylipin diversity in the diatom family Leptocylindraceae reveals DHA derivatives in marine diatoms. Marine Drugs 12 (1): 368-384. https://doi.org/10.3390/md12010368
- Natural History Museum (2025) Natural History Museum, data portal: collection specimens. Occurrence dataset. Natural History Museum, London, UK. URL: https://doi.org/10.5519/qd.f4i40jj0
- Nelson DM, Treguer P, Brzezinski MA, Leynaert A, Queguiner B (1995) Production and dissolution of biogenic silica in the ocean: revised global estimates, comparison with regional data and relationship to biogenic sedimentation. Global Biogeochemical Cycles 9 (3): 359-372. https://doi.org/10.1029/95GB01070
- Orlova TY, Stonik IV, Aizdaicher NA (2002) Morphology and biology of the diatom alga *Attheya longicornis* from the Sea of Japan. Russian Journal of Marine Biology 28: 186-190. https://doi.org/10.1023/A:1016897320307
- Ostenfeld CH (1900) Plankton. In: Knudsen M, Ostenfeld C (Eds) Iagttagelsen over overfladevandets temperatur, saltholdighed og plankton paa islandske og grønlandske skibsrouter i 1899. Bianco Lunos Kgl. Hof-Bogtrykkeri, Copenhagen, Denmark, 93 pp.
- Østrup E (1895) Marine diatoméer fra Østgrønland. Meddelelser om Grønland, Kjøbenhavn 18: 395-476.
- Park JS, Alverson AJ, Lee JH (2016a) A phylogenetic re-definition of the diatom genus *Bacterosira* (Thalassiosirales, Bacillariophyta), with the transfer of *Thalassiosira constricta* based on morphological and molecular characters. Phytotaxa 245 (1): 1-16. https://doi.org/10.11646/phytotaxa.245.1.1
- Park JS, Jung SW, Lee SD, Yun SM, Lee JH (2016b) Species diversity of the genus *Thalassiosira* (Thalassiosirales, Bacillariophyta) in South Korea and its biogeographical distribution in the world. Phycologia 55 (4): 403-423. https://doi.org/10.2216/15-66.1
- Park JS, Jung SW, Ki JS, Guo R, Kim HJ, Lee KW, Lee JH (2017) Transfer of the small diatoms *Thalassiosira proschkinae* and *T. spinulata* to the genus *Minidiscus* and their taxonomic re-description. PLOS One 12 (9): 0181980. https://doi.org/10.1371/journal.pone.0181980
- Patrick R, Reimer C (1966) The diatoms of the United States (exclusive of Alaska and Hawaii). Volume 1: Fragilariaceae, Eunotiaceae, Achnanthaceae, Naviculaceae. Monographs of the Academy of Natural Sciences of Philadelphia 13. Academy of Natural Sciences, Philadelphia, Pennsylvania, USA, 702 pp.
- Peragallo H, Peragallo M (1908) Diatomées marines de France et des districts maritimes voisins. In: Tempère MJ (Ed.) Tableaux synoptique & systématique (Tables). Micrographe-Éditeur, Grez-sur-Loing (S. et M.), France, 491 pp. https://doi.org/10.5962/bhl.title.13501
- Pérez-Burillo J, Mann DG, Trobajo R (2022) Evaluation of two short overlapping rbcL markers for diatom metabarcoding of environmental samples: effects on biomonitoring assessment and species resolution. Chemosphere 307 (pt 3): 135933. https://doi.org/10.1016/j.chemosphere.2022.135933
- Peter M, Diekötter T, Höffler T, Kremer K (2021) Biodiversity citizen science: outcomes for the participating citizens. People and Nature 3 (2): 294-311. https://doi.org/10.1002/pan3.10193
- Petit P (1877) Catalogue des diatomées. In: De Folin L, Périer L (Eds) Les fonds de la mer. Étude sur les particularités nouvelles des régions sous-marines. Tome troisième. Savy, Libraire-Éditeur, Paris, France, 426 pp.

- Petit P (1889) Diatomées recoltées dans le voisinage du Cap Horn. In: Hariot P, et al. (Ed.) Mission scientifique du Cap Horn, 1882–1883, vol. 5 (Botanique). Gauthier-Villas, Paris, France.
- Phifer LD (1932) Seasonal distribution and occurrence of planktonic diatoms at Friday Harbor, Washington. PhD thesis. University of Washington, Seattle, USA, 120 pp.
- Pienitz R, Fedje D, Poulin M (2003) Marine and non-marine diatoms from the Haida Gwaii archipelago and surrounding coasts, Northeastern Pacific, Canada. Bibliotheca Diatomologica 48. J. Cramer, Stuttgart, Germany, 146 pp.
- Pietluch F, Mackiewicz P, Ludwig K, Gagat P (2024) A new model and dating for the evolution of complex plastids of red alga origin. Genome Biology and Evolution 16 (9): evae192. https://doi.org/10.1093/gbe/evae192
- Plinski M, Witkowski A (2020) Diatoms from the Gulf of Gdańsk and surrounding waters (the southern Baltic Sea): a key to the identification of the species. Gdańsk University Press, Gdańsk, Poland, 442 pp.
- Poulin M, Bérard-Therriault L, Cardinal A (1984) Les diatomées benthiques de substrats durs des eaux marines et saumâtres du Québec. 1. Cocconeioideae (Achnanthales, Achnanthaceae). Le Naturaliste canadien (Revue d'écologie et de systématique) 111: 45-61.
- Prasad AK, Nienow JA (2006) The centric diatom genus *Cyclotella* (Stephanodiscaceae: Bacillariophyta) from Florida Bay, USA, with special reference to *Cyclotella choctawhatcheeana* and *Cyclotella desikacharyi*, a new marine species related to the *Cyclotella striata* complex. Phycologia 45 (2): 127-140. https://doi.org/10.2216/05-13.1
- Pritchard A (1861) A history of infusoria, including the Desmidiaceae and Diatomaceae, British and foreign. Fourth edition. Enlarged and revised by Arlidge JT, Archer W, Ralfs J, Williamson WC, Pritchard A. Whittaker and Co, London, England, 968 pp. https://doi.org/10.5962/bhl.title.101827
- Proshkina-Lavrenko A (Ed.) (1950) Diatomovyi analiz. Opredelitel' iskopaemykh i sovremennykh diatomikh vodorosleyi. Poryadok Pennales. Vol. 3. Gosudarstvennoye Izdatel'stvo Geologicheskoy Literatury, Moscow, Russia, 398 pp. [In Russian].
- Provoost P, Enevoldsen H (2025) Harmful algal event database (HAEDAT). Sampling event dataset. Version 2.2. Intergovernmental Oceanographic Commission–UNESCO Harmful Algal Bloom Programme. URL: https://doi.org/10.25607/0wdrmq
- Quast C, Pruesse E, Yilmaz P, Gerken J, Schweer T, Yarza P, Peplies J, Glöckner FO (2012) The SILVA ribosomal RNA gene database project: improved data processing and web-based tools. Nucleic Acids Research 41 (D1): D590-D596. https://doi.org/10.1093/nar/gks1219
- Rad-Menéndez C, Stanley M, Green DH, Cox EJ, Day JG (2015) Exploring cryptic diversity in publicly available strains of the model diatom *Thalassiosira pseudonana* (Bacillariophyceae). Journal of the Marine Biological Association of the United Kingdom 95 (6): 1081-1090. https://doi.org/10.1017/S0025315415000120
- Ramirez J, Watson K, Feder L, Gjieli E, Sessa E (2025) The New York Botanical Garden Herbarium (NY). Occurrence dataset. Version 1.79. The New York Botanical Garden, New York City, USA. URL: https://doi.org/10.15468/6e8nje
- Rampen SW, Schouten S, Panoto FE, Brink M, Andersen RA, Muyzer G, Abbas B, Sinninghe Damste JS (2009) Phylogenetic position of *Attheya longicornis* and *Attheya septentrionalis* (Bacillariophyta). Journal of Phycology 45 (2): 444-453. https://doi.org/10.1111/j.1529-8817.2009.00657.x

- Rao VN, Lewin J (1976) Benthic marine diatom flora of False Bay, San Juan Island, Washington. Syesis 9: 173-213.
- R Core Team (2023) R: a language and environment for statistical computing. Version 4.2.2. R Foundation for Statistical Computing, Vienna, Austria. URL: https://www.R-project.org
- R Core Team (2025) R: a language and environment for statistical computing. Version 4.5.0. R Foundation for Statistical Computing, Vienna, Austria. URL: https://www.R-project.org
- Riaux-Gobin C, Romero O (2003) Marine *Cocconeis* Ehrenberg (Bacillariophyceae) species and related taxa from Kerguelen's Land (Austral Ocean, Indian Sector). Bibliotheca Diatomologica 47. J. Cramer, Stuttgart, Germany, 188 pp.
- Riaux-Gobin C, Witkowski A (2017) *Cocconeis subantarctica* sp. nov. from Kerguelen Archipelago (Austral Ocean) and comparison with *Cocconeis stauroneiformis* (W.Smith) Okuno. Oceanological and Hydrobiological Studies 46 (3): 350-362. https://doi.org/10.1515/ohs-2017-0036
- Riaux-Gobin C, Ector L, Witkowski A, Igersheim A (2018) Achnanthales from historical Grunow collection in Porto Subzanski, Croatia. Botanica Marina 61 (6): 573-593. https://doi.org/10.1515/bot-2018-0045
- Rivera Ramírez P (1981) Beiträge zur Taxonomie und Verbreitung der Gattung *Thalassiosira* Cleve (Bacillariophyceae) in den Küstengewässern Chiles. Bibliotheca Phycologica 56. J. Cramer, Vaduz, Liechtenstein, 222 pp.
- Riznyk RZ (1973) Interstitial diatoms from two tidal flats in Yaquina Estuary, Oregon, USA. Botanica Marina 16 (3): 113-138. https://doi.org/10.1515/botm.1973.16.3.113
- Romagnoli T, Totti C, Accoroni S, De Stefano M, Pennesi C (2014) SEM analysis of the epibenthic diatoms on *Eudendrium racemosum* (Hydrozoa) from the Mediterranean Sea. Turkish Journal of Botany 38 (3): 566-594. https://doi.org/10.3906/bot-1305-52
- Romero OE (1996) Ultrastructure of four species of the diatom genus *Cocconeis* with the description of *C. pseudocostata* spec. nov. Nova Hedwigia 63 (3-4): 361-396. https://doi.org/10.1127/nova.hedwigia/63/1996/361
- Romero OE, Rivera P (1996) Morphology and taxonomy of three varieties of *Cocconeis costata* and *C. pinnata* (Bacillariophyceae) with considerations of *Pleuroneis*. Diatom Research 11 (2): 317-343. https://doi.org/10.1080/0269249X.1996.9705388
- Roper FC (1856) Some observations on the diatomaceae of the Thames. Transactions of the Microscopical Society of London, New Series 2: 67-80. https://doi.org/10.1111/j.1365-2818.1854.tb01845.x
- Ross R, Cox EJ, Karayeva NI, Mann DG, Paddox TB, Simonsen R, Simsy PA (1979) An amended terminology for the siliceous components of the diatom cell. Nova Hedwigia 64: 513-533.
- Round FE (1984) Structure of the cells, cell division and colony formation in the diatoms *Isthmia enervis* Ehr. and *I. nervosa* Kütz. Annals of Botany 53 (4): 457-468. https://doi.org/10.1093/oxfordjournals.aob.a086710
- Round FE, Crawford RM, Mann DG (1990) The diatoms: biology and morphology of the genera. Cambridge University Press, Cambridge, UK, 747 pp.
- Sar EA, Sunesen I, Lavigne AS (2002) The diatom genus *Thalassiosira*: species from the northern San Matias Gulf (Rio Negro, Argentina). Nova Hedwigia 74 (3-4): 373-386. https://doi.org/10.1127/0029-5035/2002/0074-0373

- Sar EA, Romero O, Sunesen I (2003) *Cocconeis* Ehrenberg and *Psammococconeis garcia* (Bacillariophyta) from the Gulf of San Matías, Patagonia, Argentina. Diatom Research 18 (1): 79-106. https://doi.org/10.1080/0269249X.2003.9705575
- Sarker S, Hossain MS, Sonia MI, Huda AN, Riya SC, Das N, Liyana E, Basak SC, Kabir MA (2023) Predicting the impacts of environmental variability on phytoplankton communities of a sub-tropical estuary. Journal of Sea Research 194: 102404. https://doi.org/10.1016/j.seares.2023.102404
- Saunders K, Lane C, Cook S, McMinn A, Hallaegraeff GM (2010) Benthic diatoms. In: Hallegraeff GM, Bolch CJ, Hill DR, Jameson I, LeRoi JM, McMinn A, Murray S, de Salas MF, Saunders K (Eds) Algae of Australia. Phytoplankton of temperate waters. Australian Biological Resources Study/CSIRO Publishing, Canberra, Australia, 421 pp.
- Schmidt A (1875) Atlas der Diatomaceen-kunde. Series I, Heft 3. Verlag von Ernst Schlegel, Aschersleben, Germany.
- Schmidt A (1899) Atlas der Diatomaceen-kunde. Series V, Heft 54. O.R. Reisland, Leipzig, Germany.
- Sentinel Hub (2025) Modified Copernicus Sentinel data (2016–2017). https://www.sentinel-hub.com. Accessed on: 2025-11-01.
- Shim JH (1976) Distribution and taxonomy of planktonic marine diatoms in the Strait of Georgia, B.C. PhD thesis. University of British Columbia, Vancouver, Canada, 248 pp. https://doi.org/10.14288/1.0093789
- Simon AD, Adamczyk EM, Basman A, Chu JW, Gartner HN, Fletcher K, Gibbs CJ, Gibbs DM, Gilmore SR, Harbo RM, Harris LH, Humphrey E, Lamb A, Lambert P, McDaniel N, Scott J, Starzomski BM (2022) Toward an atlas of Salish Sea biodiversity: the flora and fauna of Galiano Island, British Columbia, Canada. Part I. Marine zoology. Biodiversity Data Journal 10: e76050. https://doi.org/10.3897/BDJ.10.e76050
- Simon AD, Webber M, van Asselt A (2026) Diatoms (Bacillariophyta) of the Salish Sea, Northeast Pacific (1856–2026). Version 1.0. Biodiversity Data Journal. Occurrence dataset. https://ipt.pensoft.net/resource?r=salishseadiatoms&v=1.0. Accessed on: 2026-2-16.
- Simonsen R (1987) Atlas and catalogue of the diatom types of Friedrich Hustedt. Volume 1: Catalogue of Hustedt's diatom types. Volume 2: Atlas of Hustedt's diatom types, pls. 1–395. Volume 3: Atlas of Hustedt's diatom types, pls. 396–772. J. Cramer, Berlin–Stuttgart, Germany, 1,741 pp.
- Simpson A, Eglit Y (2016) Protist diversification. In: Kliman RM (Ed.) Encyclopedia of evolutionary biology. Academic Press (Elsevier), Cambridge, Massachusetts, 2,132 pp. https://doi.org/10.1016/B978-0-12-800049-6.00247-X
- Sims PA (Ed.) (1996) An atlas of British diatoms. Arranged by B. Hartley based on illustrations by H.G. Barber and J.R. Carter. Biopress Ltd, Bristol, UK, 601 pp.
- Siqueiros-Beltrones DA, Ibarra Obando SE (1985) Lista florística de las diatomeas epífitas de *Zostera marina* en Bahía Falsa, San Quintin. Ciencias Marinas 11 (3): 21-67. https://doi.org/10.7773/cm.v11i3.480
- Smith W (1856) A synopsis of the British Diatomaceae; with remarks on their structure, functions and distribution; and instructions for collecting and preserving specimens. Vol. II. John van Voorst, London, England, 107 pp.
- Snoeijs P (Ed.) (1993) Intercalibration and distribution of diatom species in the Baltic Sea, Volume 1. The Baltic Marine Biologists Publication 16a. Opulus Press, Uppsala, Sweden, 129 pp.

- Snoeijs P, Balashova N (Eds) (1998) Intercalibration and distribution of diatom species in the Baltic Sea, Volume 5. The Baltic Marine Biologists Publication 16e. Opulus Press, Uppsala, Sweden, 144 pp.
- Sobocinski K, Harvell CD, Baloy NK, Broadhurst G, Dethier M, Flower A, Delaney J (2022) Urban seas as hotspots of stress in the Anthropocene ocean: The Salish Sea example. Elementa: Science of the Anthropocene 10 (1). https://doi.org/10.1525/elementa.2022.00055
- Sobocinski KL (2021) State of the Salish Sea. Broadhurst G, Baloy NJK (Contributing Eds). Salish Sea Institute, Western Washington University, Bellingham, USA, 275 pp. https://doi.org/10.25710/vfhb-3a69
- Spalding M, Fox H, Allen G, Davidson N, Ferdaña Z, Finlayson M, Halpern B, Jorge M, Lombana A, Lourie S, Martin K, McManus E, Molnar J, Recchia C, Robertson J (2007) Marine ecoregions of the world: a bioregionalization of coastal and shelf areas. BioScience 57 (7): 573-583. https://doi.org/10.1641/b570707
- Staatliche Naturwissenschaftliche Sammlungen Bayerns (2025) The diatom collection of Franz Josef Weinzierl at the Botanische Staatssammlung München. Occurrence dataset. The Bavarian State Collections of Natural History, Munich, Germany. URL: https://doi.org/10.15468/dixlft
- Stidolph SR (1994) Observations and remarks on morphology and taxonomy of the diatom genera *Gyrosigma* Hassall and *Pleurosigma* W. Smith IV. *Gyrosigma fogedii* sp. nov., and some diatoms similar to *G. fasciola* (Ehrenb.) Griffith & Henfrey. Diatom Research 9 (1): 213-224. https://doi.org/10.1080/0269249X.1994.9705297
- Stonik IV, Orlova TY, Crawford RM (2006) *Attheya ussurensis* sp. nov. (Bacillariophyta)—a new marine diatom from the coastal waters of the Sea of Japan and a reappraisal of the genus. Phycologia 45 (2): 141-147. https://doi.org/10.2216/04-48.1
- Stonik IV, Aizdaicher NA (2016) The species composition, morphology, and seasonal distribution of diatoms of the genus *Attheya* West, 1860 from the Sea of Japan. Russian Journal of Marine Biology 42 (4): 357-361. https://doi.org/10.1134/S1063074016040118
- Stonik IV, Efimova KV (2020) *Attheya* (Bacillariophyta) from the northwestern Sea of Japan: a description of two subgenera based on molecular and morphological data. Phycologia 59 (3): 227-237. https://doi.org/10.1080/00318884.2020.1732801
- Sugie K, Kuma K (2017) Change in elemental composition and cell geometry of the marine diatom *Attheya longicornis* under nitrogen- and iron-depleted conditions. Diatom Research 32 (1): 11-20. https://doi.org/10.1080/0269249X.2017.1301999
- Sunesen I, Sar EA (2007) Marine diatoms from Buenos Aires coastal waters (Argentina). IV. *Rhizosolenia* s. str., *Neocalyptrella*, *Pseudosolenia*, *Proboscia*. Phycologia 46 (6): 628-643. https://doi.org/10.2216/07-13.1
- Suzuki H, Toyoda K, Yazaki I, Yamaguchi K (2009) Morphology of the marine benthic diatom *Achnanthes pseudogroenlandica* Hendey (Bacillariophyceae). Journal of Japanese Botany 84 (3): 131-142.
- Takano H (1965) New and rare diatoms from Japanese waters. I. Bulletin of the Tokai Regional Fisheries Laboratory 42: 1-10.
- Takano H (1983) New and rare diatoms from Japanese marine waters. IX. A new *Rhaphoneis* emitting mucilaginous threads. Bulletin of the Tokai Regional Fisheries Laboratory 109: 27-39.
- Tanaka H (2007) Taxonomic studies of the genera *Cyclotella* (Kützing) Brébisson, *Discotella* Houk et Klee and *Puncticulata* Håkansson in the family Sephanodiscaceae

Glezer et Makarova (Bacillariophyta) in Japan. Bibliotheca Diatomologica 53. J. Cramer, Berlin–Stuttgart, Germany, 204 pp.

- Tempère J, Peragallo H (1908) Diatomées du monde entier. 2nd edition, fascicles 2-7. Arcachon, Gironde, France, 480 pp.
- Theobald EJ, Ettinger AK, Burgess HK, DeBey LB, Schmidt NR, Froehlich HE, Wagner C, HilleRisLambers J, Tewksbury J, Harsch MA, Parrish JK (2015) Global change and local solutions: tapping the unrealized potential of citizen science for biodiversity research. Biological Conservation 181: 236-244. https://doi.org/10.1016/j.biocon.2014.10.021
- Throndsen J, Hasle GR, Tangen K (2007) Phytoplankton of Norwegian coastal waters. Almater Forlag AS, Oslo, Norway, 343 pp.
- Tréguer P, Bowler C, Moriceau B, Dutkiewicz S, Gehlen M, Aumont O, Bittner L, Dugdale R, Finkel Z, Iudicone D, Jahn O, Guidi L, Lasbleiz M, Leblanc K, Levy M, Pondaven P (2018) Influence of diatom diversity on the ocean biological carbon pump. Nature Geoscience 11: 27-37. https://doi.org/10.1038/s41561-017-0028-x
- Trobajo R, Mann DG (2019) A rapid cleaning method for diatoms. Diatom Research 34 (2): 115-124. https://doi.org/10.1080/0269249X.2019.1637785
- Tynni R (1986) Observations of diatoms on the coast of the state of Washington. Geological Survey of Finland, Report of Investigation 75. Geological Survey of Finland, Espoo, Finland, 25 pp.
- United Nations Global Compact (2024) The plankton manifesto—a call for plankton-based solutions to address the triple planetary crisis (biodiversity, climate & pollution). https://unglobalcompact.org/library/6242. Accessed on: 2025-10-26.
- University of British Columbia Herbarium (2024) University of British Columbia Herbarium (UBC) - algae collection. Occurrence dataset. Version 14.19. University of British Columbia, Vancouver, Canada. URL: https://doi.org/10.5886/ujwtvvs2
- University of New Hampshire Natural History Collections (2025) University of New Hampshire - macroalgal collection. Occurrence dataset. University of New Hampshire, Durham, New Hampshire, USA. URL: https://doi.org/10.15468/kembya
- Van der Werff A, Huls H (1975) Diatomeeënflora van Nederland. Drukkerij Sprey Abcoude, The Hague, Netherlands, 738 pp.
- Van Heurck H (1880) Synopsis des diatomées de belgique. Atlas (plates I–XXX). Ducaju et Cie, Antwerp, Belgium.
- Van Heurck H (1881) Synopsis des diatomées de belgique. Atlas (plates XXXI–LXXVII). Ducaju et Cie, Antwerp, Belgium.
- Van Heurck H (1882) Synopsis des diatomées de belgique. Atlas (plates LXXVIII–CXXXII). Ducaju et Cie, Antwerp, Belgium.
- Vardi A (2008) Cell signaling in marine diatoms. Communicative & Integrative Biology 1 (2): 134-136. https://doi.org/10.4161/cib.1.2.6867
- Vardi A, Thamatrakoln K, Bidle KD, Falkowski P (2009) Diatom genomes come of age. Genome Biology 9: 245. https://doi.org/10.1186/gb-2008-9-12-245
- Vasselon V, Domaizon I, Rimet F, Kahlert M, Bouchez A (2017) Application of high-throughput sequencing (HTS) metabarcoding to diatom biomonitoring: do DNA extraction methods matter? Freshwater Science 36 (1): 162-177. https://doi.org/10.1086/690649
- Vaulot D, Eikrem W, Viprey M, Moreau H (2008) The diversity of small eukaryotic phytoplankton (≤3 µm) in marine ecosystems. FEMS Microbiology Reviews 32 (5): 795-820. https://doi.org/10.1111/j.1574-6976.2008.00121.x

- Viljoen JJ, Sun X, Brewin RJ (2024) Climate variability shifts the vertical structure of phytoplankton in the Sargasso Sea. Nature Climate Change 14 (12): 1292-1298. https://doi.org/10.1038/s41558-024-02136-6
- Villac MC, Kaczmarska I, Ehrman JM (2017) Diatoms from ship ballast sediments (with consideration of a few additional species of special interest). In: Witkowski A (Ed.) Diatom Monographs. 18. Koeltz Botanical Books, Oberreifenberg, Germany, 557 pp.
- Wachnicka AH, Gaiser EE (2007) Characterization of *Amphora* and *Seminavis* from South Florida, U.S.A. Diatom Research 22 (2): 387-455. https://doi.org/10.1080/0269249X.2007.9705722
- Webber M, van Dam J, Humphrey EC (2011) Effectiveness of cleaning methods for investigating diatoms. Microscopy and Microanalysis 17 (S2): 266-267. https://doi.org/10.1017/S1431927611002200
- Wilks JV, Armand LK (2017) Diversity and taxonomic identification of *Shionodiscus* spp. in the Australian sector of the Subantarctic Zone. Diatom Research 32 (3): 295-307. https://doi.org/10.1080/0269249X.2017.1365015
- Williams DM (2025) Introduction: papers for 'Progress in diatom biogeography'. Diatom Research 40 (1): 1-7. https://doi.org/10.1080/0269249X.2024.2425707
- Witkowski A, Metzeltin D, Lange-Bertalot H, Bafana G (1997) *Fogedia* gen. nov. (Bacillariophyceae), a new naviculoid genus from the marine littoral. Nova Hedwigia 65 (1-4): 79-98. https://doi.org/10.1127/nova.hedwigia/65/1997/79
- Witkowski A, Lange-Bertalot H, Metzeltin D (2000) Diatom flora of marine coasts I. In: Lange-Bertalot H (Ed.) Iconographia diatomologica. Annotated diatom micrographs. Vol. 7, Diversity-taxonomy-identification. A.R.G. Gantner Verlag K.G., Ruggell, Liechtenstein, 925 pp.
- Witkowski A, Lange-Bertalot H, Kociolek JP, Kulikowskiy M, Bak M, Ruppel M (2010) Diatom flora of San Francisco bay and vicinity. II. *Fogedia krammeri* sp. nov. Polish Botanical Journal 55 (1): 49-53.
- Witkowski A, Li CL, Zgłobicka I, Yu SX, Ashworth M, Dąbek P, Qin S, Tang C, Krzywda M, Ruppel M, Theriot EC, Jansen RK, Car A, Płociński T, Wang YC, Sabir JS, Daniszewska-Kowalczyk G, Kierzek A, Hajrah NH (2016) Multigene assessment of biodiversity of diatom (Bacillariophyceae) assemblages from the littoral zone of the Bohai and Yellow Seas in Yantai region of Northeast China with some remarks on ubiquitous taxa. In: Harff J, Zhang H (Eds) Environmental processes and the natural and anthropogenic forcing in the Bohai Sea, eastern Asia. Journal of Coastal Research 74 (Sp 1): 166-195. https://doi.org/10.2112/SI74-016.1
- WoRMS Editorial Board (2021) World register of marine species. https://www.marinespecies.org. Accessed on: 2025-10-28.
- Wright E (2019) DECIPHER: Tools for curating, analyzing, and manipulating biological sequences. https://rdrr.io/bioc/DECIPHER/. Accessed on: 2025-12-03.
- W.S. Turrell Herbarium (2025) Miami University - algae. Occurrence dataset. Miami University, Oxford, Ohio, USA. URL: https://doi.org/10.15468/9xp52b
- Yun SM, Lee JH (2011) Morphology and distribution of some marine diatoms, family Rhizosoleniaceae, genus *Proboscia*, *Neocalyptrella*, *Pseudosolenia*, *Guinardia*, and *Dactyliosolen* in Korean coastal waters. Algae 26 (4): 299-315. https://doi.org/10.4490/algae.2011.26.4.299

Supplementary materials

Suppl. material 1: Diatoms (Bacillariophyta) of the Salish Sea, Northeast Pacific (1866–2026): Annotated Checklist

Authors: Mark Webber, Arjan van Asselt, Alice Chang, Andrew Simon
Data type: annotated checklist
Brief description: Annotated checklist of diatoms reported for the Salish Sea (1866–2026).
Download file (780.33 kb)

Suppl. material 2: Diatoms (Bacillariophyta) of the Salish Sea, Northeast Pacific (1866–2026): Annotated Checklist

Authors: Mark Webber, Arjan van Asselt, Alice Chang, Andrew Simon
Data type: annotated checklist (CSV format)
Brief description: Annotated checklist of diatoms reported for the Salish Sea (1866–2026) - summary in CSV format (used as the basis for the formatted checklist provided as PDF).
Download file (230.23 kb)

Suppl. material 3: *Scagelia* sample - Miners Bay, Mayne Island, BC - manually curated 18S ASV taxon table

Authors: Mark Webber, Evan Morien, Andrew Simon
Data type: manually curated ASV taxon table (18S)
Download file (14.23 kb)

Suppl. material 4: *Zostera marina* samples - Montague Harbour - manually curated 18S ASV taxon table

Authors: Mark Webber, Evan Morien, Andrew Simon
Data type: manually curated ASV taxon table (18S)
Download file (101.03 kb)

Suppl. material 5: *Zostera marina* samples - Montague Harbour - manually curated rbcL ASV taxon table

Authors: Mark Webber, Evan Morien, Andrew Simon
Data type: manually curated ASV taxon table (rbcL)
Download file (80.74 kb)

Suppl. material 6: plankton samples - Salish Sea - manually curated rbcL ASV taxon table

Authors: Mark Webber, Evan Morien, Andrew Simon
Data type: manually curated ASV taxon tables (rbcL)
Download file (49.97 kb)

Suppl. material 7: Galiano BioBlitz 2023 - Galiano Island, BC - manually curated rbcL ASV taxon table

Authors: Mark Webber, Evan Morien, Andrew Simon
Data type: manually curated ASV taxon table (rbcL)
Download file (118.60 kb)

Suppl. material 8: Diatoms (Bacillariophyta) of the Salish Sea, Northeast Pacific (1866–2026): Catalogue of occurrence data (aligned)

Authors: Mark Webber, Evan Morien, Arjan van Asselt, Andrew Simon
Data type: occurrences
Brief description: Catalogue of occurrence data used for baseline analysis - all records aligned with the curated summary of unique taxa reported in the annotated checklist.
Download file (6.81 MB)

Suppl. material 9: Diatoms (Bacillariophyta) of the Salish Sea, Northeast Pacific (1866–2026): Catalogue of occurrence data (complete)

Authors: Mark Webber, Evan Morien, Arjan van Asselt, Andrew Simon
Data type: occurences
Brief description: Catalogue of occurrence data - all diatom records (including taxa unresolved beyond family or genus).
Download file (8.73 MB)